Ocean carbon sequestration by direct CO_2 injection

Dissertation

zur Erlangung des Doktorgrades
der Mathematisch - Naturwissenschaftlichen Fakultät
der Christian-Albrechts Universität zu Kiel

vorgelegt von
Fabian Reith

Kiel, Dezember 2017

1. Gutachter: Prof. Dr. Andreas Oschlies

2. Gutachter: Prof. Dr. Ulf Riebesell

Tag der mündlichen Prüfung: 08.03.2018

_____

gez. Prof. Dr. Natascha Oppelt, Dekanin

"Our population and our use of the finite resources of planet Earth are growing exponentially, along with our technical ability to change the environment for good or ill."

- Stephen Hawking

Contents

Summary

The Paris Agreement of 2015 has set the specific target to limit mean global warming to well below 2°C, if not 1.5 °C above preindustrial levels in order to avoid the most dangerous consequences of anthropogenic climate change (UNFCCC, 2015). The accomplishment of this target very likely depends on the future deployment of both carbon capture and storage (CCS) and intentional carbon dioxide removal (CDR), which are measures that deliberately remove CO_2 from the atmosphere and store it somewhere else (e.g., Fuss et al., 2014; Gasser et al., 2015), e.g., in geological formations or the deep ocean (e.g., IPCC, 2005). To date, the technological development and feasibility of such methods are in their infancy and thus uncertain regarding their effectiveness, costs, side effects, and carbon-cycle implications (e.g., Field and Mach, 2017). A proposed carbon storage method for CO_2 captured from large point sources such as power plants or via some CDR method is ocean carbon sequestration by direct CO_2 injection into the deep ocean. This carbon storage method aims at the deliberate acceleration of the natural oceanic uptake of anthropogenic CO_2 by discharging it directly into the deep ocean (Marchetti, 1977; see section 1.3). Chapters 2 - 4 of this thesis revisit this idea and provide a novel evaluation of direct CO_2 injection into the deep ocean that goes well beyond previous assessments.

Chapter 2 presents a modeling study that expands on the previously studied effects of direct CO_2 injection into the deep ocean on atmospheric and oceanic reservoirs and also considers respective carbon-cycle- and climate feedbacks between the atmosphere and the terrestrial biosphere. This is of importance, because other studies have shown that backfluxes from the land to the atmosphere in response to reducing atmospheric CO_2 can further offset the target atmospheric carbon reduction (e.g., Oschlies et al., 2010). Furthermore, this study also looks at the injection-related changes in seawater carbonate chemistry.

For that purpose, we use the University of Victoria Earth System Climate Model (UVic model) of intermediate complexity to simulate the direct injection of CO_2 into the deep ocean as a means of emissions reduction during a high CO_2 emission scenario.

The effectiveness (the fraction of injected CO_2 that remains in the ocean) and seawater carbonate chemistry changes observed in this study are similar to previous studies. However, this effectiveness only accounts for the injected CO_2 and does not include possible adjustments of fluxes of other carbon in the Earth system. Accordingly, we define another effectiveness that accounts for all potential feedbacks of carbon fluxes into and out of the ocean in response to the CO_2 injections. From this carbon budget perspective, we find that the targeted atmospheric CO_2 reduction is never reached, indicating that both injected carbon has been leaking from the ocean and that atmosphere-land and/or atmosphere-ocean carbon fluxes (relative to the control run) have been affected by the reduction in atmospheric carbon.

The findings of this study show how feedbacks challenge a correct attribution of the effect of direct CO_2 injections on the targeted atmospheric carbon reduction.

Chapter 3 presents a modeling study that is the first one to look at the suitability and injection-related biogeochemical impacts of direct CO_2 injection into the deep ocean as a means to bridge the gap between CO_2 emissions and climate impacts of the Representative and Extended Concentration Pathway (RCP/ECP) 4.5 scenario and the 1.5°C climate target. Three conceptually different approaches for applying direct CO_2 injection into the deep ocean to meet the 1.5°C climate target on a millennium timescale are simulated using the UVic model. The first approach assumes that all anthropogenic CO_2 emissions are injected after a global mean temperature of 1.5°C is exceeded for the first time, the second approach injects a mass of CO_2 that prevents global mean temperature from rising beyond 1.5°C, and the third approach injects an amount of CO_2 to enable that atmospheric CO_2 concentrations follow the RCP/ECP 2.6 scenario as closely as possible. For each approach the cumulative CO_2 injections required are quantified and the collateral effects of the injections in terms of changes

of oceanic pH and carbonate ion saturation state are determined to identify trade-offs between possible benefits at the ocean surface and injection-induced harms in the deep ocean. In sensitivity simulations, this study also investigates how $CaCO_3$ sediment and weathering feedbacks influence the cumulative mass of injected CO_2 as well as the impacts on ocean biogeochemistry in each approach.

The findings of this study demonstrate the massive amounts of CO_2 that would need to be injected into the deep ocean in order to reach and sustain the 1.5°C climate target under an intermediate CO_2 emissions scenario on such a timescale. These amounts include a high portion of outgassed CO_2 that needs to be re-injected in order to maintain the targeted state.

With respect to biogeochemical impacts, the results of this study show that there is a trade-off between injection-related reductions in atmospheric CO_2 levels accompanied by reduced upper-ocean acidification and adverse effects on deep ocean carbonate chemistry. The inclusion of $CaCO_3$ sediment and weathering feedbacks, i.e., feedbacks that are always present in the real Earth system, are found to weaken the required cumulative CO_2 injections and lead to the highest benefit in the upper ocean and the lowest harm the intermediate and deep ocean.

Chapter 4 presents a study that investigates how well carbon-cycle feedbacks are represented in carbon-cycle models used in state-of-the-art integrated assessment models (IAMs). Therefore, direct CO_2 injection into the deep ocean is integrated in an economic inter-temporal optimization model as proxy for ocean-based CDR measures. Such an approach allows for the derivation of optimal CO_2 injection trajectories, which go beyond previous assessments. Here, we account for the change in CO_2 emissions as a response to CO_2 injection in the deep ocean and the potential extra amount of CO_2 injection required to compensate for outgassing. The investigation applies the benchmark IAM DICE (Dynamic Integrated Climate-Economy model), combined with different box-model representation of the global carbon-cycle, to consider different climate objectives: i) a cost-benefit framework with an endogenous level of cli-

mate change, and ii) a cost-effectiveness framework with an exogenous level of climate change, as given by the 2°C goal. In order to validate this integrated assessment of direct CO_2 injection as proxy for ocean-based CDR measures, the derived atmospheric carbon and global mean temperature trajectories are implemented in the UVic-model.

The analyses reveal that the basic carbon-cycle models have significantly improved over the past years. While with the carbon-cycle description of the DICE model in its 2013 version, there is almost no difference between deep ocean CO_2 injection and geological storage, the carbon-cycle description of the most recent version (2017) displayed the effect of the emission reduction substitution and carbon-cycle feedbacks. Accordingly, investigating deep ocean CO_2 injection, and more generally CDR, appears to be sensible in such an integrated assessment framework, however, deriving robust policy recommendation requires the validation with Earth system models.

Overall, this thesis illustrates the importance of the accounting for all carbon fluxes in the carbon- cycle when deliberately reducing atmospheric CO_2 and injecting the removed CO_2 into the deep ocean. This is especially highlighted by the fact that carbon-cycle feedbacks as well as leakage would offset any targeted atmospheric carbon reduction and thus prevent direct CO_2 injection from being 100 % efficient and capable of reducing atmospheric CO_2 by the injected amount.

Furthermore, the thesis explores the potential as well as injection-related side effects of direct CO_2 injection into the deep ocean to reach and maintain the 1.5°C climate target on a millennium timescale. The large amounts of outgassed CO_2, which would need to be re-captured by additional CDR and subsequently re-injected into the deep ocean in order to sustain the desired target, question the respective suitability of direct CO_2 injection. This re-injection also represents a burden for future generations since re-injection would be necessary for centuries after the initial injection and its associated economical benefit from energy production.

Finally, there is a trade-off between potential benefits in the upper ocean and injection-related harms in the intermediate and deep ocean. This trade-off illustrates the

challenge of evaluating the offset of local harm against global benefit, which is very likely the subject of any CDR method. Accordingly, the results of this thesis contribute to the current scientific and political debate on the deliberate removal of atmospheric CO_2 in order to reach the agreed-upon climate goals.

Zusammenfassung

Mit dem Pariser Klimaabkommen von 2015 wurde das spezifische Ziel festelegt, die mittlere globale Erwärmung auf deutlich unter 2°C, möglichst auf 1,5°C über dem vorindustriellen Niveau zu begrenzen, um die gefährlichsten Folgen des anthropogenen Klimawandels zu vermeiden (UNFCCC, 2015). Die Erreichung dieses Ziels hängt sehr wahrscheinlich vom zukünftigen Einsatz sowohl der CO_2-Abscheidung und -Speicherung (carbon capture and storage, CCS) als auch von Carbon Dioxide Removal (CDR) ab. Bei CDR handelt es sich um Maßnahmen, die der Atmosphäre gezielt CO_2 entziehen und an anderer Stelle speichern (z.B. Fuss et al., 2014; Gasser et al., 2015), z.B. in geologischen Formationen oder im tiefen Ozean (z.B. IPCC, 2005). Die technologische Entwicklung und Abschätzung der Durchführbarkeit solcher Methoden befindet sich in den Anfängen, so dass diese hinsichtlich ihrer Wirksamkeit, Kosten, Nebenwirkungen und Auswirkungen auf den Kohlenstoffkreislauf ungewiss sind (z.B. Field and Mach, 2017). Eine vorgeschlagene Methode zur Kohlenstoffspeicherung im Meer für abgeschiedenes CO_2 aus großen Punktquellen wie Kraftwerken oder entnommenem CO_2 aus der Atmosphäre durch eine CDR-Methode ist die direkte CO_2-Injektion in den tiefen Ozean. Diese Methode bezweckt, die natürliche ozeanische Aufnahme von anthropogenem CO_2 an der Grenzschicht Atmosphäre-Ozean zu beschleunigen (Marchetti, 1977; siehe Abschnitt 1.3). Die Kapitel 2 bis 4 der vorliegenden Dissertation untersuchen diese Idee und präsentieren Ergebnisse zur direkten CO_2-Injektion in den tiefen Ozean, die weit über den bisherigen Wissensstand hinausgehen.

Kapitel 2 stellt eine Modellierungsstudie vor, die die zuvor untersuchten Effekte der direkten CO_2-Injektion in den tiefen Ozean auf atmosphärische und ozeanische Reservoire erweitert und auch entsprechende Kohlenstoffkreislauf- und Klima-Rückkopplungen zwischen Atmosphäre und terrestrischer Biosphäre berücksichtigt. Dies ist von

Bedeutung, da andere Studien gezeigt haben, dass Rückflüsse vom Land in die Atmosphäre als Reaktion auf die Reduzierung des atmosphärischen CO_2 die angestrebte Reduktion des atmosphärischen Kohlenstoffs weiter verringern können (z.B. Oschlies et al., 2010). Darüber hinaus untersucht diese Studie auch die injektionsbedingten Veränderungen in der Meerwasser-Karbonatchemie.

Das University of Victoria Erdsystemmodell mittlerer Komplexität (UVic-Model) wird verwendet, um die direkte CO_2-Einleitung in den tiefen Ozean als Mittel zur Emissionsreduzierung während eines hohen CO_2-Emissionsszenarios zu simulieren.

Die Ergebnisse in Bezug auf die Effektivität (Anteil an injiziertem CO_2, der im Ozean verbleibt) und Veränderungen in der Meerwasser-Chemie sind vergleichbar mit früheren Studien. Diese Effektivität betrifft allerdings nur das injizierte CO_2 und berücksichtigt keine möglichen Veränderungen anderer Kohlenstoffflüsse im Erdsystem. Daher wird eine Effektivität der Methode definiert, die alle möglichen Rückkopplungen von Kohlenstoffflüssen in und aus dem Ozean als Reaktion auf die CO_2-Injektionen berücksichtigt. Aus dieser Perspektive des Kohlenstoffhaushalts wird die angestrebte CO_2-Reduzierung in der Atmosphäre jedoch nicht erreicht, was darauf hindeutet, dass sowohl etwas von dem eingeleiteten CO_2 ausgegast ist als auch dass die Kohlenstoffflüsse zwischen Atmosphäre-Land und/oder Atmosphäre-Ozean (relativ zur Kontrollsimulation) verringert wurden.

Die Ergebnisse dieser Studie zeigen, wie schwierig die Zuordnung der Kohlenstoffflüsse als Folge des zusätzlich injizierten CO_2 ist.

Kapitel 3 stellt eine Modellierungsstudie vor, die als erste das Potenzial sowie die einhergehenden biogeochemischen Nebenwirkungen direkter CO_2-Injektionen in den tiefen Ozean untersucht, um die Lücke zwischen den CO_2-Emissionen und Klimaauswirkungen des Repräsentativen und Erweiterten Konzentrationspfades (Representative and Extended Concentration Pathway, RCP/ECP) 4.5 und des 1,5°C Ziels zu schließen. Zu diesem Zweck werden drei konzeptionell unterschiedliche Ansätze für

direkte CO_2-Injektionen in den tiefen Ozean zur Erreichung und Erhaltung des 1,5°C Ziels über einen Zeitraum von 1000 Jahren mit Hilfe des UVic-Models simuliert.

Der erste Ansatz geht davon aus, dass alle anthropogenen CO_2-Emissionen injiziert werden, nachdem eine globale Mitteltemperatur von 1,5°C zum ersten Mal überschritten wurde, der zweite Ansatz injiziert eine Menge an CO_2, die verhindert, dass die globale Mitteltemperatur weit über 1,5°C ansteigt, und der dritte Ansatz injiziert so viel CO_2, dass die atmosphärischen CO_2-Konzentrationen dem RCP/ECP 2.6 möglichst genau folgen.

Für jeden Ansatz werden die erforderlichen kumulativen CO_2-Injektionen quantifiziert sowie die Nebenwirkungen der Injektionen untersucht, um so Grundlagen für eine Bewertung der potenziellen Vorteile an der Meeresoberfläche gegenüber den injektionsbedingten Schäden im tiefen Ozean zu ermöglichen. Des Weiteren wird in dieser Studie anhand von Sensitivitätssimulationen untersucht, inwieweit $CaCO_3$ Sedimente und Verwitterungsflüsse die kumulativen CO_2-Injektionen sowie die biogeochemischen Auswirkungen durch Rückkopplungen beeinflussen.

Die Ergebnisse dieser Studie verdeutlichen die massiven Mengen an CO_2, die in den tiefen Ozean injiziert werden müssten, um das 1,5°C Ziel unter einem mittleren CO_2-Emissionsszenario auf einer tausendjährigen Zeitskala zu erreichen und aufrechtzuerhalten. Diese Mengen beinhalten einen hohen Anteil an ausgegastem CO_2, das erneut injiziert werden muss, um das angestrebte Ziel aufrechtzuerhalten.

Hinsichtlich der biogeochemischen Auswirkungen zeigt sich, dass es einer Abwägung bedarf zwischen einer injektionsbedingten Reduktion des atmosphärischen CO_2-Gehalts bei gleichzeitiger Verringerung der oberflächennahen Ozeanversauerung sowie den negativen Auswirkungen auf die Karbonatchemie im tiefen Ozean.

Die Berücksichtigung der $CaCO_3$-Sediment- und Verwitterungsrückkopplungen, d.h. Rückkopplungen, die im realen Erdsystem immer vorhanden sind, verringern die erforderlichen kumulativen CO_2-Injektionen und führen zum höchsten Nutzen im oberen Ozean und den geringsten Schäden im mittleren und tiefen Ozean.

Kapitel 4 präsentiert eine Studie, die untersucht, wie gut die Rückkopplungseffekte des Kohlenstoffkreislaufs in Kohlenstoffkreislaufmodellen dargestellt werden, die in modernen integrierten Bewertungsmodellen (integrated assessment model, IAM) verwendet werden.

Zu diesem Zweck wird die Methode der CO_2-Injektion in den tiefen Ozean in ein ökonomisches inter-temporales Optimierungsmodell integriert und als Proxy für ozeanbasierte CDR-Methoden verwendet. Die Integration in einen solchen integrierten Bewertungsrahmen ermöglicht es, endogen bestimmte Trajektorien für die CO_2-Injektion zu bewerten, was über bisherige Untersuchungen hinausgeht. Diese Studie berücksichtigt die wirtschaftlich motivierte geringere Reduktion der CO_2-Emissionen als Reaktion auf die CO_2-Injektion in den tiefen Ozean und die potenzielle zusätzliche Menge an CO_2-Injektion, die erforderlich ist, um das ausgegaste CO_2 zu kompensieren. Die Studie verwendet das IAM DICE (Dynamic Integrated Climate-Economy Model), das im Hinblick auf die Anwendungshäufigkeit in der sozioökonomischen Literatur des Klimawandels als Standardmodell bezeichnet werden kann. In der Untersuchung wird DICE mit verschiedenen Box-Modellen kombiniert, die essentielle Prozesse des globalen Kohlenstoffkreislaufs unterschiedlich parametrisieren. Innerhalb der Untersuchung wird zwischen folgenden Entscheidungsansätzen unterschieden: i) ein Kosten-Nutzen-Ansatz mit endogenem Niveau des Klimawandels und ii) ein Kosten-Effektivitäts-Ansatz mit exogenem Niveau des Klimawandels, wie dieser durch das 2°C-Ziel vorgegeben wird. Um diese integrierte Bewertung der direkten CO_2-Injektion als Proxy für ozeanbasierte CDR-Maßnahmen zu validieren, werden die daraus abgeleiteten atmosphärischen Kohlenstoff- und globalen Mitteltemperaturverläufe in das UVic-Modell implementiert.

Die Analysen zeigen, dass sich die Darstellung des Kohlenstoffkreislaufs in IAMs in den letzten Jahren deutlich verbessert hat. Während es bei der Beschreibung des Kohlenstoffkreislaufs des DICE-Modells in der Version 2013 fast keinen Unterschied zwischen der CO_2-Injektion in den tiefen Ozean und der geologischen Speicherung gibt, zeigt die Beschreibung des Kohlenstoffkreislaufs in der neuesten Version (2017) den Substitutionseffekt von Emissionsreduzierung und Rückkopplungen im Kohlen-

stoffkreislauf. Dementsprechend erscheint die Untersuchung von CO_2-Injektion in den tiefen Ozean sowie von CDR im Allgemeinen in einem solchen integrierten Bewertungsrahmen sinnvoll, jedoch erfordert die Ableitung einer robusten politischen Empfehlung eine Validierung mit Erdsystemmodellen.

Insgesamt veranschaulicht diese Dissertation, dass für die Bewertung der gezielten CO_2-Entnahme aus der Atmosphäre und der Injektion des entfernten CO_2 in den tiefen Ozean alle Kohlenstoffflüsse im Kohlenstoffkreislauf berücksichtigt werden müssen. Dies wird vor allem deshalb notwendig, da Rückkopplungen im Kohlenstoffkreislauf sowie ausgegastes CO_2 dem atmosphärischen CO_2-Reduktionsziel entgegenwirken und somit verhindern, dass die direkte Einleitung von CO_2 in den tiefen Ozean zu 100 % effizient und damit in der Lage ist, das atmosphärische CO_2 um die injizierte Menge zu reduzieren.

Darüber hinaus untersucht diese Dissertation das Potenzial und die injektionsbedingten Nebenwirkungen der direkten CO_2-Injektion in den tiefen Ozean, um das 1,5°C Ziel über einen Zeitraum von 1000 Jahren zu erreichen und aufrechtzuerhalten. Insbesondere muss berücksichtigt werden, dass die CO_2-Einleitung in den tiefen Ozean mit großen Mengen an ausgegastem CO_2 einhergeht, das dann der Atmosphäre durch zusätzliches CDR entzogen und anschließend erneut in den tiefen Ozean injiziert werden müsste, um das gewünschte Klimaziel aufrechtzuerhalten. Wegen der zeitlichen Ungleichverteilung von zu vermeidenden Emissionen und der Wiedereinleitung des ausgegasten CO_2 geht die hier untersuchte Methode von CO_2-Einleitungen in den tiefen Ozean mit erheblichen ökonomischen Lasten für zukünftige Generationen einher. Darüber hinaus gilt es zwischen dem potenziellen Nutzen im oberen Ozean und injektionsbedingten Schäden im mittleren und tiefen Ozean abzuwägen.

Diese Überlegungen und Abwägungen veranschaulichen die Herausforderungen, die mit der Bewertung der verschiedenen CDR Methoden einhergehen: Keine der Methoden ist perfekt, und es muss zwischen lokalem Schaden und globalem Nutzen abgewogen werden. Dementsprechend tragen die Ergebnisse dieser Arbeit auch zur aktuellen wissenschaftlichen und politischen Debatte über die CDR Methoden bei, die zwar für die Erreichung ambitionierter Klimaziele unvermeidbar erscheinen, gleichzeitig aber Nebenwirkungen haben.

1 Introduction

The introduction of this dissertation first briefly describes the scientific background with regard to the anthropogenic perturbation of the global carbon cycle and the climate system. Second, the current options to address this perturbation are outlined, which provides the motivation of the research presented in the Chapters 2 – 4. Subsequently, the ocean carbon sequestration method of direct CO_2 injection into the deep ocean is introduced as well as the general tools (numerical models) that are used for the conducted investigations. The last section of the introduction presents the synopsis of the Chapters 2 – 4 and lists the respective author contributions.

1.1 Scientific background – anthropogenic perturbation of the global carbon cycle and the climate system

The earth's climate is strongly influenced by the abundance of greenhouse gases (GHG) in the atmosphere such as carbon dioxide (CO_2), water vapor, methane (CH_4) and nitrous oxide (N_2O), because these have a direct impact on the earth's energy balance (Hansen et al., 2005). Next to water vapor, atmospheric CO_2 is considered to be the most important GHG, which is due to its high abundance and long residence time in the atmosphere, when compared to other GHG (IPCC, 2013; Myhre et al., 2013).

The atmospheric CO_2 concentration is regulated by processes of the global carbon cycle, which naturally transfer carbon between the reservoirs of the atmosphere, ocean, and land on timescales from sub-daily to millennia, while carbon exchanges with the lithosphere occur at longer timescales (Archer et al., 2009). This active cycle has been roughly in steady state during the Holocene (starting 11,700 years ago) prior to the onset of the industrial era (about 1750), meaning that the sum of all carbon fluxes in and out of each carbon reservoir of the Earth system, i.e. the atmosphere, ocean and land, has been close to zero (Cias et al., 2013). This is as well represented

in the preindustrial atmospheric CO_2 concentration, which, expressed as a volume-mixing ratio, has been around 280 ppmv with minor fluctuations around this level as derived from ice-core measurements (Siegenthaler, 2005).

However, anthropogenic CO_2 emissions from human activities (fossil fuel combustion, industrial processes and land-use change) have led to a rapid build-up of CO_2 in the atmosphere, mainly since the onset of the industrial era and in consequence to a perturbed natural carbon cycle (e.g., Archer et al., 2009; Cias et al., 2013). Between 1750 and 2016, these human activities have emitted a cumulative amount of about 645 ± 80 Gt C into the atmosphere (Le Quere et al., 2017, in review). However, less than half (~ 40 %) of these anthropogenic CO_2 emissions have stayed in the atmosphere. The remaining 60 % of anthropogenic carbon have been approximately evenly taken up by the terrestrial and oceanic carbon reservoirs (Le Quere et al., 2017, in review). Accordingly, the atmospheric CO_2 concentration has increased from its preindustrial value of about 280 ppmv to about 403 ppmv in 2016 (Le Quere et al., 2017, in review; Fig. 1.1). This increase in atmospheric CO_2 has caused an imbalance in the earth's energy budget, which has led to an observed increase in the global mean temperature of about 0.8°C above preindustrial levels (IPCC, 2013). Further, the observed increase in the global mean temperature has caused many changes that are detrimental for natural and human ecosystems and considerable concerns surround these growing climate and ecosystem impacts (IPCC, 2014). The consequences of the human-induced increase in atmospheric CO_2 are referred to as anthropogenic climate change.

As illustrated in Figure 1.1, the atmospheric CO_2 concentration would have been about 157 ppmv higher in year 2016 and in turn the consequences of anthropogenic climate change larger, if the ocean and land would not have taken up a significant fraction of the anthropogenic CO_2 emissions. This highlights the importance of the ocean and land carbon sinks as their response to anthropogenic CO_2 emissions regulates the atmospheric CO_2 concentration. Consequently, the scientific understanding of the mechanisms that control the anthropogenic carbon uptake by these natural sinks is essential in order to be able to make plausible predictions of future trajectories of atmospheric CO_2 and thus the extent of anthropogenic climate

change (Houghton, 2007). The main processes that control the response of the ocean and land to the anthropogenic CO_2 perturbation are briefly described in the following.

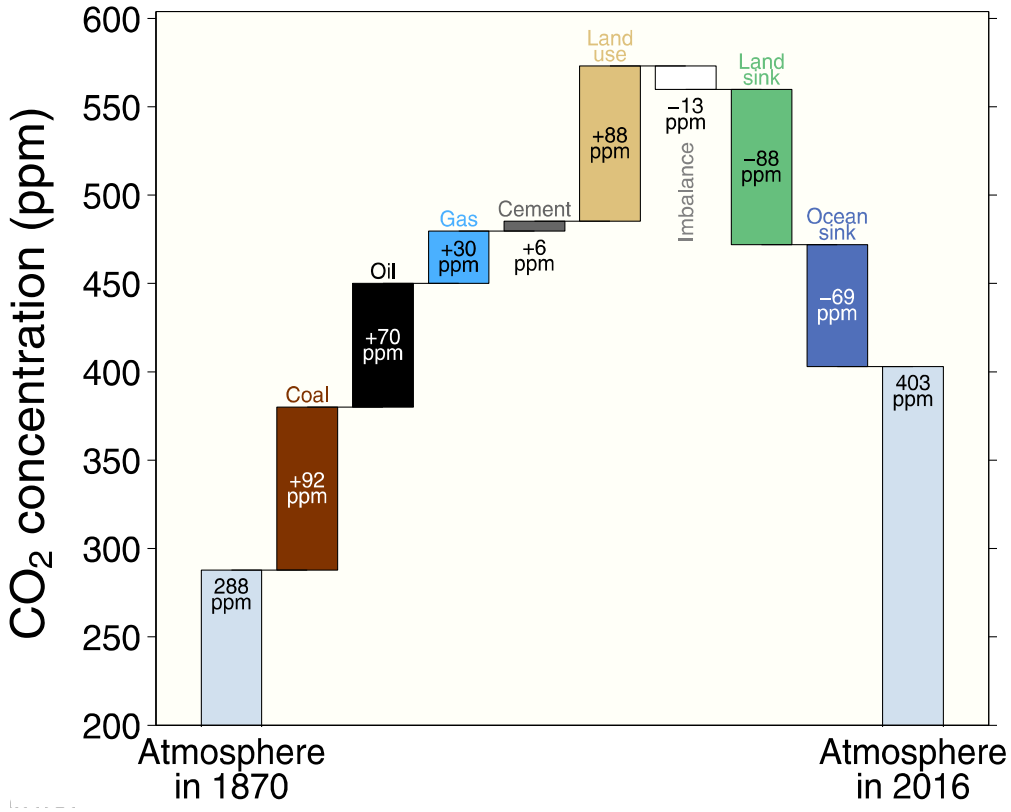

Figure 1.1: Overview of cumulative contributions to the global carbon budget from 1870 to 2016. Note that the illustrated carbon imbalance represents the knowledge gap of current carbon sources and carbon sinks. Taken from Le Quere et al. (2017, in review).

Terrestrial ecosystems take up atmospheric CO_2 through plant photosynthesis and store carbon in living organisms and soils through biotic and abiotic processes (Cias et al., 2013). Plant photosynthesis on land is affected by changes in temperature, nutrients as well as light and water availability (Prentice et al., 2001). However, as CO_2 can be one of the limiting factors for plant growth in terrestrial ecosystems, increased atmospheric CO_2 concentrations stimulate photosynthesis and thus carbon uptake. This process is known as the CO_2 fertilization effect (Mathews, 2007) and is also referred to as a negative carbon cycle feedback, because it decelerates the human-induced increase in atmospheric CO_2. This negative carbon cycle feedback has likely accounted for a considerable share of the historical land carbon sink (Friedlingstein et

al., 2006). However, at CO_2 concentrations of 800 to 1000 ppmv that are expected for the end of this century under a business-as-usual CO_2 emission scenario, the CO_2 fertilization effect is likely to be saturated (Prentice et al., 2001). Another fertilization effect is given by the increased availability of biologically active nitrogen, mainly through the production of fertilizers, which increases terrestrial net primary productivity and thus carbon storage (e.g., Houghton, 2007; Cias et al., 2013). The stored carbon on land is released to the atmosphere through respiration, including the respiration of plants, animals, and microbes (largely soil respiration) as well as through fires (Prentice et al., 2001). However, the main mechanism is soil respiration as such as if the temperature increases, the rate of soil respiration increases and thus the carbon flux from land into the atmosphere (e.g., Jenkinson et al., 1991). Hence, soil respiration functions as a positive (amplifying) climate-carbon cycle feedback.

Accordingly, anthropogenic CO_2 emissions to the atmosphere lead to both negative and positive terrestrial carbon cycle feedbacks, i.e., the biophysical effect of CO_2 helps to reduce CO_2 in the atmosphere and the warming effect of CO_2 results in a carbon flux to the atmosphere. To date, the CO_2 fertilization effect is the dominant carbon cycle feedback with the land taking up about ~ 30 % of anthropogenic CO_2 emissions (Cias et al., 2013; Le Quere et al., 2017, in review). However, it is highly uncertain whether the land will continue to be a net carbon sink for anthropogenic CO_2 emissions or if it will switch to a net source of carbon into the atmosphere later in this century (e.g., Carvalhais et al., 2014; Hagerty et al., 2014; Schimel et al., 2015).

With respect to the three carbon reservoirs that exchange carbon on timescales from sub-daily to millennia (atmosphere, land, and ocean), the ocean is by far the largest, containing about 38,000 Gt C (Cias et al., 2013). The large carbon storage potential of the ocean is well known and is due to its large volume and the slightly alkaline behavior of seawater, which enables it to keep the ionic compounds of weak acids such as carbonic acid (H_2CO_3) in solution (Volk and Hoffert, 1985; IPCC, 2005; Heinze et al., 2015).

Over the ocean the uptake of anthropogenic CO_2 occurs mainly via air-sea CO_2 fluxes that are driven by the gradient in partial pressure (pCO_2) between the atmosphere and

the ocean surface and amplified by the reaction of CO_2 with seawater (Sarmiento and Gruber, 2002).

After CO_2 has entered the air-sea interface it quickly dissociates from carbonic acid (H_2CO_3) into three main chemical species, which are cumulated as dissolved inorganic carbon (DIC) (e.g., Heinze et al., 2015). Due to the ocean's buffer factor, less than 1 % of the DIC exists as dissolved CO_2 (CO_{2aq}), about 91 % as bicarbonate ions (HCO_3^-), and about 8 % of carbonate ions (CO_3^{2-}, ~ 8 %) (Prentice et al., 2001). The chemical equilibrium between the different chemical species of DIC allows for the high solubility of CO_2 in the ocean. However, the more anthropogenic CO_2 is absorbed by the ocean the lower the amount of CO_3^{2-} becomes, which in turn decreases the buffer capacity of the ocean (Prentice et al., 2001). Further, this leads in parallel to an increase in hydrogen ions (H^+), causing a drop in ocean pH. This phenomenon has been coined as ocean acidification and has reduced ocean surface pH by about 0.1 units, relative to its preindustrial value of about 8.2 units (Caldeira and Wickett, 2006; Hofmann and Schellnhuber, 2010). If the current trend in CO_2 emissions stays unmitigated and thus continuous to follow the Representative Concentration Pathway (RCP) 8.5, which is a high CO_2 emission scenario, ocean surface pH could further decline by about 0.3 to 0.5 units until the end of this century (e.g., Bopp et al., 2013). How ocean acidification affects marine ecosystems and their services is of major concern and is currently studied intensively (e.g., IPCC, 2011).

In contrast to the rapid uptake of anthropogenic CO_2 through air-sea gas exchange at the ocean surface, the slow process of advection controls the transport of surface waters into the interior ocean. This transport of CO_2 enriched waters between the ocean surface and deeper water columns is the bottle-neck for the oceanic uptake of CO_2 (e.g., Prentice et al., 2001; Houghton, 2007). This bottle-neck has given raise to the idea of deliberately accelerating this slow natural process by directly injecting CO_2 into the deep ocean (Marchetti, 1977; see section 1.2.1).

However, the physio-chemical processes mentioned above that determine the uptake capacity of anthropogenic CO_2 and its subsequent transfer into deep ocean are referred to as the solubility pump, which acts as a strong negative feedback to

anthropogenic climate change. Yet, as anthropogenic climate change progresses, the strength of the solubility pump will very likely be weakened by positive climate feedbacks. These relate to the reduced buffer capacity of the carbonate system, the heat uptake induced increase in ocean surface temperatures that decreases the CO_2 solubility, and finally, the increase in vertical stratification, which slows down the transport of anthropogenic CO_2 into the deep ocean (e.g., Prentice et al., 2001; Cias et al., 2013).

Although physio-chemical processes (solubility pump) dominate the uptake of anthropogenic CO_2, marine biology contributes as well through the transfer of photosynthetically produced organic matter from the ocean surface to intermediate and deep waters, i.e., the biological pump (Heinze et al., 2015). The net effect of the sinking and remineralization of organic matter is the CO_2 enrichment of deeper waters when compared to the ocean surface, leading to a reduced atmospheric CO_2 concentration (Houghton, 2007). If the biological pump would be absent, it is estimated that the atmospheric CO_2 concentration would be about 30 % higher (Sarmiento, 1993). However, in contrast to the CO_2 fertilization effect on terrestrial ecosystems mentioned above, the human-induced increase in atmospheric CO_2 has no significant fertilization effect on marine biological productivity (e.g., Houghton, 2007; Körtzinger, 2010; Heinze et al., 2015).

While the positive feedbacks to anthropogenic climate change (e.g., increase in sea surface temperature and stratification) will to some extent decrease the ocean sink for CO_2 emissions, it is impossible that the ocean will transition from a carbon sink to a carbon source (e.g., Cias et al., 2013). Actually, over longer timescales (millennia), most of the anthropogenic CO_2 will end up in the ocean and eventually be neutralized by the dissolution of calcium carbonate ($CaCO_3$) sediments (e.g., Archer, 2009).

However, as the efficacy of the terrestrial and ocean carbon sink very likely decreases in the near future, more anthropogenic CO_2 will remain in the atmosphere, generating larger climate perturbations and more severe consequences for natural and human ecosystems (IPCC, 2014).

Amid the concerns about dangerous and irreversible impacts of anthropogenic climate change, scientists, engineers and policy makers and others have been searching for options that reduce the growing threat.

1.2 Motivation – What are the options to address anthropogenic climate change?

So far there have been two main options to address anthropogenic climate change: mitigation and adaptation. The most straightforward option to limit climate change is the curbing of anthropogenic greenhouse gas emissions (mitigation). Mitigation includes for example the use of new less carbon intensive technologies and renewable energies, improvement of energy efficiency, or changes of management practices or consumer behavior. Yet, in light of insufficient mitigation to prevent any climate change, some countries need to adapt to current and future impacts of climate change such as increased flood risks and sea-level rise (adaptation). However, until today mitigation success is rather low (e.g., Peters et al., 2013; Riahi et al., 2017), questioning the ability to adapt to the corresponding rather extreme climate change (Klein et al., 2014).

The Paris Agreement of 2015 has set the specific goal of limiting global warming to well below 2°C, if not 1.5°C above preindustrial levels. This target range has been chosen, because it is considered to significantly reduce the risks and impacts of anthropogenic climate change (UNFCCC, 2015). Further, the <2°C climate target is considered to ensure sustainable food production and economic development (Rockström et al., 2009; Knutti et al., 2015; Rogelj et al., 2016). To date, the National Determined Contributions (NDCs) from all countries, which outline their national post-2020 climate action plan to climate mitigation in order to meet the <2°C climate target, are the foundation of the Paris Agreement (Clemencon et al., 2016). If fully realized, the current NDCs would potentially avoid the worst effects of climate change as projected in a business-as-usual world (4-5°C), but still lead to a median warming of 2.6 to 3.1°C by the year 2100 (Rogelj et al., 2016). Hence, these pledges are inadequate to meet the agreed-upon <2°C climate target and it is therefore

questionable if conventional mitigation alone will be sufficient enough to comply with the respective target (Horton et al., 2016).

A useful metric that has been derived from observational records and models of varying complexity directly relates the primary cause of anthropogenic climate change (CO_2 emissions) to the change in global mean temperature (Allen et al., 2009; Matthews et al., 2009; MacDougall, 2016). From this transient response to cumulative carbon emissions (TCRE) it can be predicted that the total quota of CO_2 emissions from all sources (fossil fuel combustion, industrial processes and land-use change) that would comply with a 1.5°C target will be depleted in a few years at present emission rates (Knopf et al., 2017). The total quota of CO_2 emissions that would be compatible with a 2°C target is expected to be used up in the next three decades at the 2014 emissions rates (Friedlingstein et al., 2014). Consequently, the chances to reach the agreed-upon climate targets through emissions reductions alone are shrinking (Sanderson et al., 2016).

Accordingly, additional options are increasingly discussed to cope with anthropogenic climate change. Under consideration is the large-scale deliberate manipulation of the earth system, referred to as Climate Engineering (CE), Geoengineering or Climate Intervention. CE can be separated into radiation management (RM) and carbon dioxide removal (CDR) methods whereby the latter are also discussed under the term negative emission technologies.

RM methods aim to offset global warming by either causing the Earth to absorb less solar radiation (Solar Radiation Management, SRM) or by enhancing the amount of outgoing long-wave radiation into space (Long-wave Radiation Management, LRM). Accordingly, RM methods target the symptoms of anthropogenic climate change and would thus for instance leave ocean acidification unmitigated (Shepherd et al., 2009). Interested readers are referred to Rickels et al. (2011) and the National Research Council (2015a) and references therein.

CDR methods aim at the root cause of anthropogenic climate change by deliberately removing CO_2 from the atmosphere and storing it somewhere else (e.g., IPCC, 2005; Gasser et al., 2015). Over the course of the recent CE debate, the various CDR

methods can be broadly separated into three main categories. The first one includes methods that seek to sequester carbon in the terrestrial biosphere or the ocean by enhancing the natural carbon uptake mechanisms (National Research Council, 2015b). To enhance natural carbon sinks is suggested, because as mentioned above (see section 1.1), the terrestrial biosphere and ocean have already each taken up about a quarter of the anthropogenic CO_2 emissions since the onset of the industrial era (Le Quere et al., 2017, in review). Further, both of these carbon sinks have the potential to store additional carbon, although with environmental limitations (Keller et al., 2017, in review). Prominent examples of such sink enhancement methods are afforestation and reforestation, enhanced terrestrial weathering, ocean fertilization, and ocean alkalinization.

The second category entails CDR methods that engineer the CO_2 removal from the atmosphere, ocean or land and its subsequent storage (Field and Mach, 2017). Such methods are suggested because these may have smaller environmental limitations as methods of the first category (Keller et al., 2017, in review). Prominent examples include direct CO_2 air capture with storage (DACS) and seawater carbon capture and storage (National Research Council, 2015b).

The third category refers to another proposed method, bioenergy with carbon capture and storage (BECCS), which relies on both the enhancement of natural processes and technology.

None of the CDR methods mentioned above have, in a business-as-usual CO_2 emission scenario, the potential to reach the <2°C climate target, without significant impacts on land, energy, water or nutrient resources (Fuss et al., 2014; Smith et al., 2016; Williamson, 2016; Boysen et al., 2017a).

A central issue of CDR methods is the storage of the removed CO_2 in a non-atmospheric reservoir. It is still unclear if carbon storage can be created fast enough to meet the mitigation demands that are compatible with the agreed-upon <2°C climate target. Consequently, also temporary carbon storage sites have been investigated (Scott et al., 2015). Such storage sites could be especially of interest in regions where CCS into geological formations proves unpractical (Israelsson et al., 2009). Further,

carbon cycle feedbacks, saturation effects and outgassing of carbon may particularly limit the effectiveness of CDR (Vichi et al., 2013; Fuss et al., 2014; Tokarska and Zickfeld, 2015).

However, the idea of artificially increasing oceanic carbon uptake goes already back into the year 1977. Cesare Marchetti, coining the term geoengineering in the context of climate change, investigated direct CO_2 injection into the deep ocean. The idea has received some attention in the following years (e.g., Hoffert et al., 1979; Orr et al., 2001; IPCC, 2005), but is currently prohibited by the London Protocol and the Convention for the Protection of the Marine Environment of the North East Atlantic (OSPAR Convention) (Leung et al., 2014). However, ocean fertilization measures are considered to be too limited with respect to their potential and ocean alkalinity management measures are considered to be limited by their operational cost (e.g., Renforth et al., 2013). Accordingly, revisiting the idea of direct CO_2 injection into the deep ocean could become an unavoidable option in the light of insufficient emissions reductions.

This dissertation assesses the potential and risks of direct CO_2 injection with a focus on i) its effectiveness (leakage vs. C-cycle feedbacks), ii) its potential to meet stringent climate targets, and iii) its role in the context of climate policies. The following subsections provide more insight on direct CO_2 injections and state the specific research questions that are addressed in this dissertation.

1.2.1 Direct CO_2 injection into the deep ocean

Direct CO_2 injection into the deep ocean refers to the idea of deliberately accelerating the oceanic uptake of atmospheric CO_2 (Marchetti, 1977), which occurs naturally, albeit at a relatively slow rate limited by the sluggish overturning circulation (see section 1.1).

As illustrated in Figure 1.2 this ocean carbon sequestration method includes i) the capture of CO_2 from large point sources such as coastal power plants or direct air

capture facilities, ii) the transport of the captured CO_2 via pipeline or ship to the injection site(s), and iii) the direct injection of CO_2 into the deep ocean.

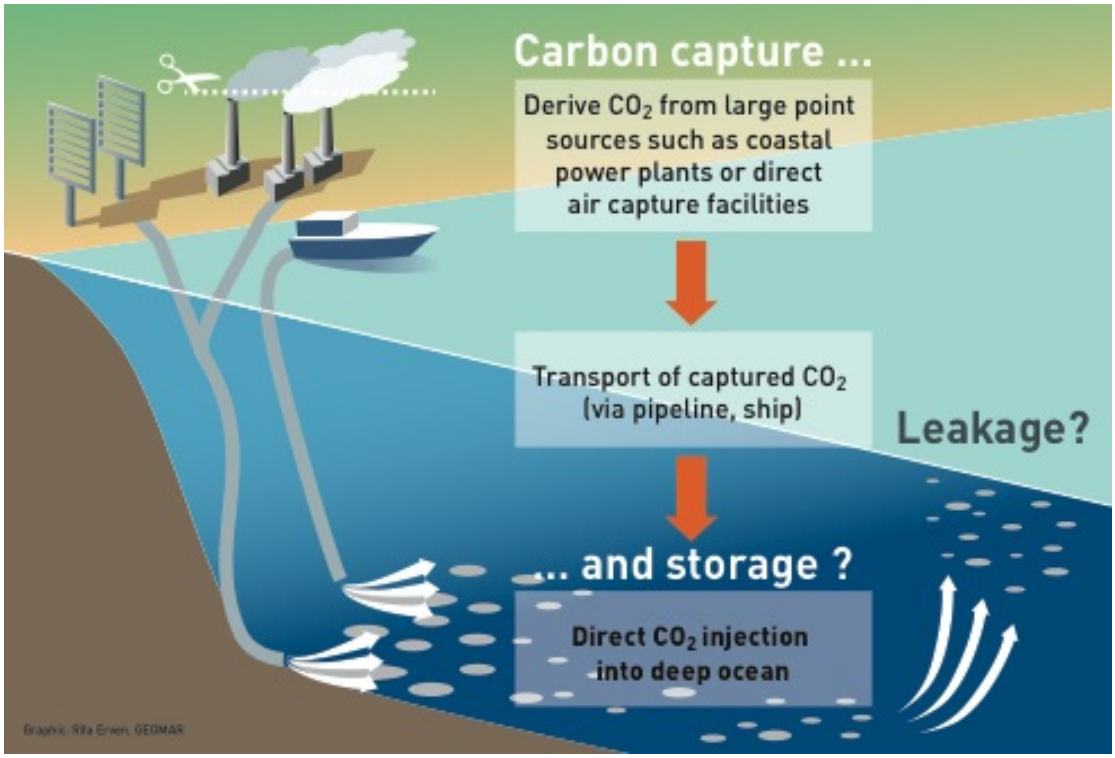

Figure 1.2: Schematic diagram of direct CO_2 injections into the deep ocean.

On millennial timescales, 65-80 % of anthropogenic CO_2 is estimated to be absorbed by the ocean through air-sea-gas exchange at the ocean surface and by its subsequent transport into the deep ocean. On timescales of tens to hundreds of millennia, this amount eventually increases to 73-93% through the neutralization of acidified water masses with $CaCO_3$ sediments (e.g., Archer et al., 2005; Zeebe, 2012). Direct injection could potentially accelerate this natural process by directly depositing CO_2 in deep waters, some of which stay isolated from the atmosphere for hundreds of thousands of years (DeVries and Primeau, 2011; their Figure 12), and by bringing it in closer contact with $CaCO_3$ sediments. Accordingly, direct CO_2 injection into the deep ocean would prevent anthropogenic CO_2 from having an effect on the climate in the near future, and speed up eventual and nearly permanent removal through the chemical reaction with $CaCO_3$ sediments (Archer et al., 1998; Archer, 2009). However, this is

completely different from just avoiding CO_2 emissions, because the injected CO_2 has been added to the carbon-cycle and may leak out of the ocean and influence the climate as well as other carbon cycle pathways. The effectiveness of this method is determined by the fraction of injected CO_2 that remains in the ocean. Analysis of ocean observations and model simulations agree that the effectiveness increases with deeper injection (e.g., Orr, 2004; IPCC, 2005)

Although the carbon sequestration potential of the ocean is well-known (e.g., Sarmiento and Toggweiler, 1984; Volk and Hoffert, 1985; Sabine et al., 2004), direct CO_2 injections into the deep ocean is as mentioned above currently prohibited. This legal ban is associated with the concern that deep-sea ecosystems such as cold-water corals and sponge communities would be harmed by rapid pH reductions, at least in the vicinity of the injection site(s) (e.g., IPCC, 2005; Schubert et al., 2006; Gehlen et al., 2014).

However, as stressed by Keeling (2009) and Ridgewell et al. (2011) there are trade-offs between injection-induced harms in the deep ocean and benefits at the ocean surface through a reduction in atmospheric pCO_2 and an accompanied decrease in surface ocean acidification. Such trade-offs should be carefully evaluated and compared to other mitigation options, that likely all imply offsetting local harm against global benefits.

1.2.2 Why simulate direct CO_2 injection into the deep ocean?

Currently, international legislation (London Protocol etc.) prohibits the injection of CO_2 into the ocean. This leaves numerical simulations as the only feasible approach to study the effectiveness of large scale CO_2 injection into the ocean (e.g., Orr, 2004), but also to quantify the intensity of local harm (at the injection sites), and the potential of global benefit (mitigation of surface ocean acidification). Most likely, CO_2 would be injected into the deep ocean. Waters there can remain isolated from the atmosphere for hundreds to thousands of years, depending on the injection site and depth. Studying the fate of injected CO_2 hence naturally involves long timescales and global

spatial scales, which again can only be meaningfully studied by numerical simulations. Further, global warming is expected to change the intensity of ocean circulation. Hence, the long-term fate of injected CO_2 in a changing future ocean can only be quantified by means of global ocean models.

In previous modeling studies of ocean CO_2 injection, relatively simple 1-D vertical box models (e.g., Hoffert et al., 1979) and 3-D global ocean circulation models (Orr, 2004) have been used with the focus on the effectiveness of direct CO_2 injection as well as injection-related changes in ocean chemistry (e.g., Orr et al., 2001; Orr 2004; Jain and Cao, 2005; IPCC, 2005; Ridgwell et al., 2011). The use of 1-D vertical box models for simulating direct CO_2 into the deep ocean, however, does not allow for an estimation of the effectiveness of different injection sites, because the injected CO_2 will spread with the global overturning circulation. The position of the injection sites relative to the outcrop of the density horizon to which CO_2 was injected will affect its residence time. Conversely, 3-D ocean models describe the ocean circulation in three dimensions and can hence be used to investigate the dependence of injection sites and –depth upon the effectiveness (Orr, 2004). However, ocean-only models used in earlier studies did not have a land component and hence did not include a fully coupled carbon cycle. Accordingly, such models could not explore the influence of oceanic and terrestrial carbon cycle feedbacks on the effectiveness of direct CO_2 injections. This is of importance because a more comprehensive assessment of the carbon sequestration and mitigation potential of direct CO_2 injection also requires accounting for the changes in all ambient carbon fluxes (Mueller et al., 2004; Vichi et al., 2013).

The conducted investigations in this dissertation (see section 1.3) are based on an Earth System Model of intermediate complexity (EMICs) with a fully coupled carbon cycle and also state-of the art Integrated Assessment Models (IAMs).

EMICs close the gap between the simplest and the most complex climate models (Claussen et al., 2002). EMICs are complex enough to simulate essential climate processes and feedbacks, however, they usually compromise on the complexity of one or more climate model component, e.g., the atmosphere. However, processes that

operate within the Earth System on very long timescales such as the burial and dissolution of carbonate sediments and terrestrial weathering can only be integrated by EMICs (Eby et al., 2013). The primary advantage of EMICs when compared to more complex models is due to the fact that simulations are several orders of magnitude faster and can be conducted on standard computers. Accordingly, such models are ideally suited for investigating direct CO_2 injections into the deep ocean on long timescale (see section 1.3)

A comprehensive assessment of direct CO_2 injection into the deep ocean also requires its integration in the context of respective climate policies. Common tools for such investigations are Integrated Assessment Models (IAMs), which couple the economy and the climate system. Scientific simulations in Earth System models such as in the study of Reith et al. (2017, see Chapter 2) are based on determined paths of CO_2 injection, neglecting therefore socioeconomic feedbacks like less emission reductions as response to ocean CO_2 injection or more CO_2 injection to compensate for outgassing. Accordingly, comprehensive assessment of direct CO_2 injection into the deep ocean requires accounting also for the non-carbon cycle feedbacks. However, state-of-the-art climate models are too computationally expensive to be used in economic analyses so that IAMs use simplified representations of the physical climate system, including the global carbon cycle (Glotter et al., 2014). An important issue with respect to direct CO_2 injections is the suitability of carbon cycle models applied in IAMs to capture the outgassing of injected CO_2 as well as carbon cycle feedbacks. Only a few carbon cycle models used in IAMs are capable of simulating these effects. Carbon cycle models that rely on empirically derived impulse response representations of the (oceanic) carbon cycle are not suitable, because those do not allow to keep track of carbon removed into other reservoirs and outgassing of sinks. While impulse response representations can capture non-linarites in the evolvement of atmospheric carbon, box-type representations become indispensable if options like direct CO_2 injections are considered under accounting for carbon-cycle feedbacks. However, box-type models suitable to be included in IAMs can only mimic the various complex processes of the global carbon cycle. For that reason, the investigation of CO_2 injection into the ocean in IAMs serves two mutually dependent

research challenges: i) accounting for socio-economic feedbacks as response to CO_2 injection into the deep ocean and ii) investigating how well the major feedbacks and saturation effects of the carbon cycle are captured in the rather simple box-type models used in IAMs.

1.3 Chapter synopsis and author contributions

Chapter 2 presents a modeling study that investigates the long-term response of the atmospheric, oceanic and terrestrial carbon reservoirs to the targeted atmospheric carbon reduction through direct CO_2 injection into the deep ocean. Previous studies have not considered carbon cycle and climate feedbacks between the atmosphere and the terrestrial carbon reservoir, because the models used did not have a land component. However, including these additional feedbacks is important, because simulations of other oceanic carbon sequestration methods have demonstrated that backfluxes from the terrestrial biosphere can partly offset oceanic carbon uptake and thus prevent the targeted atmospheric carbon reduction from being achieved (Oschlies et al., 2010).

For that purpose, the University of Victoria Earth System Climate Model (UVic model) of intermediate complexity with a fully interactive carbon cycle is used to simulate direct CO_2 injection into the deep ocean as a measure of emissions mitigation during the Representative and Extended Concentration Pathway (RCP/ECP) 8.5.

Following Orr et al. (2001) in the configuration of the CO_2 injection scenarios, three different sets of injection experiments with different injection depths (800m, 1500m, and 3000m) are conducted to simulate a continuous 100-year injection of CO_2 at seven injection sites with individual injection rates (0.1 Gt C yr^{-1} per site). At the end of the injection period, the simulations continue in order to follow global carbon cycle dynamics for another 900 years. In additional parameter perturbation simulations, the strength of the default terrestrial photosynthesis CO_2 fertilization parameterization is varied by ± 50 %. This allows for a better understanding of how differences in the

response of the terrestrial biosphere influence the targeted atmospheric carbon reduction. Accordingly, Chapter 2 addresses two main research questions:

- How do carbon cycle feedbacks and backfluxes affect the effectiveness of ocean carbon injection and thus the targeted atmospheric carbon reduction of 70 Gt C?
- How do variations of the default CO_2 fertilization parameterization alter the response of the terrestrial biosphere to the targeted atmospheric carbon reduction?

With respect to our experimental set-up the analyses reveal that the response of the carbon cycle during and after the CO_2 injections is dominated by the partial outgassing of injected CO_2 and a reduced rate of air-sea gas exchange when compared to the control simulation without injection. The models terrestrial ecosystems respond to the injections and reduced atmospheric CO_2 concentration through a decreased CO_2 fertilization effect and a temperature related decrease in soil respiration. Accordingly, we find that carbon cycle feedbacks and backfluxes in both land and ocean carbon reservoirs decrease the targeted atmospheric carbon reduction of 70 Gt C by 16 to 30 %. The targeted atmospheric carbon reduction in the parameter perturbation simulations is found to be 0.2 and 2 % more at the end of the injection period and about 9 % less to 1 % more at the end of the simulations. Furthermore, we observe that the ocean unexpectedly took up carbon after direct CO_2 injections are stopped in some of the experiments, which is caused by an ocean deep convection event in the Southern Ocean.

The results of the study demonstrate how challenging the attribution of carbon fluxes and accounting for injected CO_2 might be in the real Earth system. Further, the findings stress the importance of accounting for all carbon fluxes in the global carbon cycle and not only for those of the manipulated reservoir in order to obtain a comprehensive assessment of direct CO_2 injection into the deep ocean in particular and also marine carbon sequestration in general.

This chapter is based on the paper: Reith, F., Keller, D. P., and Oschlies, A. (2016): *Revisiting ocean carbon sequestration by direct injection: a global carbon budget perspective*, Earth Syst. Dynam., 7, 797-812, doi: 10.5194/esd-7-797-2016. F.R., A.O., and D.P.K. conceived and designed the experiment. F.R. implemented and

performed the experiments and analyzed the data. F.R. wrote the manuscript with contributions from D.P.K. and A.O..

Chapter 3 presents a modeling study that is the first one to assess the feasibility as well as the associated biogeochemical impacts of direct CO_2 injection as a measure to close the gap between the CO_2 emissions and climate impacts of the RCP/ECP 4.5 CO_2 emission scenario and the 1.5°C climate target. Accordingly, three conceptually different approaches for applying direct CO_2 injection at 3000 m water depth are simulated using the UVic model: The first approach assumes that all CO_2 emissions of the RCP/ECP 4.5 are injected after the model-predicted global mean temperature of 1.5°C is exceeded for the first time, the second one injects an amount of CO_2 such that global mean temperature does not rise well beyond 1.5°C, and the third approach injects an amount of CO_2 in order to closely follow the atmospheric CO_2 concentration of the RCP/ECP 2.6. All idealized approaches are designed to reach and maintain the 1.5°C climate target on a millennium timescale. In additional sensitivity runs, this study investigates the effect of $CaCO_3$ sediment feedbacks and continental weathering on the cumulative CO_2 injections and on the biogeochemical impacts in each approach. Respectively, Chapter 3 addresses the following research questions:

- How much CO_2 would have to be injected into the deep ocean in order to reach and maintain the 1.5°C climate target on a millennium timescale?
- Are there trade-offs between potential benefits at the ocean surface (e.g., reduced warming and acidification) and injection-related harms in the intermediate and deep ocean?
- How do sediment/weathering feedbacks influence the required cumulative CO_2 injections and the injection-related biogeochemical impacts?

Our analyses reveal that it would not be sufficient enough to inject all CO_2 emissions of the RCP/ECP 4.5 (964 Gt C in total) after a global mean temperature of 1.5°C has been exceeded for the first time. Accordingly, we find that about 600 Gt C more (62 %) would have to be injected in order to reach and maintain the 1.5°C climate target on a millennium timescale. However, this required mass includes an outgassed CO_2 amount of about 602 Gt C that needs to be re-injected in order to sustain the

respective climate target. With respect to the injection-related biogeochemical impacts, we observe that the pH in the upper ocean volume is increased by about 0.13 to 0.18 units, relative to the control simulation. Further, this increase leads to a significant increase in potential coral reef habitat size when compared to the control run. However, these benefits come at the expense of strongly acidified water masses of up to -2.37 units in the vicinity of the injection sites, which illustrates the trade-off between the ocean surface and the intermediate and deep ocean. With respect to the sensitivity runs, we observe that $CaCO_3$ sediment and terrestrial weathering feedbacks reduce the required CO_2 injections that comply with the 1.5°C climate target on a millennium timescale by about 11 %. Further, we find that the inclusion of $CaCO_3$ sediment/weathering feedbacks leads to the highest benefit in the upper ocean and the lowest harm in the intermediate and deep ocean.

Chapter 3 demonstrates the huge mass of CO_2 that would need to be injected into the deep ocean in order to reach and maintain the 1.5°C climate target under the RCP/ECP 4.5 on a millennium timescale. Further, it illustrates that direct CO_2 injections into the deep ocean results in a trade-off between local harm and global benefit, which would need to be carefully evaluated if this method would be seriously considered.

Chapter 3 is based on a manuscript in preparation by: Reith, F., Koeve, W., Keller, D. P., Getzlaff, J., and Oschlies, A. (2017). F.R. and W.K. conceived and designed the experiments. F.R. implemented the experiments with contributions from W.K. and J.G.. F.R. performed the experiments and analyzed the data. F.R. wrote the manuscript with contributions from W.K., D.P.K., J.G., and A.O..

Chapter 4 presents a study that assesses how well carbon cycle feedbacks are represented in carbon-cycle models used in state-of-the-art integrated assessment models (IAMs). Therefore, direct CO_2 injection into the deep ocean is integrated in an economic inter-temporal optimization model as proxy for ocean-based CDR measures. Such an approach allows for the derivation of optimal CO_2 injection trajectories which go beyond previous assessments because we account for i) the change in atmospheric CO_2 in response to the CO_2 injections into the deep ocean and

ii) the potential extra amount of CO_2 injections needed to compensate for the outgassed fraction.

For that purpose, we use the most recent version of the Dynamic Integrated Climate-Economy model (DICE2016R) and consider different climate objectives: i) a-cost-benefit framework with an endogenous level of climate change, ii) a cost-effectiveness framework with an exogenous level of climate change, as given by the 2°C climate target, and iii) a cost-effectiveness framework with an exogenous level of climate change to be reached at some date in the future (i.e. an overshooting target given by reaching the 2°C in the year 2100). In addition, we analyze how the results change if we replace the carbon cycle model of DICE2016R with the carbon cycle model from its previous version, i.e., DICE2013R or with the carbon cycle model from the recent IAM by Gerlagh and Liski (2017). In order to validate this integrated assessment of direct CO_2 injection as proxy for ocean-based CDR methods, the derived atmospheric carbon and global mean temperature trajectories are implemented in the UVic model.

With respect to the experimental set-up, Chapter 4 addresses the following research question:

- How well are carbon cycle feedbacks represented in the different box-type carbon cycle models used in DICE2016R?
- How strong is the substitution effect between emission reduction and deep-ocean carbon injection in the different climate policy frameworks?
- How do carbon cycle feedbacks affect the optimal amount of deep-ocean carbon injection?

The analyses reveal that DICE2016R has significantly improved compared to DICE2013R, because it captures the long-term outgassing of injected CO_2 into the deep ocean as well as the related increase in global mean temperatures. However, this improvement comes with the expense of a small near-term remaining emission budget, when compared to the UVic model, which limits the accurate assessment of low emission scenarios. As a consequence, the 2°C climate target in DICE2016R cannot be achieved without negative emissions through CDR. With respect to

DICE2013R, we find that direct CO_2 injection is close to geological storage, because the model assumes a rather slow exchange between the different carbon reservoirs. Furthermore, the strongest carbon cycle feedbacks are observed in the carbon cycle model by Gerlagh and Liski (2017). The substitution effect clearly differs between the different climate objective frameworks. Whereas in the cost-benefit framework, CDR via deep-ocean carbon injection is utilized rather as long-term strategy to accelerate the otherwise slow natural decline in atmospheric carbon concentration, CDR is already required before the year 2050 if compliance with the 2°C goals in a cost-effectiveness framework is to be achieved. In contrast to previous studies, we quantify the extra amount of CDR required to compensate for carbon cycle induced feedbacks, showing that the presence of this feedbacks result in more CDR given that the CDR cost function is sufficiently flat. Overall, the findings of this study show that the assessment of direct CO_2 injections and more generally CDR seems to be sensible in such an integrated assessment framework, although Earth system models should be used for validation in order to enable a more robust derivation of policy recommendations.

This chapter is based on a submitted manuscript to the science journal Earth's Future and is currently under review: Rickels, W., Reith, F. Keller, D. P., Oschlies A., and Quaas, M. F. (2017): *Integrated Assessment of Carbon Dioxide Removal*. W.R. and F.R. conceived and designed the experiments. W.R. implemented and performed the experiments with the Integrated Assessment Models. F.R. implemented and performed the experiments with the UVic-model. W.R. and F.R. analyzed the data. W.R. and F.R. wrote the manuscript with contributions from D.P.K., A.O. and M.F.Q..

2 Revisiting ocean carbon sequestration by direct injection: a global carbon budget perspective

This chapter is based on the paper 'Revisiting ocean carbon sequestration by direct injection: a global carbon budget perspective' published in the journal Earth System Dynamics.
Citation: Reith, F., Keller, D. P., and Oschlies, A.: Revisiting ocean carbon sequestration by direct injection: a global carbon budget perspective, Earth Syst. Dynam., 7, 797-812. Accepted Author Manuscript. doi: 10.5194/esd-7-797-2016, 2016.

Abstract. In this study we look beyond the previously studied effects of oceanic CO_2 injections on atmospheric and oceanic reservoirs and also account for carbon cycle and climate feedbacks between the atmosphere and the terrestrial biosphere. Considering these additional feedbacks is important since backfluxes from the terrestrial biosphere to the atmosphere in response to reducing atmospheric CO_2 can further offset the targeted reduction. To quantify these dynamics we use an Earth system model of intermediate complexity to simulate direct injection of CO_2 into the deep ocean as a means of emissions mitigation during a high CO_2 emission scenario. In three sets of experiments with different injection depths, we simulate a 100-year injection period of a total of 70 Gt C and follow global carbon cycle dynamics over another 900 years. In additional parameter perturbation runs, we varied the default terrestrial photosynthesis CO_2 fertilization parameterization by ± 50 % in order to test the sensitivity of this uncertain carbon cycle feedback to the targeted atmospheric carbon reduction through direct CO_2 injections. Simulated seawater chemistry changes and marine carbon storage effectiveness are similar to previous studies. As expected, by the end of the injection period avoided emissions fall short of the targeted 70 Gt C by 16–30 % as a result of carbon cycle feedbacks and backfluxes in both land and ocean reservoirs. The target emissions reduction in the parameter perturbation simulations is about 0.2 and 2 % more at the end of the injection period and about 9 % less to 1 % more at the end of the simulations when compared to the unperturbed injection runs.

An unexpected feature is the effect of the model's internal variability of deep-water formation in the Southern Ocean, which, in some model runs, causes additional oceanic carbon uptake after injection termination relative to a control run without injection and therefore with slightly different atmospheric CO_2 and climate. These results of a model that has very low internal climate variability illustrate that the attribution of carbon fluxes and accounting for injected CO_2 may be very challenging in the real climate system with its much larger internal variability.

2.1 Introduction

Anthropogenic CO_2 emissions have perturbed the natural carbon cycle (Archer et al., 2009). With an average of 8.6 ± 0.4 Gt C yr^{-1} emitted from fossil-fuel burning and 0.8 ± 0.5 Gt C yr^{-1} from land-use change in the last decade (2003–2013) (Le Quéré et al., 2014), global CO_2 emissions have continuously increased by about 2.5 $\%yr^{-1}$ (Friedlingstein et al., 2014). This trend continues to follow slightly above the trajectory of the highest emission scenario of the latest IPCC report (see Sect. 2.2.2), which makes it very difficult to keep global warming within the political 2°C guardrail (Peters et al., 2013), not to mention recent agreements to seriously consider an even more ambitious 1.5°C goal (UNFCCC, 2015). The limited success in reducing or even slowing down the increase in anthropogenic emissions through global climate accords (Rogelj et al., 2010) has led to renewed interest in engineering measures that are intended to reduce atmospheric CO_2 concentrations (e.g., Shepherd, 2009).

Marchetti (1977) proposed directly injecting CO_2 into the deep ocean, thus accelerating the oceanic uptake of atmospheric CO_2, which happens naturally via invasion and subsequent dissolution of CO_2 into the surface waters, albeit at a relatively slow rate limited by the sluggish ocean overturning circulation. On timescales of thousands of years, however, this will result in most anthropogenic CO_2 ending up in the deep ocean. The idea behind direct CO_2 injection is to speed up this slow natural process by directly depositing CO_2 in deep waters, some of which remain

isolated from the atmosphere for hundreds to thousands of years (DeVries and Primeau, 2011; their Fig. 12), thereby preventing the CO_2 from having an effect on the climate in the near future. This is fundamentally different from just avoiding emissions because the CO_2 has still been added to the carbon cycle and may leak out of the ocean and affect the climate and other carbon cycle pathways.

Over millennial timescales carbon from direct injection can simply be viewed as "delayed" emissions, in terms of its climatic effect and fate, since the carbon cycle will eventually reach a chemical equilibrium (mainly an equilibrium between the oceanic and atmospheric carbon reservoirs, although carbonate compensation and weathering feedbacks start acting on time scales longer than 5000 years; e.g., Zeebe, 2012). However, on decadal to centennial timescales, carbon that is sequestered via direct injection cannot simply be treated as delayed emissions because the injected carbon must take fundamentally different pathways than those of carbon that is emitted directly into the atmosphere. Since these pathways operate on many different timescales and are partially controlled by climate feedbacks, it takes a considerable amount of time until the carbon cycle and climate reach the same state as if the emissions had just been delayed. This is because injecting CO_2 changes ocean chemistry internally and, thus, will at some point affect ocean carbon uptake or outgassing and hence the atmospheric CO_2 concentration: when water with chemical properties altered by the injection reaches the surface, the air–sea exchange of CO_2 is fundamentally altered compared to a situation where the carbon was just emitted into the atmosphere at a later date. By sequestering carbon in the ocean instead of emitting it into the atmosphere, one would also inadvertently change terrestrial carbon cycling compared to the situation where the carbon was emitted with some delay.

Because direct injection of CO_2 is presently in conflict with the London Protocol and the Convention for the Protection of the Marine Environment of the North East Atlantic (OSPAR Convention) (Leung et al., 2014), and also because of the long timescales and global scales involved, models are ideally suited for investigating this method (Orr, 2004). Modelling studies are also safer than actual experiments because the rapid changes in seawater chemistry that could occur if direct CO_2 injections were tested might potentially harm marine ecosystems. These risks

may be especially high for deep-sea benthic environments such as cold-water corals and sponge communities, which are adapted to special living conditions and thus may have a low capacity to acclimatize to rapid pH changes in their environment (e.g., IPCC, 2005; Schubert et al., 2006; Gehlen et al., 2014). In previous studies, relatively simple box models (e.g., Hoffert et al., 1979) and first-generation global ocean circulation models (Orr, 2004) were employed, focusing on the residence time of the injected CO_2 (i.e., effectiveness), as well as on changes in ocean chemistry (e.g., Orr et al., 2001; Orr, 2004; Jain and Cao, 2005; IPCC, 2005; Ridgwell et al., 2011).

However, a more comprehensive assessment of the carbon sequestration and climate mitigation potential of direct injection also requires accounting for the changes in all ambient carbon fluxes resulting from carbon cycle and climate feedbacks (Mueller et al., 2004; Vichi et al., 2013).

In this study, which follows Orr et al. (2001) in the configuration of the CO_2 injection scenarios, we use an Earth system model of intermediate complexity and fully interactive carbon cycle to simulate the direct injection of CO_2 into the deep ocean at different depths under a high CO_2 emission scenario. Our main objective is to assess the long-term response of the atmospheric, oceanic and terrestrial carbon pools to the targeted atmospheric reduction through a continuous 100-year injection of CO_2 at seven offshore sites with individual injection rates (0.1 Gt C yr^{-1} each) that are small compared to today's global CO_2 emissions. Although previous studies (e.g., Orr et al., 2001; Orr, 2004) have looked at the effects of CO_2 injections on atmospheric and oceanic reservoirs, the carbon-cycle and climate feedbacks between the atmosphere and the terrestrial biosphere were not considered in those studies because the models used did not have a land component. Considering these feedbacks is important since simulations of other oceanic carbon sequestration methods have shown that backfluxes from the terrestrial biosphere to the atmosphere can partially offset any oceanic C uptake (Oschlies et al., 2010).

However, since the future strength of terrestrial carbon cycle feedbacks, such as the CO_2 fertilization effect, is of uncertain magnitude as atmospheric CO_2 changes (e.g., Matthews, 2007; IPCC, 2013; Hajima et al., 2014), we also conduct parameter

perturbation simulations, in which the default CO_2 fertilization parameterization of the terrestrial photosynthesis model is varied by ±50 %. This allows us to better understand how differences in the response of the terrestrial biosphere affect the targeted atmospheric carbon reduction during direct CO_2 injections. For our injection simulations we use a well-calibrated model that conserves carbon globally, features the pelagic carbonate chemistry and is run under a business-as-usual emission scenario. The model and emission forcing used are identical to the ones in the climate engineering modeling study by Keller et al. (2014)

2.2 Methodology

2.2.1 Model description

The model used is version 2.9 of the University of Victoria Earth System Climate Model (UVic ESCM). It consists of four dynamically coupled components: a three-dimensional general circulation ocean model (Pacanowski, 1996), a dynamic–thermodynamic sea-ice model (Bitz and Lipscomb, 1999), a terrestrial model (Meissner et al., 2003), and a one-layer atmospheric energy–moisture balance model (based on Fanning and Weaver, 1996). All components have a common horizontal resolution of 3.6° longitude x 1.8° latitude. The oceanic component has 19 vertical levels, with thicknesses ranging from 50 m near the surface to 500 m in the deep ocean. Formulations of the air–sea gas exchange and seawater carbonate chemistry are based on the Ocean Carbon Cycle Model Intercomparison Project (OCMIP) abiotic protocol (Orr et al., 1999). The terrestrial model of vegetation and carbon cycles is based on the Hadley Center model TRIFFID (e.g., Matthews, 2007). A more detailed description of the UVic model version used here is given in Keller et al. (2012) and Eby et al. (2013).

2.2.2 Experimental design

The model has been spun-up for 10 000 years under preindustrial atmospheric and astronomical boundary conditions and run from 1765 to 2005 using historical fossil-fuel and land-use carbon emissions (Keller et al., 2014). From the year 2006 to 2100 the model is forced with CO_2 emissions following the Representative Concentration Pathway (RCP) 8.5, which is a business-as-usual high CO_2 emission scenario. Subsequently, simulations follow the Extended Concentration Pathway (ECP) 8.5 emission scenario until the year 2500 (Meinshausen et al., 2011). Thereafter, we keep emissions constant at 1.48 Gt C yr^{-1} until the end of the simulations in year 3020. Note that non-CO_2 greenhouse gases and anthropogenic aerosol forcing agents as well as emissions from land-use change are not considered in our simulations.

Continental ice sheets, volcanic forcing and astronomical boundary conditions are held constant to facilitate the experimental setting and analyses (e.g., to prevent confounding feedback effects) (Keller et al., 2014). Parameterized geostrophic wind anomalies, which are a first-order approximation of dynamical feedbacks associated with changing winds in a changing climate (Weaver et al., 2001), are also applied.

Simulated CO_2 injections into different ocean regions are based on the Ocean OCMIP carbon sequestration protocols (see Orr et al., 2001; Orr 2004) to facilitate comparison of our model results to those of Orr et al. (2001) and Orr (2004). For simplicity, we simulate the injection of CO_2 in an idealized manner by adding CO_2 directly to the dissolved inorganic carbon (DIC) pool (Orr et al., 2001), thus neglecting any gravitational effects and assuming that the injected CO_2 instantaneously dissolves into seawater and is transported quickly away from the injection point and distributed homogeneously over the entire model grid box with lateral dimensions of a few hundred kilometers and many tens of meters in the vertical direction. Consequently, the formation of CO_2 plumes or lakes as well as the potential risk of fast rising CO_2 bubbles are neglected (IPCC, 2005; Bigalke et al., 2008). Furthermore, we do not investigate the effect of $CaCO_3$ sediments feedbacks in our experiments, although the dissolution of $CaCO_3$ sediments near or downstream of an

injection site is expected to reduce outgassing and increase the residence time of the injected CO_2 (Archer et al., 1998).

To track the physical transport of the injected CO_2 and its transport pathways from the individual injection sites, injected carbon is added to seven site-specific diagnostic marker tracers. At the sea surface, we assume that these tracers have an instantaneous gas exchange with the atmosphere, i.e., as soon as the injected carbon reaches an ocean surface grid box, the value of the marker tracer in this surface ocean grid box is set to zero. The residence time of the injected CO_2 computed from this tracer approach (i.e., fraction retained, see below) thus, provides a conservative estimate of carbon stored to carbon injected, as it is unlikely that all of the injected carbon would instantly leave the ocean upon reaching a depth of 50 m. Furthermore, the fraction retained is not affected by changes in the Revelle factor related to the invasion of anthropogenic CO_2 into the ocean.

In all of our injection simulations we subtract the amount of injected CO_2 from the emissions forcing, thus keeping the total global carbon inventory the same as in the respective control simulation without CO_2 injection. For the purpose of assessing how all ambient carbon fluxes affect the storage lifetime of the injected CO_2, it is essential to have the same carbon inventory in all of our simulations. Following Orr et al. (2001) and Orr (2004), seven injection sites are located in individual grid boxes near the Bay of Biscay (42.3° N, 16.2° W), New York (36.9° N, 66.6° W), Rio de Janeiro (27.9° S, 37.8° W), San Francisco (31.5° N, 131.4° W), Tokyo (33.3° N, 142.2° E), Jakarta (11.7° S, 102.6° E) and Mumbai (13.5° N, 63° E) (Fig. 2.1). Starting in the year 2020, the experimental simulations consist of two periods: (1) an initial 100-year period of simultaneous 0.1 Gt C yr^{-1} injections and (2) a continuation of the model simulations until the year 3020 after stopping the injections at the end of year 2119. Separate injection (I) experiments following this protocol are conducted at three different depths: 850 m (*I-800*), 1600 m (*I-1500*), and 2900 m (*I-3000*). Hereafter, these are referred to as *With Emissions* simulations.

Following previous studies (e.g., Jain and Cao, 2005; Ridgwell et al., 2011), additional simulations are conducted to investigate how climate-change-induced

feedbacks affect the fate of injected CO_2. These simulations follow the same protocols described above but with anthropogenic emissions forcing set to zero from the year 2020 until the end of the simulations (year 3020). Hereafter, these extreme scenarios are referred to as *Complete Mitigation* simulations. Note that since these simulations are forced with historical emissions and the RCP 8.5 scenario until the year 2020, the model is not in steady state in 2020 and some climatic change occurs.

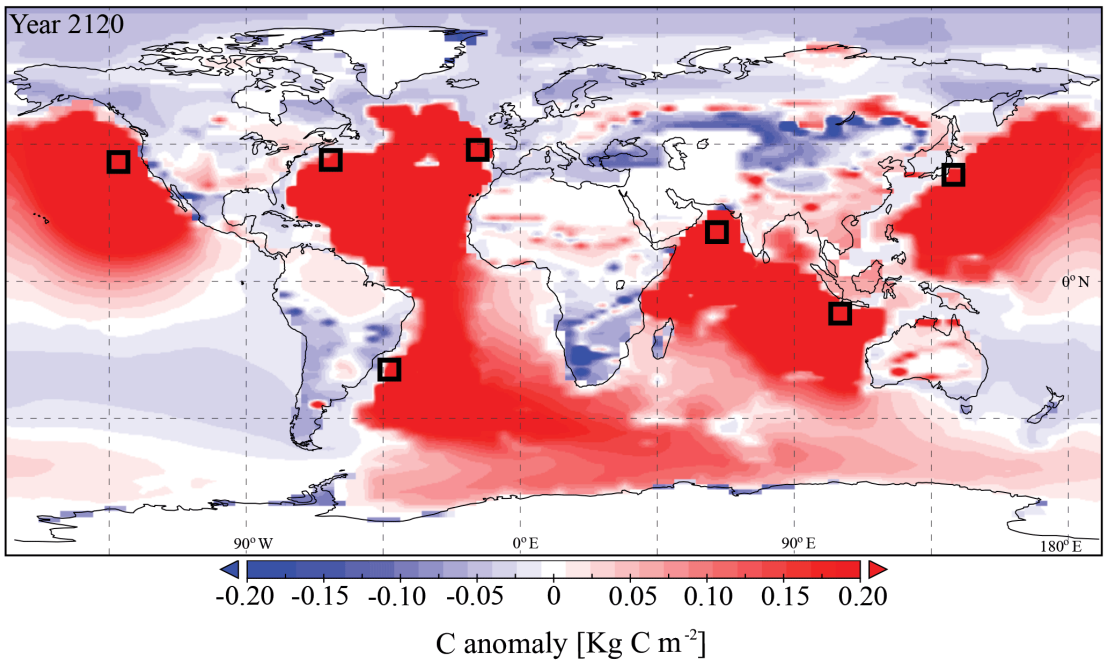

Figure 2.1: Absolute changes in oceanic and land carbon between I-3000 and the RCP 8.5 control run (I-3000 simulation minus RCP 8.5 control run) at the end of the injection period (year 2120). The black rectangles represent the locations of the seven injection sites, where the injections occurred in the center of the black rectangles.

Also, because the injected CO_2 is withdrawn from the atmosphere so that total carbon is conserved, the *Complete Mitigation* injection runs essentially have negative emissions of 0.7 Gt C yr^{-1}.

To determine how long the injected carbon stays in the ocean, we follow the IPCC (2005) and calculate a fraction retained ($FR = M_o \cdot M_i^{-1} \cdot 100$), which is the percentage ratio between the total mass of the injected carbon that remains in the ocean (M_o, determined using the diagnostic marker tracer) and the total cumulative mass injected into the ocean (M_i) since the start of the injection period (year 2020).

This metric accounts for the injected carbon atoms and does not include possible adjustments of fluxes of other carbon in the Earth system.

To assess the global carbon cycle response to the injections, we use another metric, the net fraction stored ($netFS = \Delta C_{ocean} \cdot M_i^{-1} \cdot 100$, in %), which measures total carbon reservoir changes. The *netFS* is defined as the ratio between the absolute change in globally integrated total oceanic carbon (ΔC_{ocean}), relative to the *RCP 8.5 control* run, and the total cumulative mass injected into the ocean (M_i) since the start of the injection period. In contrast to *FR*, which counts only the injected carbon atoms, *netFS* accounts for all potential feedbacks of carbon fluxes into and out of the ocean in response to the injection of CO_2 into the ocean.

To investigate if the targeted atmospheric carbon reductions in the *With Emissions* simulations differ from what would happen if CO_2 was never emitted (avoided emissions) or first emitted and subsequently removed from the atmosphere, e.g., via technology such as direct air capture (see Sect. 2.3.4.1) (Lackner, 2009) with subsequent safe and permanent storage, presumably in geological reservoirs, we performed another simulation where the atmospheric CO_2 concentration was 0.7 Gt C yr^{-1} less than in the *RCP 8.5 control* run between the years 2020 and 2120. Hereafter, this simulation is referred to as the *Direct Air Capture* run.

As mentioned in the introduction, this modelling study of direct CO_2 injection into the deep ocean is the first one to include a land component in order to assess, in addition to the atmospheric and oceanic carbon reservoirs, the long-term response of the terrestrial carbon pool to the targeted atmospheric carbon reduction through direct CO_2 injections. Since there is a significant amount of uncertainty in how the terrestrial system responds to changing atmospheric CO_2 concentrations (Friedlingstein et al., 2006), we have chosen to conduct several simulations with different terrestrial parameter values, i.e., a perturbed parameter study, to better understand how the terrestrial system could potentially respond to and affect the carbon cycle during deep ocean CO_2 injections. The parameterization that we investigate is the CO_2 fertilization effect. The process of CO_2 fertilization is thought to stimulate terrestrial carbon uptake (e.g., Matthews, 2007). This negative carbon cycle feedback results in reduced

atmospheric CO_2 concentrations and has likely accounted for a substantial portion of the historical terrestrial carbon sink (Friedlingstein et al., 2006). Accordingly, it has direct relevance for the future trajectory of atmospheric CO_2 (IPCC, 2013) and thus for our targeted atmospheric carbon reduction of 70 Gt C by the year 2120. However, the future strength of CO_2 fertilization in response to changing CO_2 is highly uncertain (e.g., Friedlingstein et al., 2006; Arora et al., 2013; Jones et al., 2013; Schimel et al., 2015). In order to better quantify the role of CO_2 fertilization in the targeted atmospheric carbon reduction in the *With Emissions* simulations (Sect. 2.3.5), we vary the CO_2 fertilization parameterization following the approach of Matthews (2007). Thereby, we scale the CO_2 sensitivity of the terrestrial photosynthesis model by ± 50 % (CO_2 fertilization is high/low) for repeated simulations that are otherwise identical to the *RCP 8.5 control* and *I-800* and *I-3000* runs. These variations scale the default strength of an increase in atmospheric CO_2 relative to preindustrial levels that is used to calculate all processes in the canopy and leaf routines within the terrestrial photosynthesis model, leading to a respective increase or decrease in terrestrial gross primary productivity. This is achieved by adding the multiplicative parameter "CO_2_fert_scale" in the routine of the photosynthesis model and setting it to 1.5 for an increase of the CO_2 fertilization effect and to 0.5 for a respective decrease.

Hereafter, the perturbed *control* runs are referred to as *RCP 8.5 control*$_{CO2\_fert\_high}$ and *RCP 8.5 control*$_{CO2\_fert\_low}$. The perturbed injections runs are denoted as *I-800* $_{CO2\_fert\_high}$, *I-800*$_{CO2\_fert\_low}$, *I-3000* $_{CO2\_fert\_high}$ and *I-3000*$_{CO2\_fert\_low}$. We did not perform an *I-1500* run because an ocean deep convection event that occurred after the injection period (see Sect. 2.3.4.2) would make it too difficult to evaluate the results. No additional spin-up is needed; since the CO_2 fertilization effect only happens when atmospheric CO_2 concentration begins to increase, e.g., from the preindustrial period onward.

An overview of all conducted simulations with their anthropogenic forcing is shown in Table 2.1.

Table 2.1: Overview of all conducted simulations and their anthropogenic forcing. "X" denotes that the respective forcing is applied. WE: With Emissions; CM: Complete Mitigation.

Simulation	Anthropogenic forcing					
	RCP 8.5 CO_2 emission scenario		Extended RCP 8.5 CO_2 emission scenario	Constant CO_2 emisions of 1.48 Gt C yr^{-1}	Continuous CO_2 injections into deep ocean of 0.7 Gt C yr^{-1}	Gt C yr^{-1} continuously subtracted from CO_2 emissions
	2006–2020	2006–2100	2100–2500	2500–onwards	2020–2120	2020–2120
RCP 8.5 control run of WE simulations		X	X	X		
I-800 WE		X	X	X	X	X
I-1500 WE		X	X	X	X	X
I-3000 WE		X	X	X	X	X
RCP 8.5 control run of CM simulations*	X					
I-800 CM	X				X	X
I-1500 CM	X				X	X
I-3000 CM	X				X	X
Direct air capture run		X	X	X		X
RCP 8.5controlCO_2_fert_high		X	X	X		
I-800CO_2_fert_high		X	X	X	X	X
I-3000CO_2_fert_high		X	X	X	X	X
RCP 8.5 controlCO_2_fert_low		X	X	X		
I-800CO_2_fert_low		X	X	X	X	X
I-3000CO_2_fert_low		X	X	X	X	X

*After the year 2020, CM simulations continue without CO_2 emissions until 3020.

2.3 Results and Discussion

2.3.1 RCP 8.5 control simulation

The physical climate and biogeochemical cycles of the Earth system during the *RCP 8.5 control* simulation are in the same state as described in Keller et al. (2014). Here, we briefly describe global carbon cycling during the control simulation so that comparisons can be made to the *With Emissions* simulations (Sect. 2.3.4). Subsequently, we briefly outline the global carbon cycling of the perturbed *control* runs *RCP 8.5 control*$_{CO2\_\ fert\_high}$ and *RCP 8.5 control*$_{CO2\_\ fert\_low}$ for comparing these simulations to the unperturbed *control* run and the respective injection experiments (Sect. 2.3.5).

By the end of the simulation in the year 3020, about 6000 Gt C have been added to the global carbon cycle. Consequently, atmospheric CO_2 has increased substantially in the *RCP 8.5 control* run, leading to a total atmospheric carbon content of about 4620 Gt C at the end of the simulation (Figs. 2.2 a and A1 in Supplement A).

By the end of the extended *RCP 8.5 control* run about 58 % of the emitted CO_2 remains in the atmosphere. The rest of the carbon has been taken up by oceanic and terrestrial reservoirs (Figs. 2.2 e, i). Oceanic carbon uptake is highest during the first few decades of the simulation, when emissions are highest, and then decreases thereafter (Fig. 2.2 c). In particular, the decrease in net oceanic carbon uptake is caused by a reduction in the ocean buffering capacity (Prentice et al., 2001), leading to a decrease in ocean carbon uptake even under increasing atmospheric CO_2 levels, a response also seen in other model simulations (Zickfeld et al., 2013).

Simulated terrestrial carbon uptake is initially high as well, but then declines rapidly, with the terrestrial reservoir becoming a source for atmospheric carbon in the year 2139 before leveling off at very little net exchange between the terrestrial

reservoir and the atmosphere after about year 2280 (Fig. 2.2 g). The initial increase in total land carbon uptake is due to the simulated CO_2 fertilization effect on vegetation (Matthews, 2007). However, as temperatures become higher, terrestrial net primary productivity (NPP) is reduced due to water stress. Moreover soil respiration increases with temperature until it eventually becomes the dominant processes, leading to a net loss of carbon from the terrestrial reservoir to the atmosphere. Projections of future net terrestrial carbon uptake or loss processes are highly uncertain (Carvalhais et al., 2014; Hagerty et al., 2014; van der Sleen et al., 2014; Sun et al., 2014), which is also reflected in the large variability between the CMIP5 (Coupled Model Intercomparison Project Phase 5) model results, with changes in terrestrial carbon budgets ranging from -0.97 to +2.27 Gt C yr^{-1} between 2006 and 2100 (Ahlström et al., 2012).

As expected, simulated terrestrial carbon uptake is higher in the *RCP 8.5 control*$_{CO2\_fert\_high}$ simulation because NPP is higher (not shown), when compared to the standard *RCP 8.5 control* run, resulting in a percentage increase in terrestrial carbon of about 5 % in the year 2120 and of about 3 % at the end of the simulation (Figs. 2.2 i, j). However, terrestrial carbon uptake declines more rapidly than in the *control* run, which is due to a faster saturation of the CO_2 fertilization effect as well as higher soil respiration. Consequently, the terrestrial biosphere switches to a stronger net carbon source about 20 years earlier (year 2121) before leveling off at very little net exchange between the terrestrial reservoir and the atmosphere after about year 2280 as occurring in the standard *control* run (Fig. 2.2 i).

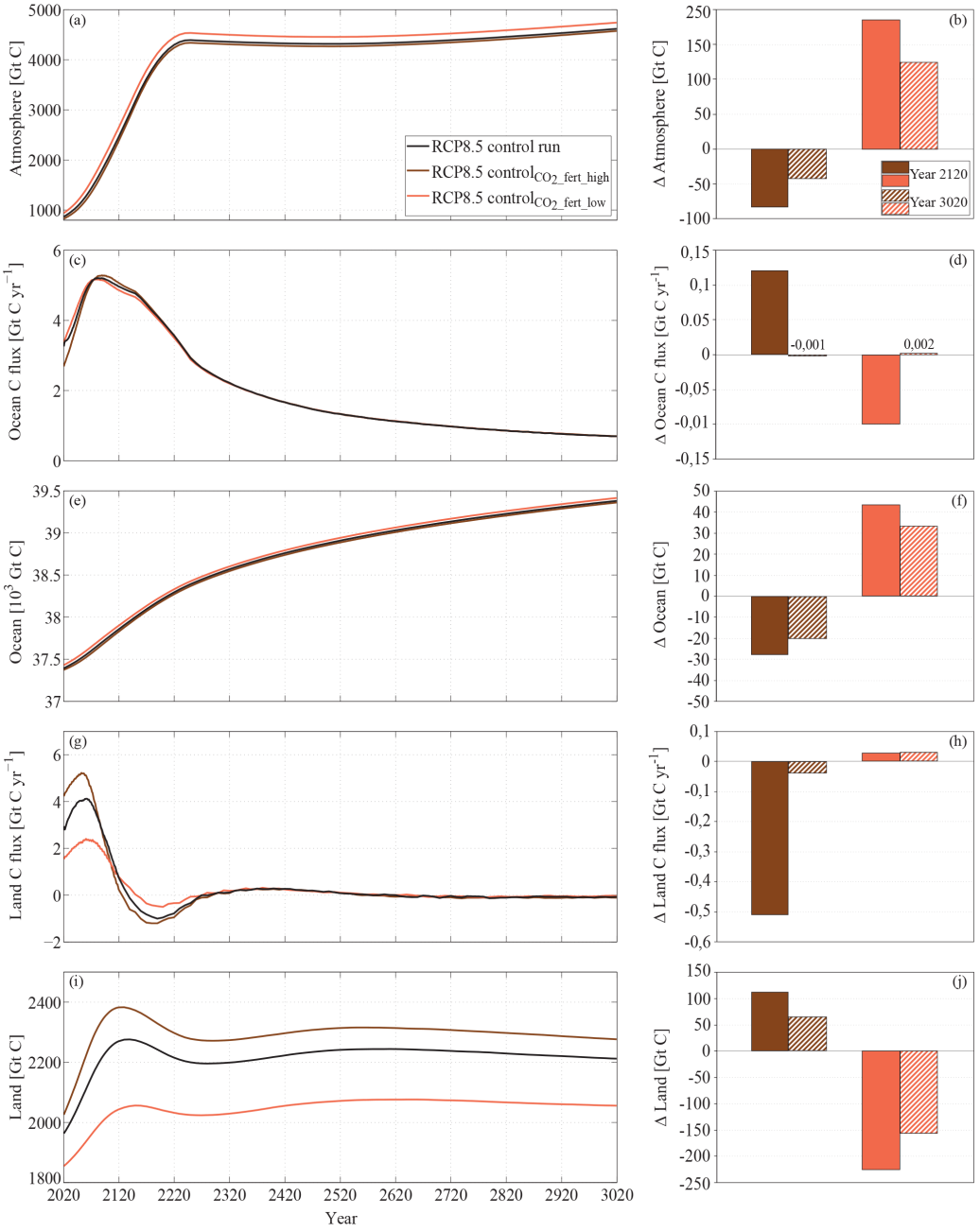

Figure 2.2: Globally integrated carbon of the RCP 8.5 control run, the RCP 8.5 control$_{CO2_fert_high}$ and RCP 8.5 control$_{CO2_fert_low}$ for **(a)** total atmospheric carbon, **(c)** carbon flux from atmosphere to ocean, **(e)** total oceanic carbon, **(g)** carbon flux from atmosphere to land and **(i)** total land carbon. Difference in carbon between the RCP 8.5 control$_{CO2_fert_high}$ (brown) (RCP 8.5 control$_{CO2_fert_low}$, orange) and the RCP 8.5 control run (perturbed control runs minus RCP 8.5 control run) for the years 2120 (filled) and 3020 (hashed) for **(b)** globally integrated total atmospheric carbon, **(d)** globally integrated carbon flux from atmosphere to ocean, **(f)** globally integrated total oceanic carbon, **(h)** globally integrated carbon flux from atmosphere to land and **(j)** globally integrated total land carbon.

Accordingly, the atmospheric carbon concentration in the *RCP 8.5 control*$_{CO2\_fert\_high}$ is lower when compared to the *RCP 8.5 control* run, although the trends are similar (Figs. 2.2 a, b). Compared to the extended *RCP 8.5 control* run, the extended *RCP 8.5 control*$_{CO2\_fert\_high}$ ends with about 1 % less atmospheric carbon (Figs. 2.2 a, b). The lower atmospheric carbon content in the *RCP 8.5 control*$_{CO2\_fert\_high}$, caused by the higher CO_2 fertilization effect, leads initially to a reduced carbon flux from the atmosphere to the ocean (Fig. 2.2 c). By the year 2075, the carbon flux from the atmosphere to ocean is slightly higher when compared to the *control* run, as the carbon flux from atmosphere to land starts to decrease with increasing CO_2 emissions (Figs. 2.2 d, g). Thus, total oceanic carbon in the *control*$_{CO2\_fert\_high}$ run stays below that of the *control* run with a percentage decrease of about 0.07 % at the year 2120 and about 0.05 % at the end of the simulation (Figs. 2.2 e, f).

Global carbon cycling in the *RCP 8.5 control*$_{CO2\_fert\_low}$ shows a similar response, although of opposite sign and higher magnitude (Fig. 2.2), which is for instance reflected in a percentage decrease in total land carbon of about 10 % in the year 2120 and about 7 % at the end of the simulation when compared to the *control* run (Figs. 2.2 i, j). This is caused by the decreased CO_2 fertilization effect, which results in less NPP and thus in lower soil respiration.

2.3.2 Changes in seawater chemistry

Here, we compare the *With Emissions* simulations to the *RCP 8.5 control* run to assess injection-related seawater chemistry changes. By the final year of the injection period (year 2119), a total of 10 Gt C is injected at each site (Fig. 2.1). The respective increases in DIC and reductions in pH depend on how quickly the injected carbon is transported away from the injection sites by local ocean currents and mixing (see Orr, 2004). Our model-predicted changes in DIC and pH at the injection sites (relative to the *control* run) are within the range of Orr (2004) (Tables A1, A2 in Supplement A).

Simulated ocean surface pCO_2 is lower in the CO_2 injection runs because of lower atmospheric CO_2 levels and the related decrease in air–sea carbon fluxes, which

results in lower surface DIC concentrations and a slightly higher surface pH (by 0.008–0.01 units compared to the *control* run).

2.3.3 Fractions retained

Here, we assess to which extent the simulated CO_2 injections are effective in keeping the injected carbon out of the atmosphere. This is described by the *FR*s. The global *FR*s of our *Complete Mitigation* and *With Emissions* simulations (Table 2.2) are within the full range of the (GOSAC)–OCMIP results (Orr et al., 2001; Orr, 2004). The simulated *FR* (Table 2.2) increases with the depth of injection because it generally takes longer for deeper waters to come into contact with the atmosphere again, as also shown in previous studies (e.g., Caldeira et al., 2001; Orr et al., 2001; Orr, 2004; Jain and Cao, 2005).

By comparing the *With Emissions* and *Complete Mitigation* simulations at all depths, we can determine how climate change affects *FR*. As in previous studies, our results show that *FR* is enhanced by climate change (Jain and Cao, 2005; Ridgwell et al., 2011). In the *With Emissions* simulations, values of *FR* are always higher than in the *Complete Mitigation* runs (Table 2.2). For *I-800* and *I-1500*, the *FR* increase due to climate change is largest in the Pacific, whereas for *I-3000*, Atlantic sites show the highest *FR* increase due to a larger ocean response to climate change (Table 2.2). However, in all simulations more of the injected carbon is retained in the Pacific compared to injections in other ocean basins.

We also assess whether the enhanced *FR* in our *With Emissions* simulations are affected by changes in the Atlantic Meridional Overturning Circulation (AMOC). Relative to preindustrial period, which has a maximum AMOC intensity of 15.98 Sv, we find AMOC decreases by 8, 29, 40 and 34 % in the years 2020, 2120, 2520 and 3020, respectively, in the *With Emissions* simulations. AMOC in the *Complete Mitigation* simulations, relative to preindustrial period, shows smaller decreases of about 7.6, 21, 8.6 and 8.6 % in the years 2020, 2120, 2520 and 3020, respectively. These differences partially explain why *FR* is enhanced in the *With Emissions*

simulations, since a reduced AMOC slows the transport of deep water masses and prolongs the time until they come into contact with the atmosphere again. As in other climate change studies (e.g., Doney, 2010; Bopp et al., 2013), we also find an increase in ocean stratification (not shown) in all respective basins in our *With Emissions* runs, relative to the *Complete Mitigation* runs, which has also led to reduced vertical mixing (Prentice et al., 2001) and increased *FR*. In contrast to Jain and Cao (2005), who found a higher *FR* mainly in the Atlantic, we find a higher *FR* in all basins (Table 2.2). This difference is likely related to the higher degree of climate change in our simulations since we use a higher CO_2 emissions scenario.

Table 2.2: Comparison of fractions retained (FR) between Orr et al. (2001), Orr (2004) (full range of their global efficiency, which is the same as the FR defined in Sect. 2.2.2 and is based on seven ocean general circulation models (OGCMs) and one zonally averaged model result) and our Complete Mitigation (CM) and With Emissions (WE) simulations for all injection sites (Global) and on an inter-basin level for the Atlantic sites (Bay of Biscay, New York, Rio de Janeiro), the Pacific sites (San Francisco, Tokyo) and the Indian sites (Jakarta, Mumbai). The FR values (%) are given for the last year of the injections (2119), 500 years after the simulations started (2519) and for the last year of the simulations (3019). For each entry of the table, numbers to the left of the vertical bars denote results of the CM runs, numbers to the right results of the WE runs. Note that the illustrated years refer to our simulations, ranging from the year 2020 until the year 3020. The GOSAC–OCMIP simulations started in the year 2000 and ended in the year 2500 (Orr et al., 2001).

Overview of FR (%)		I-800			I-1500			I-3000		
		Year								
		2119	2519	3019	2119	2519	3019	2119	2519	3019
Full range (Orr et al., 2001; Orr, 2004)		65–84	15–38	–	81–96	32–57	–	97–100	49–93	–
CM | WE	Global	68 | 75	17 | 30	8 | 17	92 | 5	40 | 56	20 | 35	99 | 100	65 | 76	38 | 54
	Atlantic sites (70° N, 35° S)	53 | 64	9 | 20	5 | 11	85 | 91	30 | 46	16 | 28	97 | 99	62 | 75	37 | 54
	Pacific sites (65° N, 35° S)	78 | 81	27 | 45	13 | 29	97 | 98	61 | 77	34 | 55	99 | 100	86 | 93	59 | 75
	Indian sites (20° N, 35° S)	80 | 84	17 | 29	6 | 14	96 | 97	34 | 49	13 | 25	99 | 100	50 | 65	20 | 34

Model-predicted *FR* (Table 2.2) refers to the injected CO_2 alone (as accounted for by the diagnostic marker tracer) and does not account for how global carbon cycle feedbacks affect net ocean carbon storage. By comparing *FR* and *netFS* (see Sect.

2.2.2) for the *With Emissions* simulations, we find that net ocean C sequestration is less efficient than would be predicted from *FR* alone (Fig. 2.4 a) because of carbon cycle and climate feedbacks (Fig. 2.1). For *I-3000*, *netFS* is about 16 % lower than *FR* at the end of the injection period (Table 2.2, Fig. 2.4 a).

These results show the importance of accounting for carbon cycle feedbacks when assessing the effectiveness of marine CO_2 injections. Interestingly, an exception occurs for the *I-1500* simulation from the last year of the injection period with a Southern Ocean deep convection event during which the ocean temporarily takes up more carbon than would be expected from the injections alone (Figs. 2.4 a, c, d). This event and its implications for carbon accounting are discussed in more detail in Sect. 2.3.4.2.

2.3.4 Response of the Global Carbon Cycle

Here we first briefly show how the atmospheric carbon reduction, relative to the *RCP 8.5 control* run (see Sect. 2.3.1), differs between *With Emissions* simulations and the *Direct Air Capture* run. Subsequently, we investigate how carbon cycle and climate feedbacks affect the distribution of carbon between different reservoirs upon injection of CO_2 in the *With Emissions* simulations. To do so, we look at the absolute changes in carbon between the *With Emissions* simulations and *RCP 8.5 control* run during and after the injection period. Finally, we show how the perturbed injection runs, in which we scaled the default CO_2 fertilization parameterization of the terrestrial photosynthesis model (Sect. 2.2.2), affect the targeted atmospheric carbon reduction as well as the other carbon reservoirs and fluxes in *I-800* and *I-3000* of the *With Emissions* simulations.

2.3.4.1 Response during injection period

In the *With Emissions* simulations and the *Direct Air Capture* run, the "globally injected carbon" denotes the targeted atmospheric carbon reduction. The globally injected carbon – in the absence of leakage and backfluxes – equals the oceanic carbon addition or atmospheric CO_2 removal of 70 Gt C by the last year of the injection period (year 2119). As presented in Figures 2.3 and 2.4b, the atmospheric carbon reduction during the injection period of the *With Emissions* simulations diverges quickly from the globally injected carbon trajectory.

This is explained by injected carbon leaking from the ocean back to the atmosphere and the response of atmosphere-to-land and atmosphere-to-ocean fluxes to the reduction in atmospheric carbon. The rapid divergence even for the deepest injection points where *FR* is high, points to carbon cycle and climate feedbacks, which are directly related to changes in atmospheric CO_2 concentrations (i.e. ocean-atmosphere pCO_2 differences and CO_2 fertilization effects) and changes in temperature. Other studies have also shown that these feedbacks occur and affect the size of the global carbon reservoirs (Arora et al., 2013). The curve progression of the atmospheric reduction in the *Direct Air Capture* run is very similar for *I-1500* and *I-3000*, which is due to the occurrence of most of the same carbon cycle and climate feedback mechanisms. However, due to no carbon injections in the *Direct Air Capture* run, the atmospheric reduction is higher as soon as injected carbon starts leaking in the *With Emissions* simulations as presented in Figure 2.3.

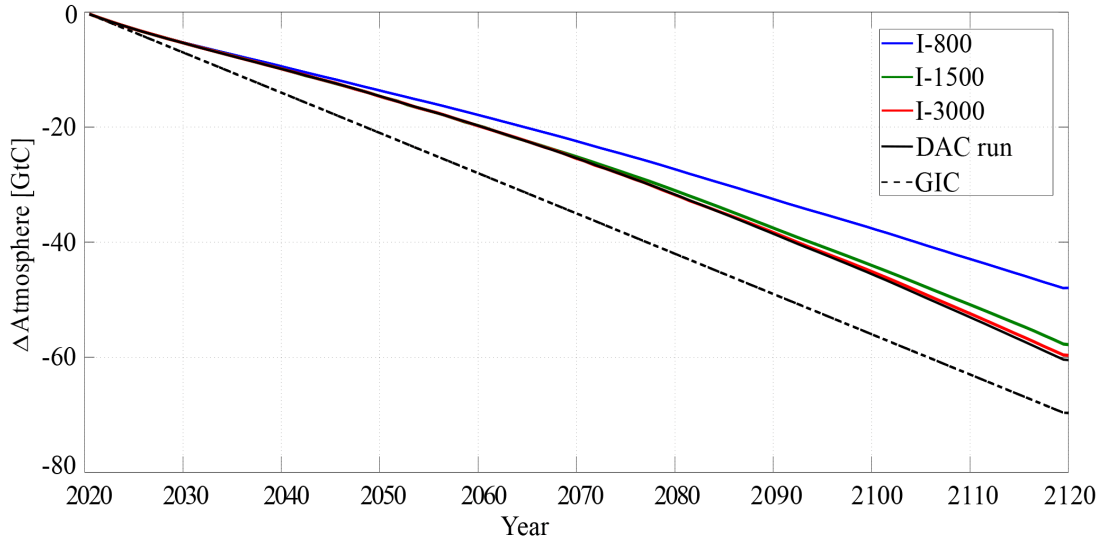

Figure 2.3: Absolute change in atmospheric carbon in the Direct Air Capture run (DAC) and in the With Emissions simulations, relative to the RCP 8.5 control run. The black dashed line denotes the globally injected carbon (GIC), which is subtracted from the emission forcing (see Sect. 2.2.2).

In the UVic model (version 2.9), the atmospheric carbon reduction of the *Direct Air Capture* run (Fig. 2.3) can also be referred to as the true atmospheric carbon reduction target. Depending on depth of injection, this implies further that direct injection of CO_2 would not be able be 100 % efficient and provide 100 % of the true atmospheric reduction target on decadal to centennial timescales (Fig. 2.3). Due to the occurrence of an ocean deep convection event in the *Direct Air Capture* run after the year 2120 (see Sect. 2.3.4.2), we cannot easily compare the *Direct Air Capture* run to the *With Emissions* simulations after the injection period.

While ocean feedbacks in response to CO_2 injection and reduced atmospheric CO_2 levels have been discussed extensively in previous studies (e.g. Orr, 2004; IPCC, 2005; Ridgwell et al., 2011), we here additionally consider land feedbacks with the purpose of accounting for the entire Earth system's response to potential marine CO_2 injections.

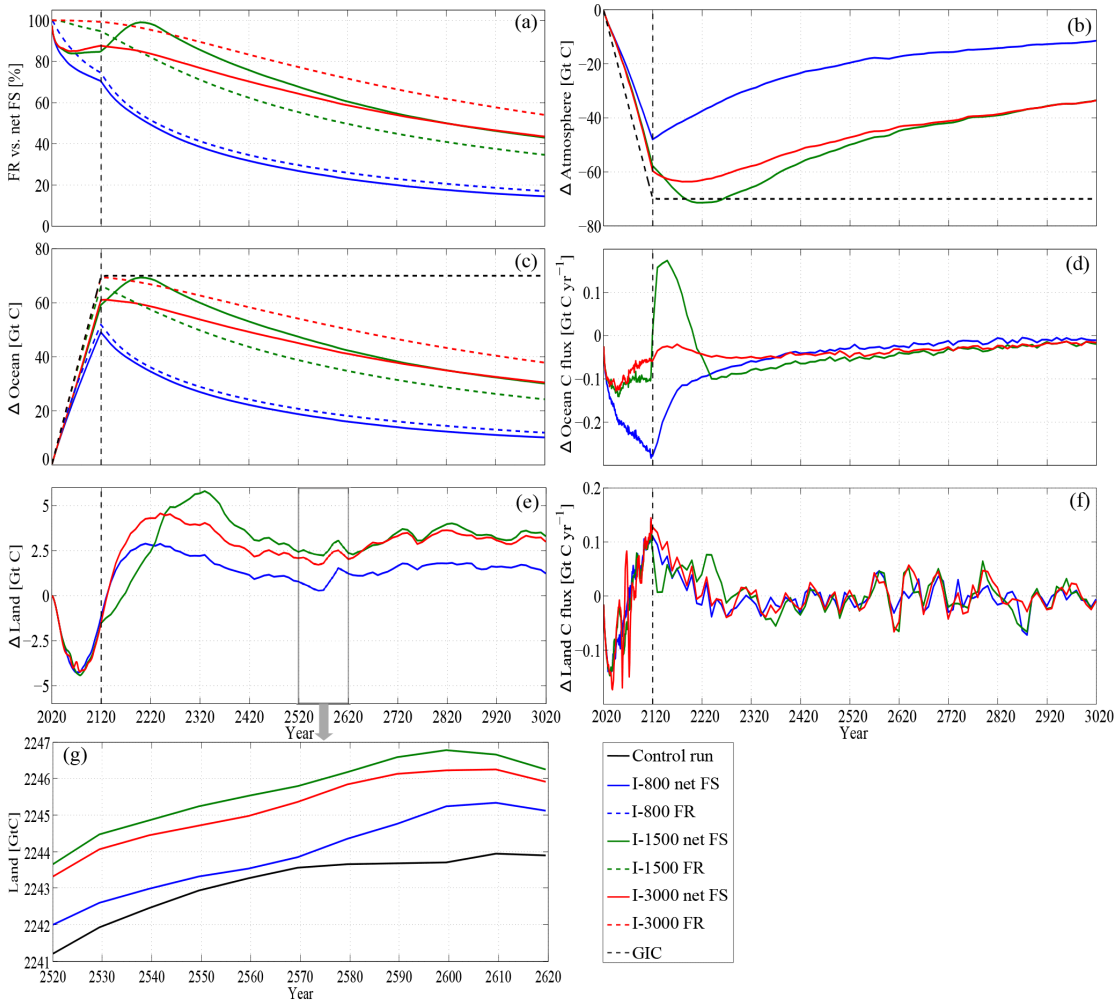

Figure 2.4: **(a)** Comparison of the fractions retained (FR, dashed) and the net fractions stored (netFS, solid) of the With Emissions (WE) simulations. Absolute changes in carbon between the WE simulations and the RCP 8.5 control run (WE simulations minus RCP 8.5 control run) for **(b)** globally integrated total atmospheric carbon, **(c)** globally integrated total oceanic carbon, **(d)** globally integrated carbon flux from atmosphere to ocean, **(e)** globally integrated total land carbon, **(f)** globally integrated carbon flux from atmosphere to land, and **(g)** absolute values of globally integrated total land carbon of the WE simulations and the RCP 8.5 control run from the year 2520 to 2620. The globally injected carbon is denoted as GIC. The vertical dashed black lines indicate the end of the injection period.

By the last year of the injection period (year 2119), *I-800* shows the highest divergence from globally injected carbon (Fig. 2.4 c) with an atmospheric carbon reduction of only 48 Gt C, which is 22 Gt C less than targeted. Since it is known from the marker tracer that 25 % (i.e. 17.8 Gt C) of the injected CO_2 leaked to the atmosphere (Table 2.2), C-cycle and temperature feedbacks must be responsible for the other 4.2 Gt C that remained in the atmosphere. This remaining amount can partially be explained by the reduced pCO_2 difference between the atmosphere and

the ocean, which leads to a smaller carbon flux into the ocean (Fig. 2.4 d). Plus, relative to the *control* run, there is a lower atmosphere-to-land carbon flux until approximately the year 2075 (Fig. 2.4 f), leading to 1.2 Gt C less total land carbon by the end of the injections (Fig. 2.4 e). After the injections start (year 2020), both NPP and soil respiration are lower in *I-800* than in the *control* run, leading to a maximum reduction in land carbon of about 4.2 Gt C in year 2075 (Fig. 2.4 e). Thereafter, total land carbon in *I-800* increases. By the end of the injections in year 2120, the terrestrial carbon pools have taken up 1.2 Gt C less than the *control* run without CO_2 injection.

Roughly similar patterns are found for injection simulations *I-1500* and *I-3000* during the injection period, although with less outgassing occurring for the deeper injections (Fig. 2.4 c), which led to a slightly larger reduction in terrestrial carbon uptake by the last year of the injection. Thus, the largest reduction in total atmospheric carbon with 60 Gt C was found for *I-3000*, followed by *I-1500* with 58 Gt C by the end of the injection period (Fig. 2.4 b).

Our results suggest that the terrestrial response due to the atmospheric carbon reduction is mainly governed by the reduced CO_2 fertilization effect on NPP and the temperature-related decrease in soil respiration. Carbon cycle-climate feedbacks on land occur because the reduced atmospheric CO_2 concentration in the *With Emissions* simulations (Fig. 2.4 c) leads to a cooling in the global mean soil temperature by about 0.08°–0.1°C in the year 2119 relative to the *control* simulation, with the lowest reduction for *I-800* and the highest one for *I-3000*. Both fertilization and temperature feedbacks on the terrestrial biosphere act simultaneously, although our results indicate that the reduced CO_2 fertilization effect, which in current models is the largest terrestrial carbon cycle feedback (Schimel et al., 2015), is the dominant one until the maximum reduction in land carbon around year 2075. Thereafter, the decrease in soil respiration leads to an increase in land carbon and becomes the dominant feedback.

Feedbacks from the terrestrial system to atmospheric CO_2 are among the largest uncertainties to projections of future climate change (Schimel et al., 2015).

According to our analysis, these would impact our ability to predict the net carbon storage associated direct injection of CO_2 into the deep ocean.

The neglected effect of the $CaCO_3$ dissolution feedback in our injection experiments (see Sect. 2.2.2) introduces another uncertainty with respect to the response of the global carbon cycle to direct CO_2 injections. Model simulations by Archer et al. (1998) have shown that $CaCO_3$ dissolution is sensitive to direct CO_2 injections throughout the Atlantic but that it leads to only a slight impact on atmospheric pCO_2. However, a slightly modified trajectory of atmospheric CO_2 may, for instance, further impact the terrestrial carbon pool and fluxes and could result in different terrestrial responses as in our *With Emissions* simulations. However, the question of how the marine $CaCO_3$ sediments feedback would affect global carbon cycling compared to the injections experiments without $CaCO_3$ sediments is the subject of future work and beyond the scope of this particular study

2.3.4.2 Response after injection period

After the injections are stopped (end of year 2119), *I-800* shows a continuous outgassing of about 40 Gt C until the end of the simulation, which is represented by the steady divergence from the globally injected carbon (denoted as GIC in Figs. 2.4 b, c). As in the *control* simulation, the terrestrial system in *I-800* becomes a source of carbon between the years 2139 and 2280, although the flux is slightly lower because of lower atmospheric CO_2 and lower temperatures. Thus, the net effect is an increase in land carbon relative to the *control* simulation with a maximum of 3 Gt C in the year 2239 (Fig. 2.4 e). Thereafter, total land carbon in *I-800* converges towards that of the *RCP 8.5 control* run but remains higher until the end of the simulation (Fig. 2.4 e).

Unlike *I-800*, *I-3000* actually gets closer to the globally injected carbon trajectory after the end of the injection period until the year 2199, with about 64 Gt C less total atmospheric carbon than in the *control* simulation, compared to about 60 Gt C at the end of the injection period in the year 2119 (Fig. 2.4 b). This is a result of the reduced carbon flux from the atmosphere to the ocean, relative to the *RCP 8.5 control*

run (Fig. 2.4 d), with only about 4 Gt C leaving the ocean by year 2199. Moreover, the land turns from a sink into a net source of CO_2 in the year 2139 (Fig. 2.4 f). Subsequently, *I-3000* shows a steady outgassing of the injected CO_2 from the year 2199 until the end of the simulation (Fig. 2.4 e), with little change in the terrestrial carbon pool (Fig. 2.4 f). The processes that govern changes in terrestrial carbon in *I-3000* are the same as for *I-800*, although more carbon is retained in the soils resulting from lower soil temperatures in *I-3000*. The relatively small responses of the terrestrial biosphere to the injections, compared to the *RCP 8.5 control* run, show a similar progression, although with different amplitudes, as illustrated in Figure 2.4f and e. After the injection period, this is especially reflected by the apparent synchronous increase in land carbon around the year 2600 and the synchronous decrease around the year 2770 (Fig. 2.4 e). This is a result of a slightly different phase of small variations in the total land carbon content of the *control* run (Figs. 2.4 , A2 a, b), which is the only simulation that has not seen any atmospheric CO_2 reduction. However, due to the same amount of atmospheric carbon being removed and injected into the ocean, the *With Emissions* runs have a similar climatic state throughout the simulations with comparable changes in global mean air and soil temperatures (0.1–0.3 % less) and precipitation over land (0.1–0.4 % more) when compared to the control run (Figs. 2.5 a, b, e). The high synchronicity (Fig. 2.4 e) can be further explained by the fact that in the *With Emissions* simulations, the same biome regions are sensitive to the changes in temperature (Figs. 2.5 a, b), although the magnitudes of the absolute changes in land carbon differ between the injection runs (Figs. A3, A4, A5). These regions are predominantly located at transition zones of different plant functional types that are in competition which each other and thus shift from one to another, leading to small changes in land carbon. The offset between *I-800* and *I-3000* (Fig. 2.4 e) is caused by higher soil respiration in *I-800* (Fig. 2.5 d), which is due to slightly higher global mean air and soil temperatures (Figs. 2.5 a, b).

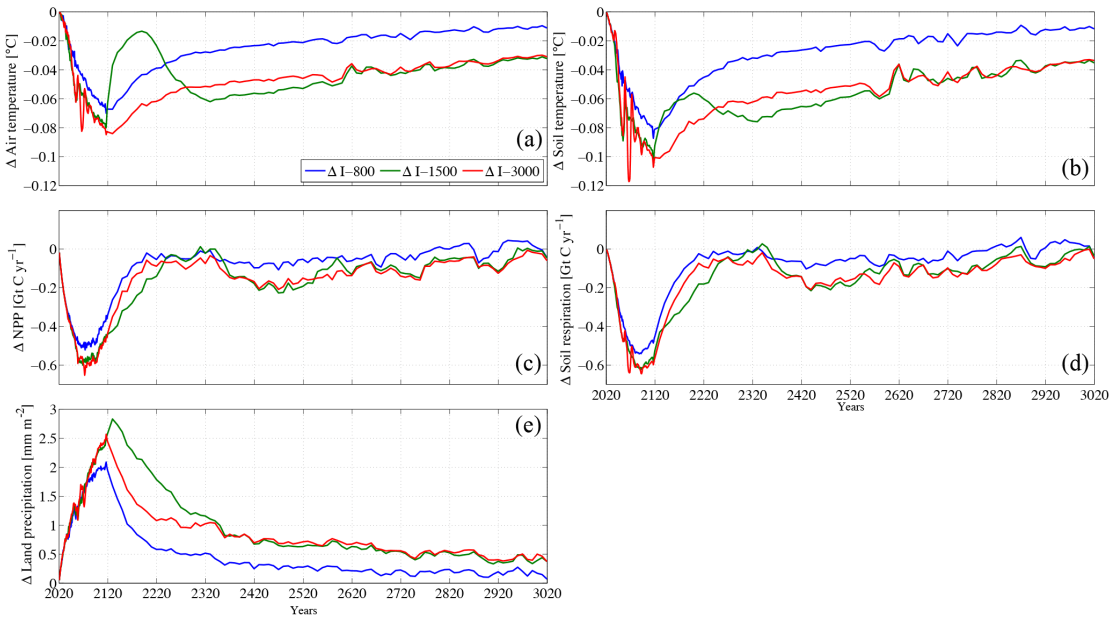

Figure 2.5: Absolute changes between the WE simulations and the RCP 8.5 control run for **(a)** global mean surface air temperature, **(b)** global mean soil temperature, **(c)** globally integrated net primary productivity on land, **(d)** globally integrated soil respiration and **e)** global mean precipitation over land.

For *I-1500*, an unexpected oceanic carbon uptake event is observed from the last year of the injection period (Figs. 2.4 c, d). This is caused by a large temporary carbon flux from the atmosphere into the ocean (Fig. 2.4 d), with a total of ~13 Gt C taken up in a region of the Southern Ocean (~ 0°–20° E; 60°–70° S) between the years 2119 and 2209 (Fig. A6). Because this event is not simultaneously present in the reference simulation without injection, the difference in atmospheric carbon between run *I-1500* and the reference run even exceeds the globally injected carbon between the years 2189 and 2262 (Fig. 2.4 b). For standard accounting of carbon removed from the atmosphere with respect to a reference simulation, this would correspond to sequestration effectiveness greater than 100 %. The oceanic *netFS* is just less than 100 % of the GIC (Fig. 2.4 c). Our analysis for *I-1500* suggests that the regional carbon uptake is due to an intermittent ocean deep convection event that occurs in the *I-1500* simulation. Using an earlier version of the UVic model (version 2.8), Meissner et al. (2007) found that under a CO_2 concentration of 440 ppm or higher, the modeled climate system started oscillating between a state with open-ocean deep convection in the Southern Ocean, causing massive bottom water formation, and a state without. In

their runs, which were spun-up to equilibrium under constant atmospheric CO_2, the simulated deep convection event led to a rapid increase in atmospheric temperatures, carbon outgassing and a subsequent increase in atmospheric CO_2 concentrations. In contrast to Meissner et al. (2007), we here find that a deep convection event during a transient high CO_2 emission scenario can result in carbon uptake, as also found in CMIP5 model runs (Bernardello et al., 2014). This can be explained by the fact that the pCO_2 of the old (preindustrial) water masses that reach the surface during deep convection is lower than the atmospheric pCO_2 in the *I-1500* simulation at the end of the 22nd century. Compared to the injected carbon content of 70 Gt C at the end of the injection period, the deep convection event leads to a significant carbon uptake of about 19 %. Compared to the oceanic uptake of anthropogenic CO_2 by the end of the simulation, the carbon uptake associated with the deep convection event amounts to less than 1 %. The deep convection event also causes the ocean to lose a substantial amount of heat, which causes regional warming and thus partially counteracts the cooling effect associated with the direct CO_2 injection in *I-1500*. This is also reflected in a slower increase in total land carbon (Figs. 2.4 e, f) through more soil respiration than in *I-800* and *I-3000*.

Recurring open-ocean deep convection in the Southern Ocean has been found in many CMIP5 models (De Lavergne et al., 2014) and also in the Kiel Climate Model, for which the driving mechanism could be linked to internal climate variability (Martin et al., 2013). Although the modeled deep convection events feature similarities to processes associated with the Weddell Polyna of the 1970s (Martin et al., 2013), uncertainty remains regarding their realism. An important model constraint in this respect is a coarse grid resolution, which hinders, for instance, the correct representation of bottom water formation processes on the continental shelf and instead might favor open-ocean deep convection (Bernardello et al., 2014).

It is intriguing that among 19 millennial-scale simulations performed for this study, a deep convection event occurred only in 3 simulations: the *I-1500*, an injection run with a 10-year injection period (not shown) and the *Direct Air Capture* run. Apparently, small internal variability combined with certain CO_2 levels can give rise to such events (Meissner et al., 2007). The only means to discriminate between the

feedbacks of the ocean deep convection event, which are driven by the removal of atmospheric carbon and the little internal variability in the UVic model, would be to run ensembles with different initial conditions. This is how one would also discriminate between other feedbacks and internal variability in models with more intense - and more realistic - levels of internal variability. Furthermore, ensembles would allow one to assess of the robustness of the occurrence of ocean deep convection events, which might become more significant or different for slightly perturbed initial conditions. Such open-ocean deep convection can cause an inter-model spread in projections of future ocean carbon uptake (Bernardello et al., 2014) and may make accounting for the injected CO_2 as the *netFS* very difficult. As shown by the dashed lines in Fig. 2.4, the *FR* of the injected CO_2, which could in principle be tracked via a marker tracer, is more robust to internal variability of the model and, presumably, of the real world. A pragmatic and robust way to account for the storage of injected CO_2 might therefore well be based on *FR* despite its neglect of carbon cycle and climate feedbacks. To account for these feedbacks, *FR* could possibly be augmented by some model-derived correction factors to account for the ensemble-averaged interaction of the ocean with the other carbon pools under changing climate conditions.

2.3.5 Sensitivity to variations in the CO_2 fertilization parameterization

Here we show how varying the CO_2 fertilization parameterization in the perturbed injection runs (i.e., $I\text{-}800_{CO2\_\ fert\_high\ and\ low}$ and $I\text{-}3000_{CO2\_\ fert\_high\ and\ low}$) changes carbon cycling and the leakage of injected CO_2 when compared to the standard *I-800* and *I-3000* experiments of the *With Emissions* simulations.

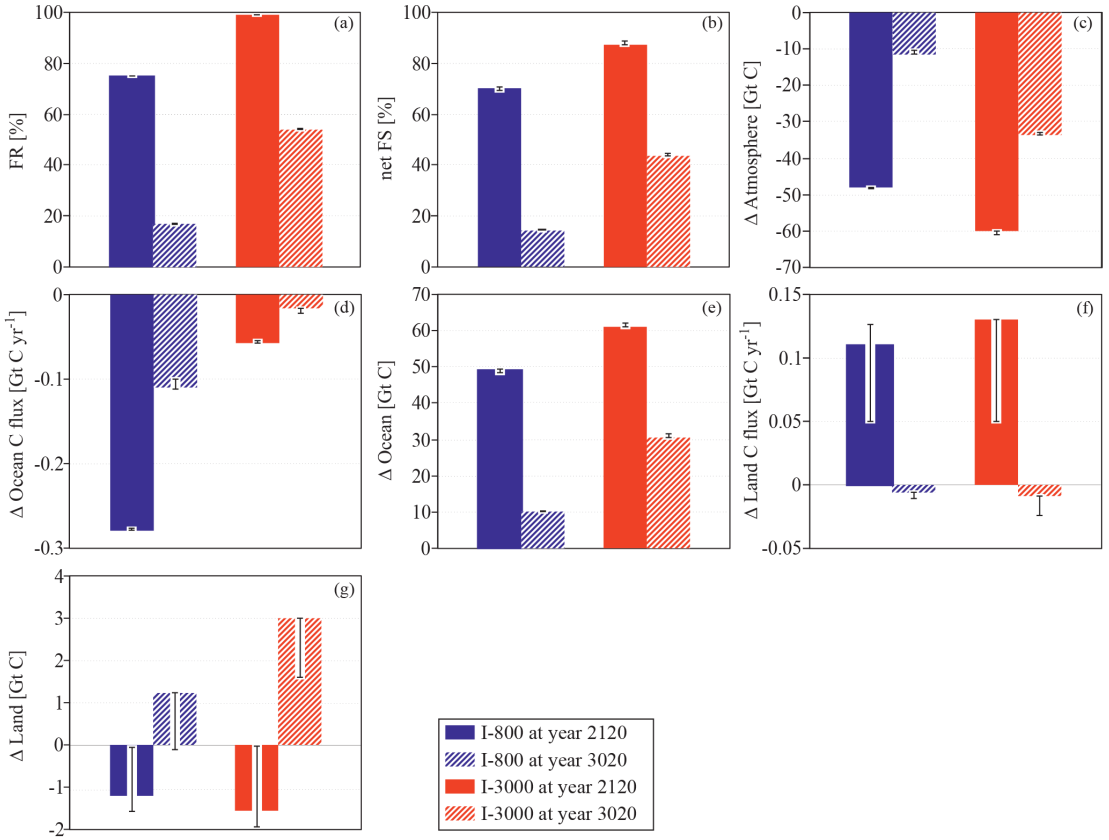

Figure 2.6: (a) Fraction retained (FR) for I-800 (blue) and I-3000 (red) for the years 2120 (filled) and 3020 (hashed) with error bars. In all panels, the error bars are defined as the difference of absolute changes between the perturbed injection runs and the respective control runs and the absolute change between the unperturbed injection runs and the control run of the With Emissions simulations. **(b)** Net fraction stored (netFS) for I-800 and I-3000 for the years 2120 and 3020 with error bars. Absolute changes in carbon between I-800 (I-3000) and the RCP 8.5 control run (With Emissions simulations minus RCP 8.5 control run) error bars for the years 2120 and 3020 for **(c)** globally integrated total atmospheric carbon, **(d)** globally integrated carbon flux from atmosphere to ocean, **(e)** globally integrated total oceanic carbon, **(f)** globally integrated carbon flux from atmosphere to land and **(g)** globally integrated total land carbon.

As illustrated by the error bars in Figure 2.6 c, varying the CO_2 fertilization effect impacts the targeted atmospheric carbon reduction in *I-800* of the *With Emissions* experiments, leading to a difference of –0.5 to 0.02 Gt C in the year 2120 and of 0.4 to 1.1 Gt C in the year 3020. Absolute changes in total oceanic carbon are also rather insensitive in these simulations with differences of only about –0.7 to 0.4 Gt C (0.01 to 0.3 Gt C) in the year 2120 (3020) (Figs. 2.6 d, e). Accordingly, the difference in the *netFS* in *I-800* lies between –1 and 0.5 % (Fig. 2.6 b) at the respective times. The slight differences in the fraction retained in *I-800* (between –0.2 and 0.3 % at the respective times) are due to a slightly different climate in the

perturbed simulations when compared to the standard *With Emissions* runs, which is caused by the different atmospheric carbon concentrations (Fig. 2.6 c).

Absolute changes in terrestrial land carbon uptake and total land carbon show the largest sensitivities to the scaled CO_2 fertilization effect in *I-800* (Figs. 2.6 f, g). By the end of the injection period, the difference in total land carbon between *I-800* and the *RCP 8.5 control* run shows that this terrestrial response could result in almost the same or less carbon storage, depending on the scaling of the CO_2 fertilization parameterization (Fig. 2.6 g). Higher CO_2 fertilization, i.e. $I\text{-}800_{CO2\_\ fert\_high}$, leads to a higher carbon flux from the atmosphere to land than in *I-800*, which counteracts the lower CO_2 fertilization effect that occurs in the standard *I-800* because of less atmospheric carbon, when compared to the *RCP 8.5 control* run (see Sect. 2.3.4.1). This results in more land carbon of about 1.1 Gt C (Fig. 2.6 g). The opposite is true for $I\text{-}800_{CO2\_\ fert\_low}$, leading to less land carbon by about 0.4 Gt C in the year 2120 when compared to the difference between *I-800* and the *RCP 8.5 control* run. By the end of the simulation, the perturbed injection simulation $I\text{-}800_{CO2\_\ fert\_high}$ has about 0.4 Gt C less land carbon, relative to the difference of *I-800* and the *control* run, which is caused by a slightly stronger cooling effect, because there is less atmospheric carbon than in *I-800* (Fig. 2.6 g). This cooling also results in less soil respiration. $I\text{-}800_{CO2\_\ fert\_low}$ has about 1.3 Gt C less land carbon at the end of the simulations, when compared to the absolute change between *I-800* and the respective *control* run. This can be explained by the reduced CO_2 fertilization effect that has led to a decreased NPP and consequently to a reduced soil respiration when compared to *I-800*.

The magnitude of the responses that can be seen in the perturbed injection runs $I\text{-}3000_{CO2\_\ fert\_high}$ and $I\text{-}3000_{CO2\_\ fert\_low}$ are similar as in the perturbed *I-800* runs.

Although the above response is informative, the future strength of the CO_2 fertilization effect also depends on other factors, such as water and nutrient availability (IPCC, 2013), which may be poorly simulated by our model. A key update since the Fourth Assessment Report by the IPCC is the implementation of nutrient dynamics in some of the CMIP5 land carbon models, such as in the Norwegian Earth System Model (intermediate resolution with carbon cycle)

(NorESM-ME) and the Community Earth System Model, version 1.0, biogeochemical cycles (CESM1-BGC) (Arora et al., 2013; Hajima et al., 2014). There is high confidence that low nitrogen availability will limit land carbon uptake. Models that combine nitrogen limitation with rising CO_2 as well as changes in temperature and precipitation predict a larger increase in projected future atmospheric CO_2 for a given CO_2 emission scenario (e.g., IPCC, 2013; Hajima et al., 2014). Models including terrestrial nutrient limitation would likely be subject to a smaller terrestrial response if direct CO_2 injections into the deep ocean occurred. Thus, the introduction of nitrogen limitation in the land component of the UVic model would presumably result in less total simulated land carbon because of lower NPP and soil respiration throughout the simulation when compared to the terrestrial response in the shallow injection run (*I-800*) or for delayed emissions.

2.4 Conclusions

We use an Earth system model of intermediate complexity to simulate direct CO_2 injections into the deep ocean under a high CO_2 emission scenario. The model-predicted *FR*s are found to be within the range of the values found by Orr et al. (2001). In agreement with earlier studies (Jain and Cao, 2005), we also find that the *FR* is enhanced as global warming progresses. In our simulations, this enhancement amounts to about 7–16 % at the end of the simulations (year 3020). Injection sites in the Pacific are the most effective ones on the millennial timescale considered in our simulations. The neglect of the effect of the dissolution of $CaCO_3$ sediments near or downstream of the injection sites (see Sect. 2.2.2) may have led to an underestimation of the *FR* and *netFS* in our injection experiments. The impact of this process would presumably be largest in the Atlantic due to the lower abundance of $CaCO_3$ sediments in the Pacific and Indian Ocean.

The response of the carbon cycle during and after the injections is dominated by the partial outgassing of injected CO_2 and a reduced rate of air–sea gas exchange compared to the *control* run without injection. Relative to the *control* run, the model's

terrestrial ecosystems respond to the marine CO_2 injection and reduced atmospheric CO_2 concentrations via a reduced CO_2 fertilization effect and a temperature-related decrease in soil respiration. This leads to a maximum reduction in total land carbon by about 4 Gt C (relative to the *control* run) during the injection period in all *With Emissions* simulations (Fig. 2.4 e). After the injection period, total land carbon becomes higher than in the *control* simulation, mainly due to a terrestrial carbon-cycle–climate feedback, with a maximum increase of about 5 Gt C for *I-3000* in the year 2230 (Fig. 2.4 e).

Further, we find that varying the CO_2 fertilization parameterization results in changes of the targeted atmospheric carbon reduction in *I-800* and *I-3000* of the *With Emissions* simulations that lay between 0.2 and 2 % less atmospheric carbon at the end of the injection period (year 2120) and between 9 % less and 1 % more atmospheric carbon at the end of the simulations. The sensitivity of the terrestrial carbon cycle to the different CO_2 fertilization parameterizations in *I-800* and *I-3000* of the *With Emissions* runs ranges from 30 % less to 98 % more land carbon by the year 2120 and up to 108 % less land carbon by the end of the simulations. The larger signal of the terrestrial response to the scaled CO_2 fertilization parameterization when compared to the targeted atmospheric carbon reduction, highlights that further research on the future strength of terrestrial carbon cycle feedbacks is needed if direct CO_2 injections were to be seriously considered.

Furthermore, the influence of the highly uncertain carbon-cycle and climate feedbacks in our findings, in addition to the sporadic deep convection event in *I-1500*, illustrates the difficulty of quantitatively detecting, attributing, and eventually accounting for carbon storage and carbon fluxes generated by individual carbon sequestration measures even in relatively coarse-resolution models with little internal climate variability (“noise”). Nevertheless, our findings point to the importance of accounting for all carbon fluxes in the carbon cycle and not only for those of the manipulated reservoir to obtain a comprehensive assessment of direct oceanic CO_2 injection in particular and carbon sequestration in general.

Acknowledgments

The model data used to generate the table and figures is available at http://thredds.geomar.de/thredds/catalog/open_access/reith_et_al_2016_esd/catalog.html

The Deutsche Forschungsgemeinschaft (DFG) financially supported this study via the Priority Program 1689. We thank Torge Martin, Wolfgang Koeve, Nadine Mengis, Julia Getzlaff, Levin Nickelsen, Peter Vandromme, Markus Pahlow, Wilfried Rickels and Ell Yuming Feng for their thoughtful discussions and advice.

3 Direct CO_2 injections to meet the 1.5°C target: What price would the ocean have to pay?

This chapter is a manuscript in preparation by Reith, F., Koeve, W., Keller, D. P., Getzlaff, J., and Oschlies, A. (2017).

Abstract. The potential and collateral effects of direct CO_2 injections into the deep ocean are investigated as a means to close the gap between an intermediate CO_2 emission scenario and the 1.5°C target of the Paris agreement. For that purpose, three conceptually different approaches for applying direct CO_2 injections at 3000m water depth are implemented in an Earth System Climate Model of intermediate complexity with a fully coupled carbon cycle.

For a medium mitigation scenario of anthropogenic CO_2 emissions following the representative concentration pathway RCP 4.5, cumulative CO_2 injections required to closely meet the 1.5°C climate goal are found to be 1562 Gt C at the end of simulations, by the year 3020.

This injected CO_2 amount includes a cumulative leakage of 602 Gt C that needs to be re-injected. Furthermore, the CO_2 amount that needs to be injected in order to cool global mean temperature by 1°C is found to be about 446 Gt C in the near-term (year 2100) and about 951 Gt C in the long-term (year 3020).

$CaCO_3$ sediment and weathering feedbacks reduce the required CO_2 injections that comply with the 1.5°C target by about 11 %.

With respect to the injection-related impacts we find that average pH values in the surface ocean are increased by about 0.13 to 0.18 units, when compared to the control run. In the model, this results in significant increases in potential coral reef habitats compared to a business-as-usual scenario without direct injection. The potential benefits in the upper ocean come with the expense of strongly acidified water masses, with maximum pH reductions of about -2.37 units, relative to preindustrial, in the vicinity of the injection sites. Overall, the results of this study demonstrate that

massive amounts of CO_2 would need to be injected into the deep ocean in order to reach and maintain the 1.5°C climate target in a medium mitigation scenario on a millennium timescale, and that there is a trade-off between injection-related reductions in atmospheric CO_2 levels accompanied by reduced upper-ocean acidification and adverse effects on deep ocean chemistry, particularly near the injection sites.

3.1 Introduction

The Paris Agreement of December 2015 has set the political target of keeping global warming well below 2°C, if not 1.5°C, above preindustrial levels (UNFCCC, 2015). Staying within the Paris target range is perceived as a safe limit that avoids dangerous anthropogenic climate change and ensures sustainable food production and economic development (Rockström et al., 2009; Knutti et al., 2015; Rogelj et al., 2016). As a first step towards meeting the Paris climate goals, countries have outlined national post-2020 climate action plans by submitting their Nationally Determined Contributions (NDCs) to climate mitigation in order to meet the <2°C climate target (e.g., Clémençon, 2016). However, even if these NDCs are fully realized, it is estimated that a median warming of 2.6 to 3.1°C will occur by they year 2100 (Rogelj et al., 2016). Consequently, it is questionable whether conventional measures currently considered by individual states will be sufficient to reach and maintain the <2°C climate target (e.g., Horton et al., 2016).

The scientific rationale of such claims is based on observational records and results of climate models of varying complexity that have found a tight correlation between cumulative CO_2 emissions and global mean temperature (Allen et al., 2009; Matthews et al., 2009; MacDougall, 2016). From this transient climate response to cumulative carbon emissions (TCRE) it can be estimated that the total quota of CO_2 emissions from all sources (fossil fuel combustion, industrial processes and land-use change) that is compatible with a 1.5°C target will be used up in a few years at current emission rates (Knopf et al., 2017), and for a 2°C target it is likely to be reached in the

next 2 to 3 decades (Friedlingstein et al., 2014). Thus, the window of opportunity for deep and rapid decarbonization that would allow for such a climate target through emissions reduction alone is closing soon (Sanderson et al., 2016).

Given the very challenging and urgent nature of the task of reaching the agreed-upon Paris climate goals, unconventional methods are being discussed. Under specific consideration are negative emission technologies, i.e., measures that deliberately remove CO_2 from the atmosphere (e.g., Gasser et al., 2015) and store it somewhere else, e.g., in geological reservoirs or the deep ocean (e.g., IPCC, 2005). Negative emissions are already included in most of the scenarios from integrated assessment models (IAMs) that predict a >50 % chance of limiting global warming to well below 2°C and in all scenarios that give a >50 % chance of reaching the 1.5°C target (Clarke et al., 2014; Fuss et al., 2014; Rogelj et al., 2015). However, none of the currently debated negative emissions technologies, such as bioenergy with carbon capture and storage (BECCS), direct air capture with carbon storage (DACCS) and enhanced weathering (EW), appears to have, in a business-as-usual emission scenario, the potential to meet the <2°C target without significant impacts on land, energy, water or nutrient resources (Fuss et al., 2014; Smith et al., 2016; Williamson, 2016; Boysen et al., 2017a).

In the absence of plausible scenarios that meet the Paris climate targets, also unconventional ideas to reduce atmospheric CO_2 are being considered. One option that has been researched on is ocean carbon sequestration by direct injection of CO_2 into the deep ocean (e.g., Marchetti, 1977; Hoffert et al., 1979; Orr et al., 2001; Orr, 2004; IPCC, 2005; Reith et al., 2016). The CO_2 could be derived from point sources such as power plants or direct air capture facilities, and thereby contribute to the carbon sequestration part of CCS, DACCS or BECCS. Direct injection of CO_2 into the deep ocean is the deliberate acceleration of the oceanic uptake of atmospheric CO_2, which happens naturally via invasion and dissolution of CO_2 into the surface waters, albeit at a relatively slow rate limited by the sluggish overturning circulation. On millennial timescales, about 65-80 % of anthropogenic CO_2 is thought to be taken up by the ocean via gas exchange at the ocean surface and by entrainment of surface

waters into the deep ocean, which rises to 73-93 % on timescales of tens to hundreds of millennia via neutralization of carbonic acid with sedimentary calcium carbonate ($CaCO_3$) (e.g., Archer et al., 2005; Zeebe, 2012). Directly injecting CO_2 into the deep ocean could speed up this natural process by directly accessing deep waters, some of which remain isolated from the atmosphere for hundreds or thousands of years (DeVries and Primeau, 2011; their Figure 12), and by bringing it in closer contact with the sediment. This would prevent anthropogenic CO_2 from having an effect on the climate in the near future, and accelerate eventual and nearly permanent removal via reaction with $CaCO_3$ sediments.

Despite the well-known potential of the ocean to take up and store carbon (e.g., Sarmiento and Toggweiler, 1984; Volk and Hoffert, 1985; Sabine et al., 2004;), direct CO_2 injection into the deep ocean is currently not allowed by the London Protocol and the Convention for the Protection of the Marine Environment of the North East Atlantic (OSPAR Convention) (Leung et al., 2014). A main concern that led to the current ban is that direct CO_2 injection will harm marine ecosystems in the deep sea, e.g., cold-water corals and sponge communities at least close to the injection site (e.g., IPCC, 2005; Schubert et al., 2006; Gehlen et al., 2014). As emphasized by Keeling (2009) and Ridgwell et al. (2011) there are, however, trade-offs between injection-related damages in the deep ocean and benefits at the ocean surface via a reduction in atmospheric pCO_2 and a decrease in upper ocean acidification. These should be discussed in relation to other mitigation options, that probably all imply offsetting some local harm against global benefits. Our current study aims to inform such a debate by providing quantitative information about impacts on ocean carbonate chemistry caused by direct injection of CO_2 into the deep ocean as a potential measure to reach and maintain the Paris climate targets.

For this purpose, we consider direct injection of CO_2 into the deep ocean as ‘oceanic CCS’, deposing CO_2 from point sources such as fossil fuel or biomass-based power plants or direct air capture plants. We assume that aggressive emissions reduction has led from a business as usual CO_2 emission scenario to a world with intermediate CO_2 emissions such as represented by the Representative Concentration Pathway (RCP)

4.5. Model-predicted global mean surface air temperatures for the RCP 4.5 CO_2 emission scenario range between 1.7°C and 3.2°C in the year 2100 (Clarke et al., 2014), which is approximately in agreement with the warming after full achievement of current NDCs. Consequently, the 1.5°C climate target would not be reached under the RCP 4.5 scenario and is likely to be exceeded after the year 2050 (IPCC, 2014). We here explore the potential as well as collateral oceanic effects of 'oceanic CCS' as a means to fill the gap between emissions and climate impacts of the RCP 4.5 and the 1.5°C target of the Paris agreement.

The paper is organized as follows: In section 3.2 we address the methodological framework by describing the UVic model and the experimental setup of our experiments. In section 3.3 the results and the discussion of our model simulations are presented. Section 3.4 outlines the conclusions.

3.2 Methods

3.2.1 Model description

The model used is version 2.9 of the University of Victoria Earth System Climate Model (UVic ESCM). It consists of three dynamically coupled main components: a three-dimensional general circulation ocean model based on the Modular Ocean Model MOM2 (Pacanowski, 1996) including a marine biogeochemical model (Keller et al., 2012), a dynamic-thermodynamic sea-ice model (Bitz and Lipscomb, 1999) and a sediment model (Archer, 1996), a terrestrial vegetation and carbon-cycle model (Meissner et al., 2003) based on the Hadley Center model TRIFFID (Top-down Representation of Interactive Foliage and Flora Including Dynamics) and the hydrological land component MOSES (Met Office Surface Exchange Scheme), and a one-layer atmospheric energy-moisture balance model (based on Fanning and Weaver, 1996). All components have a common horizontal resolution of 3.6° longitude x 1.8° latitude. The oceanic component has 19 vertical levels with

thicknesses ranging from 50 m near the surface to 500 m in the deep ocean. Formulations of the air-sea gas exchange and seawater carbonate chemistry are based on the OCMIP abiotic protocol (Orr et al., 1999). Marine sediment processes of $CaCO_3$ burial and dissolution are simulated using a model of deep ocean sediment respiration (Archer, 1996).

3.2.2 Experimental design

For our default control run and injection experiments, the model has been spun up for 10,000 years under preindustrial atmospheric and astronomic boundary conditions and run from 1765 to 2005 using historical fossil-fuel and land-use carbon emissions (Keller et al., 2014). From the year 2006 onwards simulations are forced with CO_2 emissions according to the RCP 4.5 and the Extended Concentration Pathway (ECP) 4.5, which runs until the year 2500 (Meinshausen et al., 2011). This forcing includes CO_2-emissions from fossil fuel burning as well as land-use carbon emissions, e.g. from deforestation. After the year 2500, CO_2 emissions are assumed to decrease linearly until they cease at the end of the simulations in year 3020. In the default control run and injection experiments we do not apply greenhouse gas emissions other than CO_2, nor do we simulate the effect of sulfate aerosols or non-CO_2 effects of land use change. Further, prescribed, monthly varying, National Center for Environmental Prediction (NCEP) reanalysis winds are used together with a dynamical feedback from a first-order approximation of geostrophic wind anomalies associated with changing winds in a changing climate (Weaver et al., 2001).

Simulated CO_2 injections are based on the OCMIP carbon sequestration protocols (see Orr et al., 2001; Orr, 2004) and carried out in an idealized manner by adding CO_2 directly to the dissolved inorganic carbon (DIC) pool (Orr et al., 2001; Orr, 2004), thus neglecting any gravitational effects and assuming that the injected CO_2 instantaneously dissolves into seawater and is transported quickly away from the injection point and distributed homogenously over the entire model grid box with lateral dimensions of a few hundred kilometers and many tens of meters in the vertical

direction (Reith et al., 2016). Consequently, the formation of CO_2 plumes or lakes as well as the potential risk of fast rising CO_2 bubbles are neglected (IPCC, 2005; Bigalke et al., 2008).

The physical transport of the injected CO_2 and its transport pathways from the individual injection sites towards the surface of the ocean are tracked by means of inert 'dye' tracers (one per injection site). At the injections sites, these tracers are loaded at rates proportional to the amount of CO_2 injected. At the sea surface the tracers are subject to a loss to the atmosphere, which is computed in proportionality to the total gas exchange and fractional contribution to total DIC of the respective tracer at the ocean surface. The sum of tracer loss to the atmosphere from the individual 'dye' tracers provides an estimate of the loss of injected carbon to the atmosphere.

Following Orr et al. (2001; Orr, 2004; Reith et al., 2016) CO_2 is injected at seven separate injections sites, which are located in individual grid boxes near the Bay of Biscay (42.3° N, 16.2° W), New York (36.9° N, 66.6° W), Rio de Janeiro (27.9° S, 37.8° W), San Francisco (31.5° N, 131.4° W), Tokyo (33.3° N, 142.2° E), Jakarta (11.7° S, 102.6° E) and Mumbai (13.5° N, 63° E) (Reith et al., 2016; their Figure 1). Injected CO_2 is distributed equally between the seven injection sites. Direct CO_2 injections are carried out at 2900 m depth (hereafter referred to as 3000 m) to minimize leakage and maximize retention time. At this depth, liquid CO_2 is denser than seawater, which has the additional advantage that any undissolved droplets would sink to the bottom rather than rise to the surface.

3.2.3 Model experiments

Three conceptually different approaches for applying oceanic CCS are simulated using the UVic model: The first approach assumes that all anthropogenic CO_2 emissions are injected after a warming of 1.5°C is realized for the first time, the second approach injects, in every year, an amount of CO_2 that ensures that temperatures do not rise well beyond the 1.5°C target, and the third approach injects

an amount of CO_2 to ensure that atmospheric CO_2 concentrations follow the RCP/ECP 2.6 scenario as closely as possible. All idealized approaches are designed to counter the excessive emissions of the RCP 4.5 scenario to reach and maintain the 1.5°C target until the end of this century and for another millennium by direct CO_2 injections into the deep ocean. In order to avoid interference with natural fluctuations of temperature and atmospheric pCO_2, respectively, we apply restoring time scales detailed below for runs of approaches two and three. CO_2 injections needed to reach the respective target are updated every 5 days. Injections are interrupted when the simulated annual mean surface air temperature (atmospheric pCO_2) falls below the respective climate target. Table 3.1 provides an overview of all conducted simulations and their set-up from the year 2006 onwards.

Table 3.1: Overview of all conducted simulations and their set-up. The "X" denotes that the respective feature is applied.

Simulations	Set-up							
	RCP 4.5 CO_2 emission scenario	Extended RCP 4.5 CO_2 emission scenario	Linearly decline in CO_2 emissions until zero Gt C yr^{-1} in 3020	$CaCO_3$ sediment feed-backs	Direct CO_2 in-jections at 3000 m depth	Approach		
	2006-2100	2100-2500	2500-onwards	2006-3020	2020-3020	1st	2nd	3rd
RCP 4.5 control run	X	X	X					
1.5°C_target_Cemit	X	X	X		X	X		
1.5°C_target_Cemit_Comitw	X	X	X			X		
1.5°C_target	X	X	X		X		X	
CO_2target_RCP2.6	X	X	X		X			X
RCP 4.5 $control_{sed}$ run	X	X	X	X				
1.5°C_target_$Cemit_{sed}$	X	X	X	X	X	X		
1.5°C_target_$Comitw_{sed}$	X	X	X	X		X		
1.5°C_target	X	X	X	X	X		X	
CO_2target_$RCP2.6_{sed}$	X	X	X	X	X			X

We further study to what extent the required CO_2-injection needed as well as the impacts on ocean biogeochemistry depend on the inclusion of $CaCO_3$ sediment feedbacks on deep-ocean CO_2 injections and continental weathering. These aspects will be investigated in sensitivity experiments for all three oceanic CCS approaches described below.

In the first approach (*1.5°C_target_Cemit*), all further CO_2 emissions of the RCP 4.5 scenario are completely re-directed to the injections sites after the global mean air surface temperature has once exceeded the 1.5°C target. Some committed warming (e.g., Matthews and Caldeira, 2008; Gillet et al., 2011) occurs in these simulations due to past emissions and climate cycle feedbacks. This committed warming is at some point overlaid by oceanic and terrestrial carbon cycle feedbacks that lead to a CO_2 increase in the atmosphere and respective additional warming (see section 3.1). Suspecting that injected carbon that outgasses from the ocean to the atmosphere after arriving at the ocean surface is a considerable part of these carbon cycle feedbacks we design a sensitivity simulation (*1.5°C_target*_Cemit_Comitw*)*, in which CO_2 emissions are set to zero once the *1.5°C* target is reached, and no CO_2 is injected into the deep ocean.

In contrast to the first approach, the second one (*1.5°C_target)* keeps the global mean temperature at the defined threshold of 1.5°C, relative to preindustrial, by injecting an adequate amount of CO_2 into the deep ocean. We diagnose this amount of CO_2 using the transient response to emissions (TCRE, Allen et al., 2009; Matthews et al., 2009; MacDougall, 2016) of our model and the difference of the modeled annual mean atmospheric temperature and the target temperature. CO_2 is only injected if the modeled temperature is above the target temperature. In order to avoid interference with seasonal and longer periodic fluctuations of atmospheric temperature we apply a restoring time scale of 1000 days. The injected CO_2 that is taken out of the atmosphere can be larger than the applied CO_2-emissions (RCP/ECP 4.5) and eventually may cause net CO_2 emissions to be negative.

In the third approach (*CO_2target_RCP2.6*), we inject the amount of CO_2 that is needed to follow the atmospheric CO_2 concentration of the extended Representative

Concentration Pathway RCP 2.6 and Extended Concentration Pathway ECP 2.6. From year 2500 onwards, the targeted atmospheric CO_2 concentration is held constant until the end of the simulations. Therefore, the model computes at every atmospheric time step the difference between its current atmospheric CO_2 concentration, given the RCP 4.5 CO_2-emissions and all model derived CO_2-fluxes into and out of the atmosphere, and the targeted atmospheric CO_2 concentration from the RCP 2.6 pathway. By applying a restoring time scale of one month, this difference is used to diagnose a CO_2-injection needed to keep the models annual mean atmospheric CO_2 concentrations as close as possible to the RCP 2.6 concentration pathway. This amount of CO_2 is injected and subtracted from the prescribed CO_2 emissions to the atmosphere, which eventually results in net negative emissions.

In sensitivity experiments we further investigate the effect of $CaCO_3$ sediment feedbacks and continental weathering on the cumulative CO_2 injections and on seawater carbonate chemistry for the different approaches. The effect of $CaCO_3$ sediment dissolution is thought to be relevant as CO_2 injected at depth may react relatively directly with sedimentary $CaCO_3$ and increases $CaCO_3$ dissolution near or downstream of the injection sites, resulting in an acceleration of the neutralization of anthropogenic CO_2 compared to a situation where CO_2 emissions slowly invade the ocean via air-sea gas exchange (Archer et al., 1998; IPCC, 2005). Therefore, we investigate the effect of $CaCO_3$ sediment feedbacks in our simulations by running the model with and without a sediment sub-model. The global average percent of $CaCO_3$ in sediments in our "*sed*" simulations (section 3.2) is about 31 % in the year 2020 and compares well to about 34.5 % derived from observed data as reported in Eby et al. (2009). The UVic model with sediment module also has a simple representation of continental weathering, which ensures that in the steady state burial of $CaCO_3$ in the deep ocean is compensated by adequate fluxes of DIC and alkalinity from continental weathering. From the model spin-up we diagnose the global terrestrial weathering flux of DIC as 0.12 Gt C yr^{-1}, and an alkalinity flux of 0.02 Pmol yr^{-1}. During the transient runs with sediment module, this weathering flux is held constant, whereas sedimentary $CaCO_3$ accumulation or dissolution is allowed to evolve freely.

Consequently, ocean alkalinity and DIC adjust in response to interactions between seawater, injected CO_2, and sediments. Simulations with the sediment/weathering sub-model are based on a separate set of spin-up experiments (50 000 years), drift runs and historical simulation that all employ the sediment/weathering sub-model. Hereafter, simulations performed with the sediment/weathering model are referred to by the subscript "*sed*" (Table 3.1).

Relevant carbonate system parameters that are not computed at model run-time are derived offline for all simulations by means of the Matlab-version of *CO2SYS* (Lewis and Wallace, 1998; van Heuven et al., 2009; Koeve and Oschlies, 2012; http://cdiac.ornl.gov/oceans/co2rprt.html), using carbonic acid dissociation constants of Mehrbach et al. (1973), as refitted by Dickson and Millero (1987), and other related thermodynamic constants (Millero, 1995).

3.3 Results and Discussion

3.3.1 Oceanic CCS and the 1.5°C climate target

Here, we present the cumulative mass of CO_2 injected in the default runs (CO_2-only experiments) of the different approaches and show how effective these are in reaching and maintaining the 1.5°C climate target.

In the default simulation of the first approach (*1.5°C_target_Cemit*) oceanic CCS starts in the year 2045 after the 1.5°C climate target has been passed for the first time at a corresponding atmospheric CO_2 concentration of about 466 ppmv (Figs. 3.1 a, b, c). Between year 2020 and 2045, about 278 Gt C of the total CO_2 emissions between years 2020 and 3020 of 1242 Gt C applied here (RCP 4.5 scenario, section 3.2.2) have been emitted into the atmosphere. From 2045 until year 3020, CO_2 emissions (964 Gt C in total) are directly injected into the deep ocean (Fig. 3.1 a), resulting in zero anthropogenic CO_2 emissions into the atmosphere for the remaining simulation. After injection starts in year 2045, the atmospheric CO_2 concentration

decreases, but only until the year 2341, when a minimum of about 409 ppmv is reached (Fig. 3.1 c). The increase of atmospheric CO_2 observed from year 2342 onwards is a result of leakage of CO_2 injected into the deep ocean earlier. Until the end of the simulation, a total amount of 437 Gt C is diagnosed to have leaked back into the atmosphere (Fig. 3.1 d). Thus, only about 55 % of the total mass injected (964 Gt C) remains in the ocean until year 3020. From 2078 onwards, the land perennially turns into a carbon source with a total carbon loss of about 21 Gt C to the atmosphere.

Global mean temperature, relative to preindustrial, oscillates around the 1.5°C climate target by up to ± 0.02°C after injections started until the year 2200. Until then, the *1.5°C_target_Cemit* simulation of the first approach is thus nearly successful in reaching and maintaining the 1.5°C climate target. Subsequently, however, global mean surface air temperature shows a slow increase of up to 0.02°C until 2341 although atmospheric CO_2 still decreases. This warming signal is owed to the lagged response of the deep ocean to previously increasing atmospheric CO_2, i.e. committed warming, resulting in a decline of the ocean heat uptake from the atmosphere and thus in an increase in the global mean temperature (Zickfeld and Herrington, 2015; Zickfeld et al., 2016). However, this feedback mechanism (see also Fig. B1) is overlaid by increasing leakage of injected CO_2 back into the atmosphere, which becomes the dominating process for atmospheric warming as obvious from the atmospheric CO_2 increase after year 2342 (Figs. 3.1 c, d). Hence, the global mean air temperature shows a steeper increase until it reaches a maximum of about +2.2°C above preindustrial level at the end of the simulation (Fig. 3.1 b). Thus, the *1.5°C_target_Cemit* simulation overshoots the 1.5°C climate target by about 0.7°C. As mentioned above, the diagnosed mass of injected CO_2 that has leaked into the atmosphere during the entire simulation adds up to about 437 Gt C (Fig. 3.1 d). By subtracting this diagnosed leakage from the cumulative CO_2 injections (964 Gt C), we determine the required CO_2 emission reduction (527 Gt C) (Fig. 3.1 e) relative to the RCP/ECP 4.5 scenario to comply with a global mean temperature of about +2.2°C, relative to preindustrial, on a thousand-year timescale.

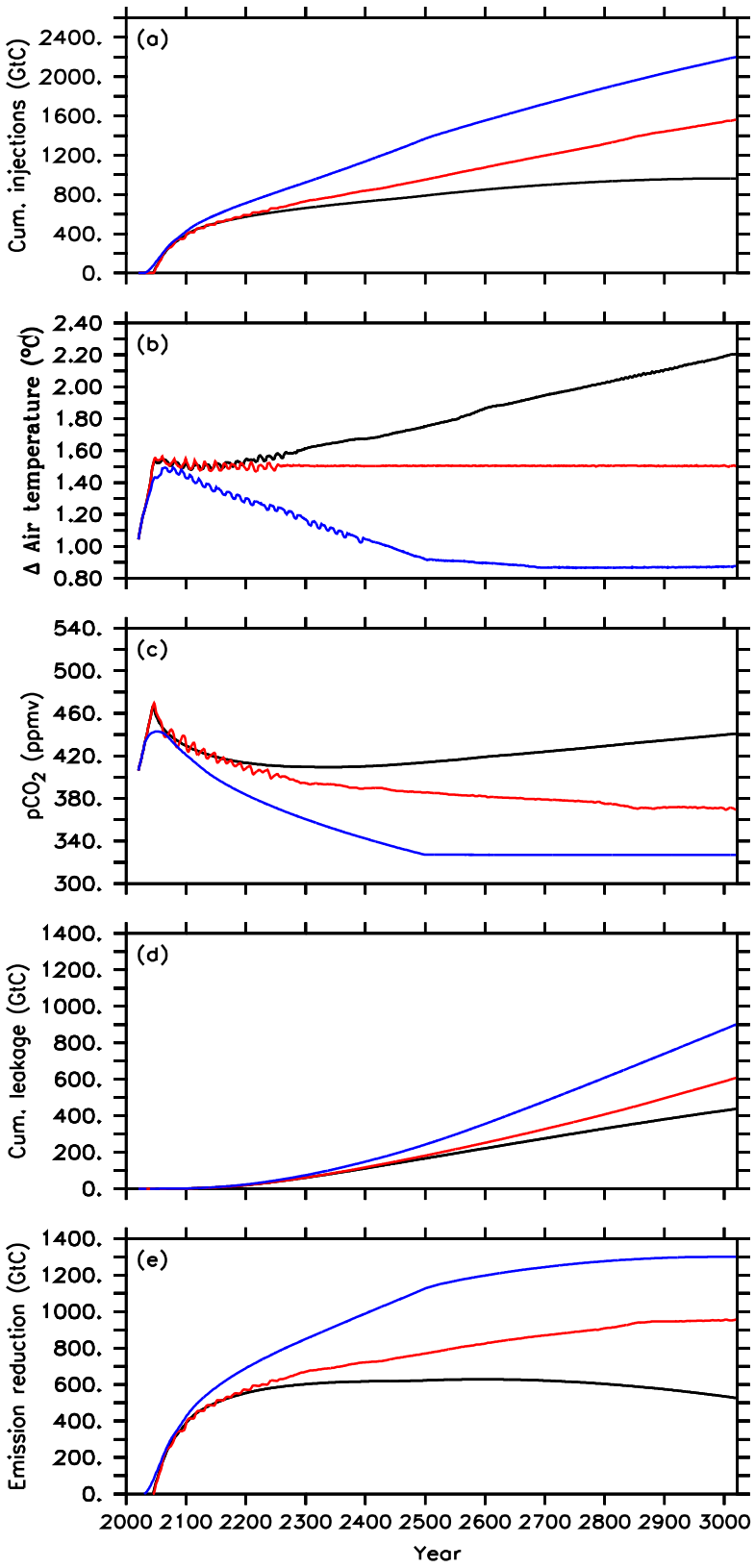

Figure 3.1: Time-series of the different default injection experiments, i.e., 1.5°C_target_Cemit simulation (black lines), 1.5°C_target simulation (red lines) and CO_2target_RCP2.6 simulation (blue lines) for (a) cumulative CO_2 injections, (b) global mean surface air temperature, relative to preindustrial, (c) atmospheric CO_2 concentration, (d) cumulative leakage of injected CO_2, and (e) required emission reduction.

Oceanic CCS in the second approach (*1.5°C_target*) starts as well in 2045 (Figs. 3.1 a, c). Relative to preindustrial, global mean surface temperature continues to increase until 2061 with a maximum of about +1.56°C (Fig. 3.1 b). Subsequently, global mean temperature oscillates around the 1.5°C climate target until year 2300 (Fig. 3.1 b). These oscillations get smaller over time until global mean temperature essentially stays at 1.5°C until the end of the simulation. We find that the oscillations are not related to our experimental design, but arise in the applied model from climate-sea-ice feedbacks under the near-term 1.5°C conditions (see Fig. B2). The terrestrial biosphere turns into a carbon source in 2061 and land-atmosphere carbon fluxes oscillate around zero until the end of the simulation. The total carbon loss from land to the atmosphere is about 75 Gt C. Atmospheric CO_2 concentrations show a continuous decline when global mean temperature is held at the aspired climate target (Figs. 3.1 b, c). This is caused by a decline in ocean heat uptake as mentioned above and consistent to an additional accumulation of heat in the atmosphere at constant atmospheric CO_2 concentrations (e.g., Zickfeld and Herrington, 2015; Zickfeld et al., 2016), and which, in our second approach, needs to be counteracted by further CO_2 injections into the deep ocean.

By the end of the *1.5°C_target* run, cumulative CO_2 injections amount to about 1562 Gt C, which is about 600 Gt C (62 %) higher than in the *1.5°C_target_Cemit* simulation. This amount of additional CO_2-injections is needed in order to reduce global mean warming at the end of the thousand-year simulation from 2.2°C in run *1.5°C_target_Cemit* to 1.5°C in run *1.5°C_target*.

In the *1.5°C_target* run, the diagnosed mass of injected CO_2 that has leaked into the atmosphere and has been reinjected into the deep ocean during the entire simulation adds up to about 607 Gt C until year 3020 (Fig. 3.1 d). Hence, about 61 % of the total mass injected (1562 Gt C) stays in the ocean. This results in a required CO_2 emission reduction of about 955 Gt C (Fig. 3.1 e), i.e., the amount of emission reduction necessary to comply with the 1.5°C climate target on a 1000 year timescale.

In the third approach, *CO_2target_RCP2.6*, oceanic CCS starts in the year 2031 (Fig. 3.1 a) as the atmospheric CO_2 concentration caused by the RCP 4.5 CO_2 emission scenario starts to exceed the targeted atmospheric CO_2 concentration of the RCP 2.6. Relative to preindustrial, global mean temperature continues to increase to a maximum of approximately +1.5°C in the year 2078 with a corresponding atmospheric CO_2 concentration of 433 ppmv (Figs. 3.1 b, c). Subsequently, temperature decreases until it reaches about +0.9°C relative to preindustrial temperature and at the end of the simulation with an atmospheric CO_2 concentration of 327 ppmv (Figs. 3.1 b, c). Up to that point in time, cumulative CO_2 injections in the default *CO_2target_RCP2.6* simulation amount to about 2200 Gt C (Fig. 3.1 a). The land turns into a source between year 2076 and 2600 with a total loss of about 144 Gt C to the atmosphere. From year 2600 onwards, the carbon flux between the atmosphere and land is nearly zero. By the end of the simulation, the diagnosed leakage of injected carbon adds up to about 900 Gt C (Fig. 3.1 d), resulting in about 59 % of injected CO_2 that remains in the ocean until year 3020. Further, the required emission reduction in the *CO_2target_RCP2.6* run is about 1300 Gt C (Fig. 3.1 e).

By the end of the *CO_2target_RCP2.6* simulation, cumulative CO_2 injections are about 636 Gt C (29 %) higher than in the *1.5°C_target* simulation. This is also reflected in the higher diagnosed leakage by about 293 Gt C in total, when compared to the *1.5°C_target* simulation. In the attempt to follow the atmospheric CO_2 concentration of the RCP2.6 (section 3.2.3), cumulative CO_2 injections are almost twice the amount of the cumulative CO_2 emissions difference between the RCP 4.5 scenario and the RCP 2.6 scenario as applied here. This can be explained by the fact that oceanic CCS into the deep ocean steepens the surface to deep DIC-gradient (Fig. B3 a) fostering a back transport to the surface ocean. Most of this enhanced deep water DIC is transported with the meridional overturning circulation to the Southern Ocean (south of 40° S), where the largest fraction of the total leakage occurs in our injection experiments (Fig. B3 b). By the end of the *1.5°C_target_Cemit* simulation, we find that about 60 % of the diagnosed leakage has outgassed in the Southern Ocean compared to about 77 % in *1.5°C_target* run and about 80 % in the

CO_2target_RCP2.6 simulation. Overall, we find that, the higher the direct CO_2 injections into the deep ocean are, the higher the leakage (Figs. 3.1 a, d), the higher the relative portion leaked out in the Southern Ocean and, in the case of the simulations of the second and third approach, the amount of CO_2 that needs to be re-injected.

What this means in terms of the effectiveness of oceanic CCS is further highlighted by the comparison of the required cumulative CO_2 injections in the default simulations of the three different approaches and the respective required emission reductions needed to reach the run's specific climate target under a RCP/ECP 4.5 CO_2 emission scenario. As illustrated in Figs. 3.2 a, b, c, the approaches one, two and three represent increasingly stringent climate targets as evident from decreasing atmospheric warming relative to preindustrial conditions. Cumulative CO_2 injections by the year 2100 are largely equivalent to the required emission reduction, because only a tiny fraction of injected CO_2 has outgassed until that point in time (Figs. 3.1 d, 3.2 a). However, by the end of the injection experiments, cumulative CO_2 injections are much larger than the required emission reductions in year 3020 as indicated by the slopes of the eye-fitted lines in Figs. 3.2 b, c. This is due to the fact that the leakage in the injection experiments (Fig. 3.1, d) results in a larger CO_2 removal effort.

3.3.2 Sensitivities to $CaCO_3$ sediment feedbacks and weathering fluxes

As illustrated in Fig. 3.2 b, cumulative CO_2 injections in the *1.5°C_target$_{sed}$* simulation are about 165 Gt C (11 %) smaller until the year 3020 when compared to the *1.5°C_target* run (1562 Gt C). This smaller CO_2 injection is a result of two processes ($CaCO_3$ sediment dissolution and terrestrial weathering), which both have the net effect of adding alkalinity to the model ocean, when compared to the standard experiments without sediment feedbacks and continuous weathering fluxes. Until the end of the simulation, average ocean alkalinity has increased by 32 mmol/m^3 in the *1.5°C_target$_{sed}$* run compared to 2422 mmol/m^3 in the *1.5°C_target* run. About 84 % of this increase in global mean alkalinity can be attributed to ocean CCS, the rest is

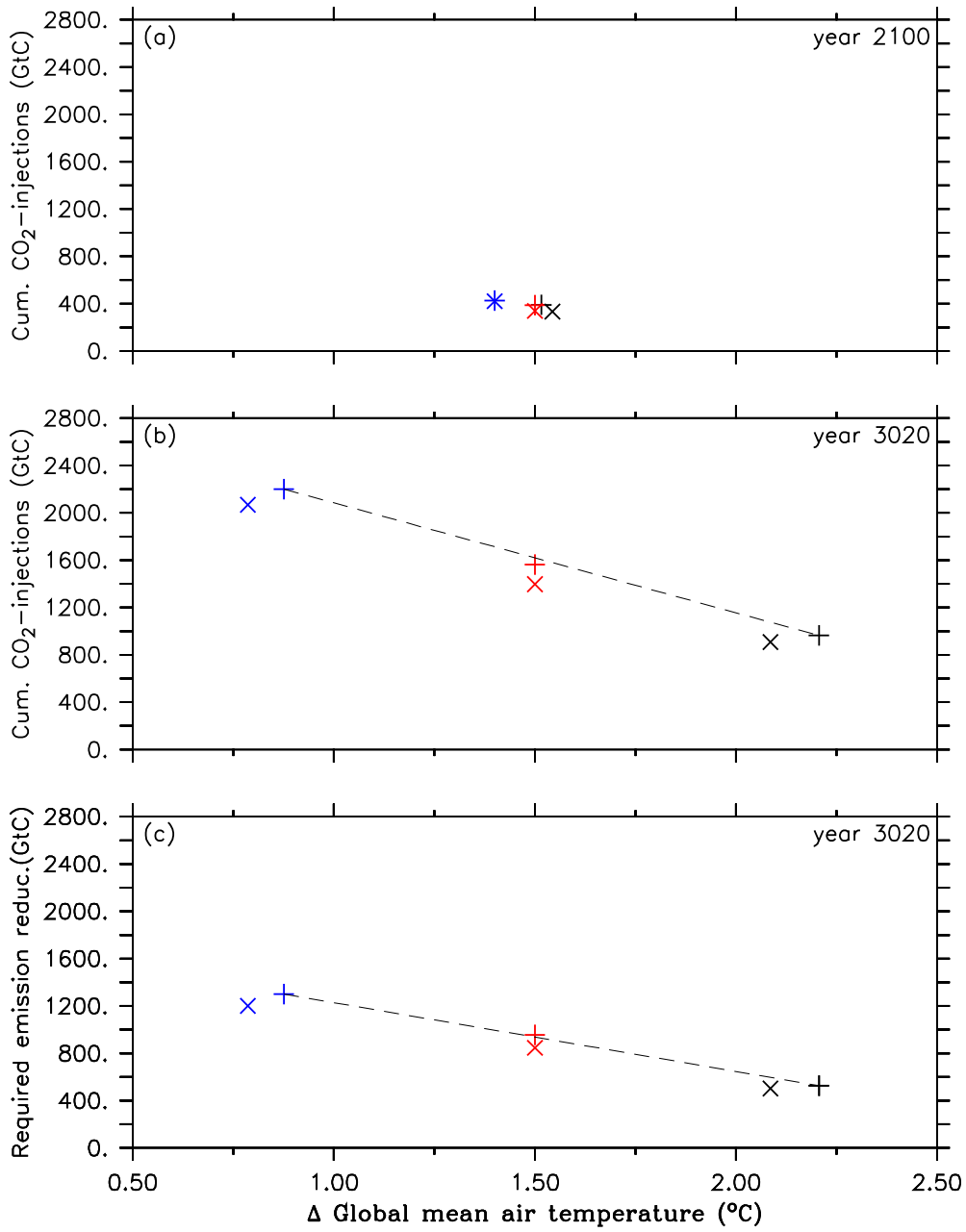

Figure 3.2: Comparison between simulations of the first approach (black symbols), simulations of the second approach (red symbols) and simulations of the third approach (blue symbols). The cross symbols refer to the default simulations with CO_2 emission forcing only and the X symbols denote simulations with CO_2 forcings and $CaCO_3$ sediment and weathering feedbacks. These symbols represent for (a) cumulative CO_2 injections and corresponding global mean temperature, relative to preindustrial, in year 2100 (b) cumulative CO_2 injections and corresponding global mean temperature, relative to preindustrial, at the end of the simulation (yr 3020), and (c) required emission reduction and corresponding global mean temperature, relative to preindustrial, at the end of the simulations. Note that the dashed black lines are eye-fitted to the results of the standard runs.

from ocean acidification according to the RCP 4.5 CO_2-emission scenario, as evident from the control run with sediment and weathering feedback. An increase in ocean alkalinity may enhance the oceanic uptake of atmospheric CO_2, however, only if waters with increased alkalinity arrive at the surface waters and lower surface-ocean pCO_2. This, in turn, reduces the required CO_2 injections to reach and maintain the 1.5°C climate target. Dissolution of $CaCO_3$ deep-sea sediments caused by the injection of CO_2 into the deep ocean at 3000m causes the dissolution of 11.8 Pmol $CaCO_3$ in the *1.5°C_target*$_{sed}$ simulation by year 3020 releasing 11.8 Pmol DIC and 23.6 Pmol alkalinity to the deep ocean. Highest $CaCO_3$ dissolution rates occur in the vicinity of the seven injection sites (Figs. B4 a, b). Hence, ocean acidification arriving in the deep ocean and ocean CCS convert sediments from a $CaCO_3$ sink (116 Gt $CaCO_3$-C at the end of the respective spin-up run) to a source of its dissolution products. A second process that contributes to the increase in ocean alkalinity is the terrestrial $CaCO_3$ weathering flux which arrives in the surface ocean via river discharge, and amounts to about 19.3 Pmol alkalinity and 9.7 Pmol C (116 Gt C) until the end of the *1.5°C_target*$_{sed}$ simulation.

Disentangling the relative role of the two processes (turning $CaCO_3$ burial into $CaCO_3$ dissolution; continuous flux of alkalinity from terrestrial weathering) with respect to stabilizing the oceanic CO_2 uptake and thereby affecting the required CO_2 injections is not trivial. Waters affected by $CaCO_3$ sediment dissolution in the deep ocean need to return to the ocean surface before having an effect on surface ocean pCO_2 and oceanic CO_2 uptake (Cao et al., 2009). The fluxes from terrestrial weathering, however, are in our simulation, continuous and constant with time (no sensitivity of weathering to changes in atmospheric pCO_2, surface air temperature or terrestrial production), and directly arrive in the surface ocean. It is thus likely that, in comparison to the standard experiments without terrestrial weathering, the latter affect atmosphere-ocean CO_2-flux well before the alkalinity input related to $CaCO_3$ dissolution. Quantifying the effect of each process to reduce the required CO_2 injection individually, however, would require additional simulations, e.g. experiments with $CaCO_3$ dissolution turned on but terrestrial weathering turned off. This is beyond the scope of this study. In

consequence of the two processes mentioned above, the required emission reduction amounts to about 846 Gt C, i.e. ~ 109 Gt C (11 %) less when compared to the *1.5°C_target* run (Fig. 3.2 b).

The net effects of sediment/weathering feedbacks on the required CO_2 injections in simulations of the second approach described above are as well represented in the injection experiments of the first and third approach, but are of smaller magnitude, i.e., 5 % less (Fig. 3.2 a, b, c).

The neglect of non-CO_2 greenhouse gases in our injection experiments may underestimate the required cumulative CO_2 injections in each approach. This is due to the fact that non-CO_2 greenhouse gases directly affect the Earth's energy balance, resulting in either warming or cooling of the atmosphere. Gases like methane and nitrous oxide warm the Earth, while aerosols such as sulfate cool it (e.g., Myhre et al., 2013). The current net effect is a small positive radiative forcing, which, although controversially debated, is expected to increase as the cooling effect of sulfate aerosols is predicted to decline over the half of this century (Moss et al., 2010; Hansen et al., 2017; Rao et al., 2017).

3.3.3 Biogeochemical impacts

Here, we present injection related biogeochemical impacts with respect to changes in pH and the saturation state of aragonite in the default simulations of the second (*1.5°C_target*) and third approach (*CO_2target_RCP2.6*) and of the respective RCP 4.5 control run. Simulations of the first approach are neglected here, because none of these are successful in reaching and maintaining the 1.5°C climate target.

At the beginning of our default simulations (year 2020), the uptake of anthropogenic CO_2 has lowered average pH at the ocean surface by about 0.12 units, relative to its preindustrial value of about 8.16 (Fig. 3.3 a). This trend continues in the control simulation until its maximum reduction of about -0.25 units in the year 2762, which stays nearly constant until the end of the simulation (Fig. 3.3 a).

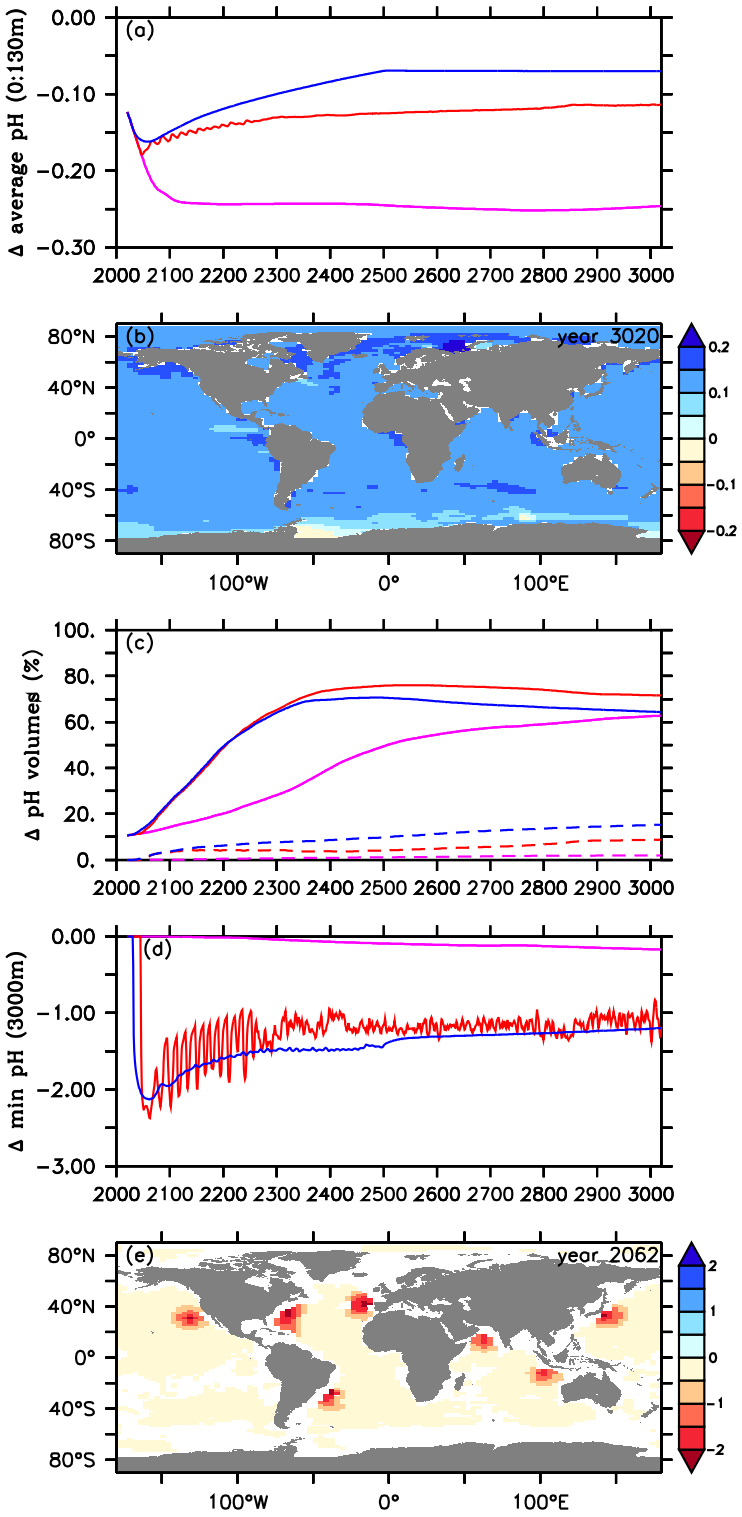

Figure 3.3: Comparison of pH values between the default RCP 4.5 control run (purple lines), the 1.5°C_target simulation (red lines) and the CO_2target_RCP2.6 simulation (blue lines) for (a) average ocean surface pH (0 to 130 m depth), (b) difference in ocean surface pH, relative to preindustrial, between the 1.5°C_target simulation and the default RCP 4.5 control run in yr 3020, (c) pH volumes of first ($\leq$ 7.8 and $\geq$ 7.4, solid lines) and second category ($<$ 7.4, dashed lines), (d) minimum pH values at 3000 m depth, and (e) difference in minimum pH at 3000 m depth between the 1.5°C_target simulation and the default RCP 4.5 control run in yr 2062.

As direct CO_2 injections lead to a decline in the atmospheric CO_2 concentration (Fig. 3.1 c) and in consequence to a lower upper-ocean carbon uptake via air-sea gas exchange, we find smaller reductions in average ocean surface pH, i.e. a reduced upper ocean acidification, after year 2045 in the *1.5°C_target* simulation and after year 2031 in the *CO_2target_RCP2.6* run (Fig. 3.3 a), i.e., shortly after their respective starting points of oceanic CCS (Fig. 3.1 a). In year 3020 the average ocean surface pH in the *1.5°C_target* simulation is about +0.13 units higher, when compared to the control run (Fig. 3.3 a). Using global mean surface ocean pH as a metric, surface ocean acidification in year 3020 is slightly more intense in the *1.5°C_target* simulation, but even reduced in the *CO_2target_RCP2.6* run. In both cases this is a direct effect of a lower atmospheric pCO_2 (Fig. 3.1 c) compared to year 2020. Amelioration of surface ocean pH shows regional variability (Fig. 3.3 b), with local maxima of the pH difference between the *1.5°C_target* simulation and the control run in the year 3020 up to +0.23 units, in particular in higher latitudes (Fig. 3.3 b). However, surface ocean acidification is less reduced in the Southern Ocean and even slightly increased in parts of the Weddell Sea, where most of the injected CO_2 leaks back into the atmosphere (Fig. 3.3 b).

The simulated ameliorations in the surface ocean pH are expected to come at the expense of strongly acidified water masses in the vicinity of the seven injection sites at 3000m depth, when compared to the RCP 4.5 control run. In order to assess how much of the global ocean volume (~ 1.3577e9 km^3) shifts to biotically critical pH values in our simulations, we define two pH categories. The first category is defined as $7.4 \leq pH \leq 7.8$ (solid lines in Fig. 3.3 c) and is chosen because studies have shown that all calcifiers such as coralline algae and foraminaferans are strongly reduced or are absent from acidified areas ($pH < 7.8$) and the overall benthic community is about 30 % less compared to normal conditions (e.g., IPCC, 2011; Fabricius et al., 2015). The second category includes pH values that are < 7.4 (dashed lines in Fig. 3.3 c). Such low pH values are for instance found in the vicinity of volcanic CO_2 vents and cause a massive drop in biodiversity (e.g., Ogden, 2013).

In our control simulation, we find a steady increase in the ocean volume characterized by 7.4 ≤ pH ≤ 7.8, from about 11 % of total ocean volume in year 2020 to about 63 % in year 3020 (Fig. 3.3 c). Oceanic CCS in the *1.5°C_target* and *CO_2target_RCP2.6* simulation leads to a much steeper increase of 'moderately' acidified waters (7.4 ≤ pH ≤ 7.8) with maximum values of 76 % and 71 %, respectively, in year 2551 (Fig. 3.3 c), but decreasing to 72 % and 64 % in year 3020. Considering our chosen category (7.4 ≤ pH ≤ 7.8) ocean CCS mainly speeds up interior-ocean acidification but does not increase the acidified volume at the end of the simulation very much. At the end of the simulation the *CO_2target_RCP2.6* simulation and the *1.5°C_target* run show an increase of affected interior-ocean water by 1 and 13 %, respectively, compared to the control run.

Respective pH volumes of the second category (< 7.4) start to appear around the year 2400 in the control simulation and then slowly increase to about 2 % until the end of the simulation (Fig. 3.3 e). In contrast, oceanic CCS directly results in volumes of the second category, which steadily increase until the year 3020 where it reaches 9 % of total ocean volume in the *1.5°C_target* simulation and 15 % in the *CO_2target_RCP2.6* run (Fig 3.3 c). The differences in both categories between the injection experiments are due to the higher cumulative mass of injected CO_2 in the *CO_2target_RCP2.6* run, leading to a smaller volume in the first category and to a bigger volume in the second one (Figs. 3.1 a, 3.2 b).

In order to further identify extreme pH related to the injections, we look at minimum pH values. These are found at 3000m depth, i.e., the depth at which oceanic CCS is carried out. Relative to preindustrial conditions, the highest reductions are found in the *1.5°C_target* simulation with about -2.37 units in year 2062, however with large regional variability (Fig. 3.3 d, e). Subsequently, the pH values in the *1.5°C_target* simulation show strong oscillations until about the year 2400, which are caused by the different annual CO_2 injection rates. By the end of the *1.5°C_target* simulation, minimum pH values in 3000m depth are up to 1 unit lower than in the control run (Fig. 3.3 d). We find a similar pattern in the *CO_2target_RCP2.6* simulation, although the pH reductions show only slight oscillations, resulting in a more constant pH

reduction than in the *1.5°C_target* simulation (Fig. 3.3 d). In comparison to the injection experiments, minimum pH values in the control run start to appear from the year 2300 onwards, leading to a reduction of about -0.17 units in the year 3020 (Fig. 3.3 d), i.e. the deep ocean feels OA very slowly.

Summarized, we observe an increasing benefit in average pH at the ocean surface with higher cumulative CO_2 injections, which comes at the expense of increasing acidified water masses in the intermediate and deep ocean with strongest reductions in the vicinity of the injection sites (Fig. 3.3 e). Figure 3.4 a, b illustrates this trade-off for the injection experiments of the second and third approach as well as for the respective control runs in year 3020. By comparing the different simulations with each other, we find that continental weathering and $CaCO_3$ sediment feedbacks lead to a slightly higher increase in average pH at the ocean surface as well as smaller minimum pH values at 3000m depth, when compared to preindustrial. This is caused by the dissolution of $CaCO_3$ sediments and the terrestrial weathering flux, which both have the net effect of adding alkalinity to the ocean and thereby increasing the buffer capacity of seawater.

The reported reductions in global average surface pH in our control simulation caused by the partial oceanic uptake of the RCP 4.5 CO_2 emissions correspond to an increase in hydrogen ions (H^+), which partly react with carbonate ions (CO_3^{2-}) to form bicarbonate ions (HCO_3^-). This leads in consequence to a reduction in the surface saturation state (Ω) with respect to the $CaCO_3$ minerals aragonite and calcite. This is of importance to marine calcifiers, because the formation of shells and skeletons generally occurs where $\Omega > 1$ and dissolution occurs where $\Omega < 1$ (unless the shells or skeletons are protected, for instance, by organic coatings) (Doney et al., 2009; Guinotte and Fabry, 2008). Since aragonite is about 1.5 times more soluble than calcite (Mucci, 1983) and since aragonite is the mineral form of coral reefs, which are of large socio-economic value, we only report here on simulated changes in the saturation state of aragonite.

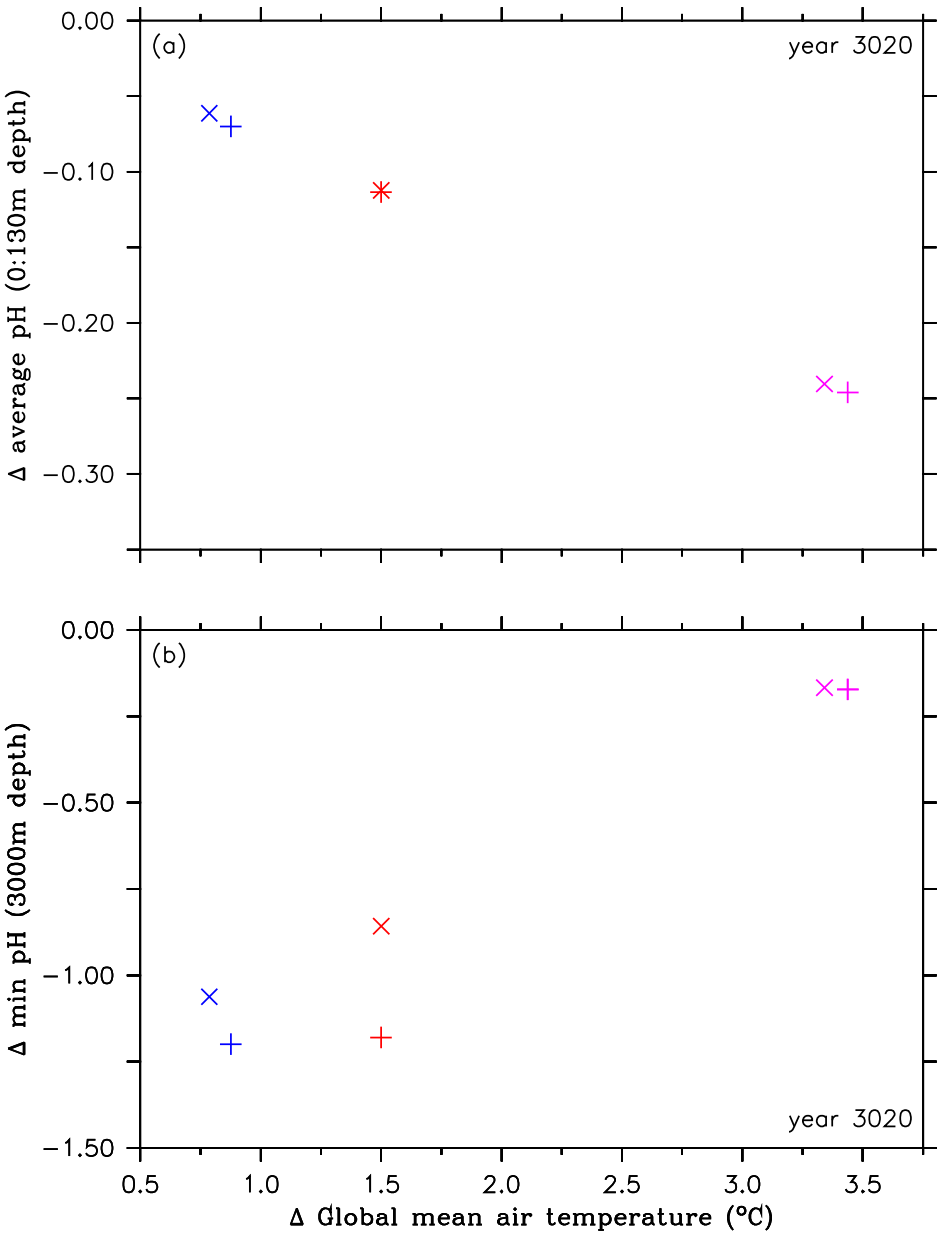

Figure 3.4: Comparison of pH values and corresponding global mean temperature in the year 3020, both relative to preindustrial, between the control simulations (purple symbols), simulations of the second approach (red symbols) and simulations of the third approach (blue symbols). The cross symbols refer to the default simulations with only CO_2 forcing and the X symbols denote simulations with CO_2 forcings and $CaCO_3$ sediment feedbacks. These symbols represent for (a) changes in ocean surface pH (0 to 130m depth), relative to preindustrial, and (b) changes in minimum pH values at 3000 m depth, relative to preindustrial.

To investigate how coral reef habitats might be impacted in our simulations, we here define the potential coral reef habitat as the volume of the global upper ocean (0:130 m, the two topmost model grid cells), which is characterized by $\Omega_{AR} > 3.4$ and ocean temperatures between 21°C and 28°C, where most coral reefs exist (Kleypas et al., 1999). We present this volume as the percent fraction of the total upper ocean volume (4.637×10^7 km^3) in our model.

For preindustrial conditions (year 1765), we find that about 37 % of the upper ocean volume are within our defined thresholds (green star in Figs. 3.5 a, b). At the beginning of our simulations (year 2020), this coral reef habitat volume has already declined to about 13 %, consistent with the current observation that many coral reefs are already under severe stress (e.g., Pandolfi et al., 2011; Ricke et al., 2013). Under the conditions of the RCP 4.5 CO_2 emissions in the control run, we observe that the potential tropical coral reef habitat volume reaches 0 % in the year 2056 and is persistently zero until the end of the simulations (Fig. 3.5 a) with a decrease in aragonite oversaturation levels being the main driver.

In our injection experiments, we find an increase in the potential tropical coral reef habitat volume right after the start of oceanic CCS (Fig. 3.5 a). In the *1.5°C_target* simulation the respective volume approaches zero (0.2 %) in the year 2044 and then steadily increases until it reaches 21 % at the end of the simulation, i.e. still 16 % less than its preindustrial state, but also 8 % more compared to the current situation (Figs. 3.5 a, b). The respective volume in the *CO_2target_RCP2.6* simulation shows an earlier and stronger increase, resulting in a volume of about 34 %, i.e. 3 % less than preindustrial, at the end of the model experiment (Fig. 3.5 a).

At preindustrial times, water masses in the upper ocean (0 - 130 m) that are undersaturated with respect to aragonite ($\Omega_{AR} < 1$) are negligible (0.2 %; Fig. 3.5 c, green star). This volume has increased to about 1 % at the beginning of our simulations. Over the course of the control run, we observe an increase with a maximum of about 9 % in the year 2212. Subsequently, the respective volume slightly decreases until it reaches a volume of about 7 % at the end of the simulation.

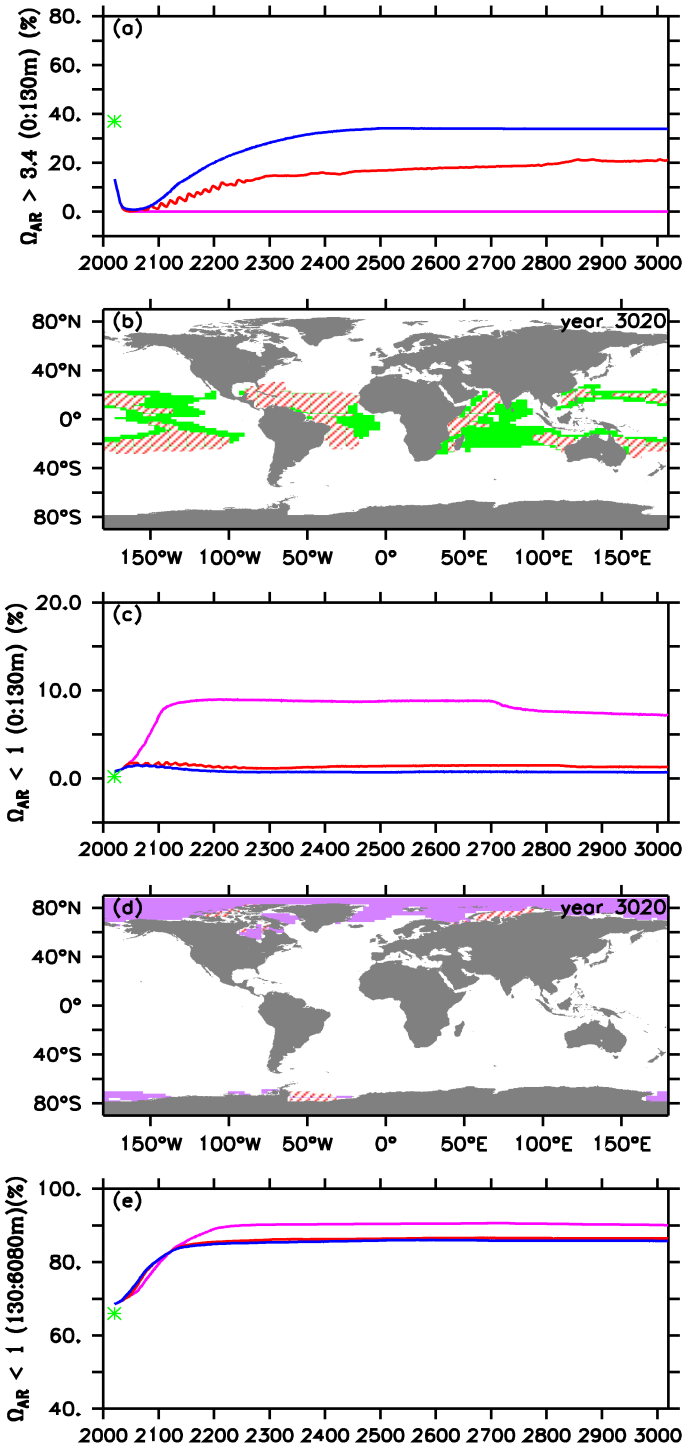

Figure 3.5: Comparison of volumes for different saturation states between preindustrial (green stars), the default RCP 4.5 control run (purple lines), the 1.5°C_target simulation (red lines), and the CO_2target_RCP2.6 simulation (blue lines) for (a) omega aragonite > 3.4 in the upper ocean (0 to 130m depth), (b) global distribution of omega aragonite > 3.4 for preindustrial (green) and the 1.5°C_target simulation (red hatching) in in the year 3020, (c) omega aragonite < 1 in the upper ocean (0 to 130m depth), (d) global distribution of omega aragonite < 1 for the default control run (purple) and the 1.5°C_target simulation (red hatching), and (e) omega aragonite < 1 in the intermediate and deep ocean (130 to 6080m depth).

As expected, undersaturated surface waters are located in higher latitudes (Fig. 3.5 d), which is for instance considered a threat to pteropods like Limacina helicina (e.g., Lischka et al., 2011). In the *1.5°C_target* and *CO_2target_RCP2.6* simulations, the respective volumes are significantly smaller and never exceed 2 % of the surface ocean volume (Fig 3.5 c, d). Undersaturated surface-water volumes in the *1.5°C_target* run are slightly higher than those in the *CO_2target_RCP2.6* simulation.

Further, we assess the volume that is undersaturated with respect to aragonite in the intermediate and deep ocean (130 - 6080 m) and present it as %-fraction the entire interior ocean volume (1.311e9 km^3). This is of interest since changes in interior-ocean Ω_{AR} may affect the growth conditions of cold-water corals (e.g., Guinotte et al., 2008; Flögel et al., 2014; Roberts and Cairns, 2014) and the dissolution depth of sinking aragonite particle.

At the beginning of the simulations, we find 69 % of the interior oceans are undersaturated with respect to aragonite, which is about 3 % more than preindustrial (Fig. 3.5 e). Subsequently, we observe a similar increase in all simulations until about the year 2122, when the control simulations continues to increase until its maximum of about 91 % in the year 2713. The volumes in the injection experiments show only a very small increase after year 2122, leading until year 3020 to values of about 86 % in both injection simulations (Fig. 3.5 e). The bigger volume in the control run is likely caused by acidified waters at the ocean surface that ventilate intermediate and mode waters (Resplandy et al., 2013).

As shown in Figs. 3.6 a, b we observe a similar trade-off in the injection experiments of the second and third approach in year 3020 as for pH (Figs. 3.4 a, b), i.e. an increase of the aragonite saturation states in the upper ocean and an increase of undersaturated conditions in the intermediate and deep ocean. Further, the effects of $CaCO_3$ sediment dissolution and continental weathering lead to the highest benefit in the upper ocean and the lowest harm in the intermediate and deep ocean (Figs. 3.6 a, b).

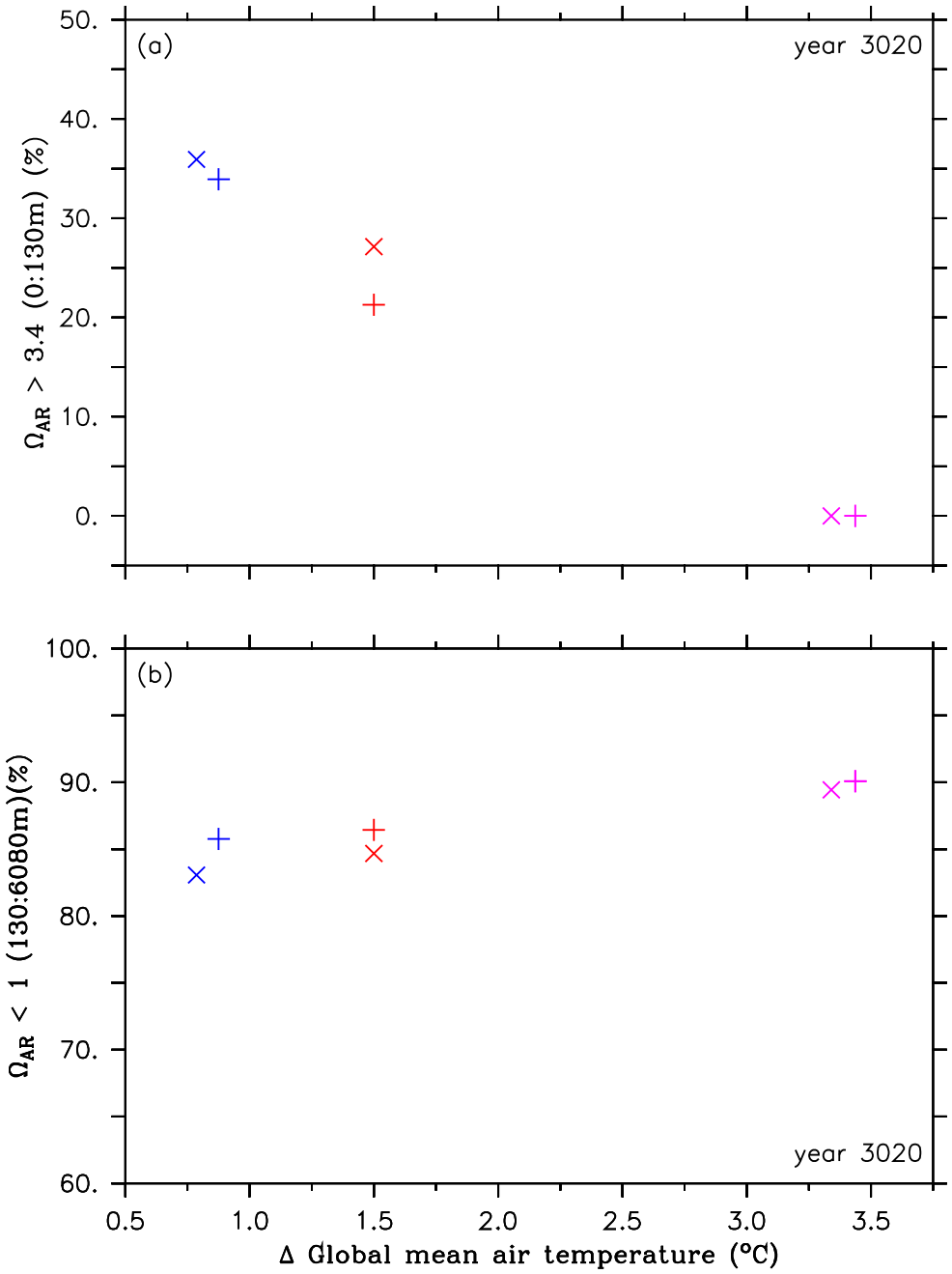

Figure 3.6: Comparison of volumes for different aragonite saturation states and corresponding global mean temperature in the year 3020, both relative to preindustrial, between the control simulations (purple symbols), simulations of the second approach (red symbols) and simulations of the third approach (blue symbols). The cross symbols refer to the default simulations with only CO_2 forcing and the X symbols denote simulations with CO_2 forcings and $CaCO_3$ sediment feedbacks. These symbols represent for (a) omega aragonite > 3.4 in the upper ocean (0 to 130m depth), relative to preindustrial, and (b) changes in minimum pH values at 3000 m depth, relative to preindustrial.

3.4 Conclusions

This modeling study explores the potential and biogeochemical impacts of three different oceanic CCS approaches as a means to fill the gap between the CO_2 emissions and climate impacts of the RCP 4.5 and the 1.5°C climate target.

The analysis of the *1.5°C_target_Cemit* simulation (first approach) reveals that it would not be sufficient to inject the residual of the RCP 4.5 CO_2 emissions (964 Gt C in total) until the year 3020 once a global mean temperature of 1.5°C is exceeded for the first time (year 2045). In order to overcome the observed overshoot of +0.7°C by year 3020 in the first approach, we find that about 600 Gt C (62 %) more need to be injected as indicated by the default simulation of the second approach, i.e., *1.5°C_target* run (Figs. 3.1 a, b, 3.2 b).

To follow the atmospheric CO_2 concentration of the RCP/ECP 2.6 as closely as possible by applying oceanic CCS would require cumulative CO_2 injections of about 2200 Gt C until the year 3020. However, global mean temperature reaches +0.9°C by the end of the *CO_2target_RCP2.6* simulation and thus undershoots the respective climate target.

The comparison between the cumulative CO_2 injections in the second and third approach and the respective required emission reductions questions the suitability of oceanic CCS for the aspired target on such a timescale, because the outgassed CO_2 amounts, which are 607 and 900 Gt C by year 3020, respectively (Figs. 3.1 d, 3.2 b, c), would need to get re-captured by additional technologies such as DACS and subsequently re-injected into the deep ocean. Nevertheless, the required emission reductions of about 955 Gt C in the second and about 1300 Gt C in the third approach, point to the massive CO_2 amounts that would need to get removed from the atmosphere under the RCP/ECP 4.5 CO_2 emission scenario in order to be compatible with the 1.5°C climate target on a millennium timescale.

Furthermore, we quantify the amount of emission reduction and oceanic CCS, respectively, required to cool the model predicted global mean temperature by 1°C

from the integrated analysis of the model runs from all three approaches (i.e. eye-fitted lines in Figs. 3.2 b, c). In the near-term (2100) this amount is found to be 446 Gt C / 1°C, which is approximately the same for both oceanic CCS and the required emission reductions as only a tiny fraction has outgassed until that point in time (see section 3.3.1). On a millennial timescale this amount is about 951 Gt C / 1°C for oceanic CCS and about 595 Gt C / 1°C (37 % less) for the required emission reductions, respectively.

Inclusion of $CaCO_3$ sediment and weathering feedbacks reduces the required cumulative CO_2 injections and required emission reductions by about 6 % in the first and third approach and by about 11 % in the second approach, respectively (Fig. 3.2 b, c). The neglect of non-CO_2 greenhouse gases in the applied forcing of the injection experiments may underestimate the cumulative CO_2 injections. In general, it is estimated that non-CO_2 climate agents contribute between 10-30 % of the total forcing (Friedlingstein et al., 2014) until the year 2100 and for business as usual simulations. Extrapolating the current contribution of greenhouse gases other than CO_2 qualitatively into the future we expect that CO_2-injections of the magnitude of the *CO_2target_RCP2.6* simulation may be required to stay safely below +1.5°C on a millennium timescale.

With respect to the biogeochemical impacts in the injection simulations of the second and third approach, we observe an increase of average pH and aragonite saturation states in the surface ocean (0 - 130 m) after the start of oceanic CCS, when compared to the RCP 4.5 control run. These are due to the direct effect of a lower atmospheric pCO_2 in the injection experiments, i.e., reduced upper ocean acidification (section 3.3.3).

Potential coral reef habitats in the upper ocean volume, which are here defined as Ω_{AR} > 3.4 and ocean temperatures between 21°C and 28°C, are observed to steadily increase after the start of oceanic CCS in the *1.5°C_target* run and the *CO_2target_RCP2.6* simulation (Fig. 3.5 a) almost reaching preindustrial levels in the *CO_2target_RCP2.6* simulation. However, the potential coral reef habitats in the

respective injection experiments are close to zero for several decades (Fig. 3.5 a), raising the question if coral reefs would be able to recover from globally inhabitable conditions during this period of time. Local application of ocean alkalinization (Feng et al., 2016) may be a technical solution to protect coral reefs during this time period, in particular in regions where coral reefs are essential for shoreline protections.

The observed reduction of ocean acidification in the surface ocean comes at the expense of more strongly acidified water masses in the intermediate and deep ocean, with strongest reductions in pH in the vicinity of the seven injections sites (Figs. 3.3 d, e). Although it is difficult to predict how this would impact marine ecosystems, it is very likely that such conditions would put them under severe stress.

Overall, the trade-off between injection-related damages in the deep ocean and benefits in the upper ocean illustrate the challenge of evaluating the offset of local harm against global benefit, which is very likely the subject of any deliberate CO_2 removal method. Leaving aside the massive economic effort associated to ocean CCS of the size needed to reach the 1.5°C climate target, humanity will have to decide whether severe stress, potentially loss, of deep-sea ecosystems is acceptable when paid off by conserving or restoring surface ocean ecosystems to a large extent.

Acknowledgements

The model data used to generate the table and the figures will be made available at http://thredds.geomar.de/de. The Deutsche Forschungsgemeinschaft (DFG) supported financially this study via the Priority Program 1689.

4 Integrated Assessment of Carbon Dioxide Removal

This chapter is based on a submitted manuscript to the science journal Earth's Future and is currently under review: Rickels, W., Reith, F., Keller, D. P., Oschlies, A., and Quaas, M. F. (2017).

Abstract. To maintain the chance of keeping the average global temperature increase below 2°C and to limit long-term climate change, removing carbon dioxide from the atmosphere (Carbon Dioxide Removal, CDR) is becoming increasingly necessary. We analyze optimal and cost-effective climate policies in the Dynamic Integrated Assessment Model of Climate and the Economy (DICE2016R) and investigate i) the utilization of CDR under different climate objectives, ii) the sensitivity of policies with respect to carbon cycle feedbacks, and iii) how well carbon cycle feedbacks are captured in the carbon-cycle models used in state-of-the-art integrated assessment models. Overall, the carbon cycle model in DICE2016R shows clear improvements compared to its predecessor, DICE2013R, capturing much better long-term dynamics and also oceanic carbon outgassing due to excess oceanic storage of carbon from CDR. However, this comes at the cost of a (too) tight short-term remaining emission budget, limiting the suitability to analyze low emission scenarios accurately. With DICE2016R, the compliance with the 2°C goal is no longer feasible without negative emissions via CDR. Overall, the optimal amount of CDR has to take into account i) the emission substitution effect and ii) compensation for carbon cycle feedbacks.

4.1 Introduction

Achieving the 2°C and even more the 1.5°C goal is unrealistic without intentional atmospheric carbon dioxide removal (CDR) (Collins et al., 2013; Rockström et al., 2016; Rogelj et al., 2016b). How effectively CDR could contribute to mitigate climate change is still very uncertain (Fuss et al., 2014; Smith et al., 2015; Tokarska and

Zickfeld, 2015; Anderson and Peters, 2016; Field and Mach, 2017). One central issue is the storage of the carbon removed from the atmosphere. Especially carbon cycle feedbacks, saturation effects, and outgassing of carbon may limit the effectiveness of CDR (Vichi et al., 2013; Fuss et al., 2014; Tokarska and Zickfeld, 2015, Jones et al., 2016). For assessing the potential of CDR in economically efficient climate policies, the central methodological question thus is how well these feedbacks and effects are reflected in carbon cycle models used in integrated assessment models (IAM).

A rigorous scientific assessment of these issues is lacking so far, in particular when taking the economic feedbacks and efficient choice of CDR patterns into account. Here, we analyze optimal climate policies (including CDR) in the dynamic integrated assessment model of climate and the economy DICE and investigate i) the utilization of CDR under different climate objectives, ii) the sensitivity of policies with respect to carbon cycle feedbacks, and iii) how well carbon cycle feedbacks are captured in the carbon-cycle box models used in state-of-the-art integrated assessment models.

We use DICE in its most recent version (Nordhaus, 2017) and analyze in addition how the results change if we replace the current carbon cycle model with the carbon cycle model from the previous version DICE2013R (Nordhaus and Sztorc, 2013) or with the carbon cycle model from the recent integrated assessment model by (Gerlagh and Liski, 2017). We focus on storage of carbon from CDR in the ocean, covering a broad range of specific CDR methods that are utilized incrementally according to their marginal deployment costs. To validate our integrated assessment of CDR we implement the optimal climate policies in the non-linear Bolin and Eriksson Adjusted Model (BEAM) (Glotter et al., 2014) and the intermediate complexity University of Victoria Earth System Climate Model (UVic ESCM) (Weaver et al., 2001; Eby et al., 2013).

CDR simulations in Earth system models suggest that the efficiency decreases with the total amount of “negative emissions” (i.e. carbon dioxide removed from the atmosphere and stored in the ocean or some other reservoir) (Vichi et al., 2013; Tokarska and Zickfeld, 2015; Jones et al., 2016). Removing carbon from the

atmosphere results in reduced uptake of or even release of carbon from the terrestrial biosphere and the ocean for modest or strong removal scenarios, respectively. Enhancing oceanic carbon uptake (by for example ocean alkalinity management) implies that not only atmospheric but also terrestrial carbon is added to the ocean and vice versa in case of terrestrial carbon uptake enhancement (by for example afforestation) (Keller et al., 2014). Without "extra" carbon removal to compensate for these carbon cycle feedbacks, desired atmospheric carbon reduction targets cannot be achieved (Jones et al., 2016).

The integrated assessment of CDR so far has focused on the role of terrestrial CDR (in particular Bioenergy with Carbon Capture and Storage, BECCS), analyzing how this sector would contribute to the required energy transition to achieve low-emission pathways (Azar et al., 2010; Kriegler et al., 2013; van Vuuren et al., 2013; Rose et al., 2014). Integrated assessment models (IAMs) have been used to analyze implications of terrestrial CDR for land use, water consumption, and food production (Smith et al., 2015; Boysen et al., 2017b; Boysen et al., 2017a). The influence of carbon cycle feedbacks on the efficiency of CDR has received less attention. One exemption is the study of (Chen and Tavoni, 2013) who investigate CDR by direct air capture (DAC) as additional mitigation option in the integrated assessment model WITCH (World Induced Technological Change Hybrid). Based on their standard DAC deployment scenario (without oceanic outgassing) they use information from Vichi et al. (2013) to estimate the average reduction in effective atmospheric carbon removal and correct the effectiveness of DAC for this outgassing. With this general correction, they find that instead of extra removal to compensate for this outgassing about 30 percent less DAC is deployed compared to their standard specification. This can be explained by the fact that in their specification the effectiveness of DAC is explicitly reduced and not implicitly determined by carbon cycle feedbacks as we do in our study.

Few studies investigate whether and under which conditions IAMs produce climate and carbon cycle outcomes which are consistent with outcomes of state-of the art earth system models (Warren et al., 2010; van Vuuren et al., 2011; Hof et al., 2012). Warren et al. (2010) find that the selected IAMs show a significant variation in

climate outcomes whereby some even result in inconsistent estimates for carbon concentrations and temperature response, compared to IPCC simulations. They suggest for example that FUND underestimates the temperature response and results therefore in less ambitious mitigation strategies than optimal. However, van Vuuren et al. (2011) finds that the outcomes of the IAMs are within the range of more complex models. Still, they conclude that differences between carbon and climate outcomes across IAMs are significant and matter with respect to the derived policy advice. Hof et al. (2012) also find significant differences but conclude that the implications on optimal policies is small, relative to other factors, and argue that for example a rather strong carbon cycle feedback found in the PAGE-2002 model has only modest impacts on near term mitigation due to discounting. In conclusion, the differences between carbon cycle models in IAMs matter in particular when considering exogenously given climate targets like the 2°C goal instead of endogenously derived optimal climate outcomes.

Furthermore, the carbon cycle models applied in the IAMs are continuously reviewed and updated with respect to new findings. For example, Glotter et al. (2014) show that the carbon cycle in DICE2013R fails to properly describe the long-term development of in particular oceanic carbon uptake. In response, the carbon cycle model in DICE2016R is calibrated to include improved long-run dynamics (up to 4000 years) (Nordhaus, 2017). Yet, DICE2016R has not yet been part of a comprehensive assessment with respect to the appropriateness of its carbon cycle model. Furthermore, the suitability of carbon cycle models applied in IAMs to capture carbon cycle feedbacks with respect to CDR has not yet been systematically assessed.

Only few carbon cycle models used in IAMS are capable of capturing these feedbacks with respect to (oceanic) CDR. For example, PAGE, MERGE, FUND, and REMIND rely on impulse response representations of the (oceanic) carbon cycle (van Vuuren et al., 2011). This type of carbon cycle model does not allow keeping track of carbon removed into other reservoirs and outgassing of sinks. While impulse-response representations can capture very well non-linarites in atmospheric carbon development, box-type representations become indispensable if options like (oceanic) CDR are considered under accounting for carbon cycle feedbacks (Rickels and

Lontzek, 2012). In this paper, we thus focus on box-type carbon cycle models that are used in IAMs.

The paper is structured as follows. Section 2 presents our methodical approach, explaining first the derivation of optimal mitigation policies (including CDR) in DICE and explaining secondly the comparison of the results obtained with linear carbon cycle models to non-linear carbon cycle and Earth system models. Section 3 presents and discusses our results, Section 4 discusses potential limitations of our study, and Section 5 concludes.

4.2 Methods

4.2.1 Derivation of optimal climate policies including CDR

We derived optimal climate policies with the widely used integrated assessment model DICE in its most recent version (i.e. DICE2016R) (Nordhaus, 2017). The time horizon we considered is the DICE2016R planning period, starting in year 2015 and running until year 2500. We used three different carbon cycles models in combination with the economic and climate module from DICE2016R: i) the carbon cycle model from DICE2016R itself (labeled *CC16* in the following), ii) the carbon cycle model from DICE2013R (Nordhaus and Sztorc, 2013) (labeled *CC13*), and iii) the carbon cycle model from (Gerlagh and Liski, 2017) (labeled *CCGL*). All three carbon cycles models are box-models with linearized carbon fluxes between the boxes. Our research question restricts the carbon cycle models we consider to those that allow the tracking of carbon removed from the atmosphere and added to non-atmospheric carbon reservoirs like the ocean. The box models we have chosen have this property. In both, *CC16* and *CC13*, the three boxes represent atmosphere, upper ocean, and lower ocean. *CCGL* is instead based on the assumption that atmosphere and upper ocean instantaneously equilibrate, implying that atmospheric carbon stock is a constant fraction of the carbon stock in the first box, whereas the second and third box

represent the terrestrial biosphere and the deep ocean carbon stocks, respectively. *CC16* and *CC13* differ only in their calibration. While *CC13* is primarily calibrated to capture short-term dynamics of the global carbon cycle (until the first 100 years), *CC16* is calibrated to capture also long-term dynamics (up to 4000 years) (Nordhaus, 2017). DICE2016R operates in 5 year time steps and the carbon cycle models are calibrated accordingly. In *CCGL* changing the time steps does not only imply an adjustment of the transition matrix between the boxes but also the share of emissions (and CDR) entering the different boxes. While for one year time steps all emissions enter the upper box (atmosphere and upper ocean), for time steps larger than one year, a certain fraction enters directly the other two boxes. For all three carbon cycle model specifications we used the climate model (forcing and temperature specifications) from DICE2016R, its assumptions about the development of exogenous forcing (resulting from other GHG emissions and aerosol emissions), its specification of economic dynamics, and the objective function. More details and the parametrization of the three carbon cycles are presented in the Supplementary Information C1.

We analyze three different mitigation frameworks: i) optimal mitigation where the cost of mitigation are weighted against the benefits of reduced climate damages (labeled *CBA* in the following), ii) cost-minimal mitigation under compliance with the 2°C goal (labeled *2C*), and iii) cost-minimal mitigation under compliance with the 2°C goal from the year 2100 onwards (labeled *2C2100*). In *CBA* the optimal level of climate change is endogenously determined, in *2C* and *2C2100* the level of climate change is exogenously constrained, whereas in the latter the level of overshooting is endogenously determined. We neglected the possibility to consider another overshooting framework where compliance with the 1.5°C goal would be achieved from 2100 onwards, as investigation of such a tight climate target is only sensible under additional mitigation options for non-CO_2 emissions and for land-use change emissions (Rogelj et al., 2016a; Su et al., 2017). Here, we focused on the role of CDR and carbon cycle feedbacks and left therefore as many other components of the original DICE2016R model as possible unchanged (including its assumptions about exogenous forcing resulting for example from non-CO_2 emissions).

In addition to abatement-only scenarios, we analyzed abatement with CDR within the three mitigation frameworks, distinguishing between three CDR options: i) (hypothetical) perfect storage in some reservoir disconnected from the boxes of the carbon cycle model, ii) oceanic CDR, i.e. storage in the deep ocean box, and iii) and oceanic CDR under the (false) assumption of perfect storage. With the first option, carbon was actually removed from the carbon cycle. Such an option would correspond to geological storage under the unrealistic assumptions that there are no scarcity issues and no leakage. The first option was primarily used as benchmark for the second option to investigate how carbon cycle feedbacks in the simple carbon cycle models change the optimal CDR application. With the second option, carbon was removed from the atmosphere and added to the deep ocean. Here, we considered rather generic oceanic CDR and accordingly, such an option would correspond to a set of CDR methods, aiming at increasing deep ocean carbon uptake. Probably the best analogy is achieved by considering deep ocean carbon injection (Marchetti, 1977; IPCC, 2005), however, also other CDR methods with significant deep ocean carbon uptake are relevant. With the third option, carbon was removed from the atmosphere under the assumption of perfect storage, however, actually added to the deep ocean. Accordingly, the decision-maker observes in the next period that his expectations about carbon stocks were wrong. Thus, after each time step a new optimal policy is derived, however with the actual values for the carbon stocks in the different boxes resulting from oceanic CDR. Consequently, here the mitigation policy was iteratively derived under constant updating with respect to the *true* values for the carbon stocks and corresponding forcing and temperature change. The third option provides insights regarding unforeseen leakage from submarine geological storage (here with the extreme assumption of full leakage into the deep ocean) under the condition that changes in carbon stocks are properly monitored. The third option also provides insights to which extend an inaccurate carbon cycle model results in less efficient climate policies under the condition of perfect monitoring.

We introduced CDR as new variable into DICE2016R. The original specification of DICE2016R allows “net negative emissions” from the year 2165 onwards. Negative emissions are simply abatement rates larger than one under the

assumption of perfect storage as discussed above. However, the negative emissions in the original DICE2016R specification are constrained to not exceed 20 percent of the business-as-usual industrial emissions in each time step. In contrast, we imposed no constraints on the amount of CDR except that atmospheric carbon concentration cannot be reduced below preindustrial levels (below we discuss the implication of relaxing this assumption).

There is a broad range of unit cost estimates for the various CDR measures in the literature, ranging for example for ocean alkalinity management from 40 USD/t CO_2 up to 144 USD/t CO_2 (Harvey (2008) and (Paquay and Zeebe, 2013) respectively). The differences arise from different assumptions regarding the implementation (e.g. scale and technology applied) and from the uncertainty about cost components. Furthermore, the studies neglect potential cost-savings via technological progress and economies of scale, but also neglect potential cost increases via (general equilibrium) price effects if the methods are applied on a larger-scale. We believe that the operational cost are best described by a convex cost function capturing increasing marginal costs, which holds a) within a specific CDR method and b) across CDR methods: a) because specific CDR methods are most likely applied to the most suitable locations first (e.g. close to an appropriate lime deposite in case of alkalinity management) while increasing the amount of CDR requires more effort (e.g. larger transport distance for lime and larger transport distance on sea); b) because generic (oceanic) CDR implies that a set of CDR methods are considered which can be ordered according to their unit cost (like the Mc Kinsey abatement cost curve, (McKinsey&Company, 2010)). While almost certainly small-scale CDR (in the ton or even small megaton scale) can be carried out rather cheaply, the major uncertainty surrounds the operational cost of large-scale CDR application (in the gigaton scale). Accordingly, we assumed a simple linear-quadratic cost function for CDR operation:

$$CDRcost(GtC) = c_1 * CDR + c_2 * (GtC)^2 \quad (1).$$

CDR is measured in *Gt C,* and c_1 in σ_{13} and c_2 in $10^{12} USD/GtC^2$. Parameter c_1 was set to 0.29328 $10^{12} USD/GtC$, corresponding to 80USD/tCO_2 for the initial amount of (oceanic) CDR (Klepper and Rickels, 2012). For parameter σ_{22} we considered a broad parameter range (to reflect the uncertainty about the scale of CDR), ranging from 0.01833 $10^{12} USD/GtC^2$ to 18.33 σ_{32}, corresponding to marginal CDR cost at the first Gt C of 90 USD/t CO_2 and 10,080 USD/t CO_2, respectively. The marginal CDR cost curve is linear in the amount of CDR, and increasing with a slope c_2. In order to study the effect of CDR cost we vary this parameter c_2, i.e. the slope of the marginal CDR cost curve, in our analysis.

An extra social cost of CDR arises in case of non-perfect storage from carbon cycle feedbacks and is determined by the carbon cycle models. Consequently, CDR allows saving the atmospheric social cost (i.e. the carbon price) but causing at the same time oceanic social cost (arising from the carbon cycle feedbacks). Accordingly, for equal operational cost, the optimal amounts of CDR (and subsequently the optimal amount of emission via the substitution effect) differ for the three different carbon cycle models. Note that this approach is different to (Chen and Tavoni, 2013) who explicitly corrected the effectiveness of the CDR methods (i.e. increasing effectively its units costs.)

The DICE model with the different carbon cycles for the different mitigation frameworks has been solved with the constrained optimization package Knitro in AMPL. All model files are included in the supplementary information.

4.2.2 Assessment of optimal climate policies with respect to carbon cycle feedbacks

For the assessment of the appropriateness of linear box models for the investigation of CDR in integrated assessment models, we implemented the derived optimal policies in the i) the non-linear Bolin and Eriksson Adjusted Model (BEAM) (Glotter et al. (2014)) and the intermediate complexity University of Victoria Earth System Climate Model (UVic ESCM) (Weaver et al., 2001; Eby et al., 2013). For this exercise, we

followed Glotter et al. (2014) by extending the time-horizon until the year 4000. Until the year 2500 we imposed the optimal climate policies derived by the integrated assessment model and beyond 2500 we assumed that both emissions and CDR were zero. This allowed investigating how well the linear box models simulate potential outgassing events and corresponding temperature responses of long-term CDR policies. Note that with a time-horizon beyond the year 2500 in the optimization exercise, the optimal policies would have suggested to sustain positive CDR in case of outgassing. We compare the distribution of carbon in the carbon cycle for the various mitigation scenarios in the year 4000 against a reference scenario (with zero emissions from 2015 onwards). In both models (BEAM and UVic ESCM) we imposed the same assumptions about the development of exogenous forcing as in DICE2016R.

BEAM is also a three-box model, containing the atmosphere, upper ocean, and deep ocean carbon stocks. However, the carbon fluxes between atmosphere and upper ocean are influenced explicitly by the nonlinear ocean carbonate chemistry and a temperature feedback (affecting the carbon storage and CO_2 solubility) (Glotter et al. (2014). Oceanic CDR is implemented by simply adding carbon to the carbon stock in the deep ocean. The application of BEAM is restricted to the carbon cycle which we combined with the climate model from DICE2016R.

UVic consists of three dynamically coupled main components: a three-dimensional general circulation ocean model based on the Modular Ocean Model MOM2 (Pacanowski, 1996) including a marine biogeochemical model (Keller et al., 2012) and a dynamic-thermodynamic sea-ice model (Bitz and Lipscomb, 1999), a terrestrial vegetation and carbon-cycle model (Meissner et al., 2003) based on the Hadley Center model TRIFFID (Top-down Representation of Interactive Foliage and Flora Including Dynamics) and the hydrological land component MOSES (Met Office Surface Exchange Scheme), and a one-layer atmospheric energy-moisture balance model (based on (Fanning and Weaver, 1996). All components have a common horizontal resolution of 3.6° longitude x 1.8° latitude. The oceanic component has 19 vertical levels with thicknesses ranging from 50 m near the surface to 500 m in the

deep ocean. Formulations of the air-sea gas exchange and seawater carbonate chemistry are based on the OCMIP abiotic protocol (Orr et al., 1999).

CDR in UVic was simulated by injecting CO_2 at seven separate injections sites, which are located in individual grid boxes near the Bay of Biscay (42.3° N, 16.2° W), New York (36.9° N, 66.6° W), Rio de Janeiro (27.9° S, 37.8° W), San Francisco (31.5° N, 131.4° W), Tokyo (33.3° N, 142.2° E), Jakarta (11.7° S, 102.6° E) and Mumbai (13.5° N, 63° E) (Reith et al., 2016, Figure 1). Injections were simulated to be carried out at 2900 m depth to minimize leakage and maximize retention time. At this depth, liquid CO_2 is denser than seawater, which has the additional advantage that any undissolved droplets would sink rather than rise to the surface (e.g., IPCC, 2005). The simulated injection were based on the OCMIP carbon sequestration protocols and carried out in an idealized manner by adding CO_2 directly to the dissolved inorganic carbon (DIC) pool (Orr et al., 2001). Thus, we neglected any gravitational effects and assumed that the injected CO_2 instantaneously dissolves into seawater and is transported quickly away from the injection point and distributed homogenously over the entire model grid box with lateral dimensions of a few hundred kilometers and many tens of meters in the vertical direction (Reith et al., 2016).

We also conducted sensitivity experiments for our CDR simulations that focus on the parameterization of vertical ocean mixing. Vertical ocean mixing plays a key role in i) determining ocean circulation, ii) biogeochemical cycles, and iii) ocean to atmosphere heat and carbon fluxes. We varied this parameterization by increasing and decreasing it by 50 % (hereafter, denoted by Kv_low and Kv_high), which is within the range of observational estimates (Duteil and Oschlies, 2011). Further details about the application of BEAM and UVic ESCM are presented in the Supplementary Information C2.

4.3 Results and Discussion

Figure 4.1 shows that there is a significant difference between oceanic CDR and perfect CDR for the *CCGL* carbon cycle model and almost no difference for *CC13* carbon cycle model, reflecting that *CCGL* has the fastest exchange between the boxes, whereas *CC13* has the lowest exchange, such that oceanic CDR is almost "perfect" in *CC13*. The CCGL box model assumes that atmospheric carbon is a constant fraction of the carbon stock in the upper box. Consequently, excess carbon in the deep ocean enters directly the atmosphere, while in the specification with *CC13* and *CC16* it needs to pass through the upper ocean box. However, with the updated calibration of *CC16* (in comparison to *CC13*), excess deep ocean carbon is more easily returned to the atmosphere, as becomes evident by the lower amount of CDR required with perfect storage in comparison to oceanic storage.

In contrast to (Chen and Tavoni, 2013) we find that the presence of carbon cycle feedbacks does not necessarily result in lower CDR deployment compared to the "perfect storage" case. While obviously higher operational cost result in less CDR deployment, the difference between oceanic CDR and perfect storage indicate that as long CDR is sufficiently cheap (from an operational cost perspective), extra CDR is carried out to compensate for leakage to the atmosphere and carbon cycle feedbacks (less ambient carbon uptake by the sinks). However, this holds only true until a certain value for the operational cost, as measured by the slope of the marginal cost curve: if the marginal cost function becomes too steep, it becomes too costly to carry out the extra CDR and in case of fast exchange between the boxes (*CCGL* carbon cycle model) less oceanic CDR is carried out compared to perfect storage.

The plots for the cumulative amount of CDR in the *CBA* framework show a few kinks. For all three carbon cycles we observe a kink towards the right end side of the plots, for *CC16* close to 1, for *CC13* around 0.8, and for *CCGL* (even though less pronounced) around 0.4. These kinks are explained because i) we constraint atmospheric carbon concentration by its preindustrial level and ii) we leave the other assumptions of DICE2016R with respect to exogenous forcing and land-use emissions unchanged.

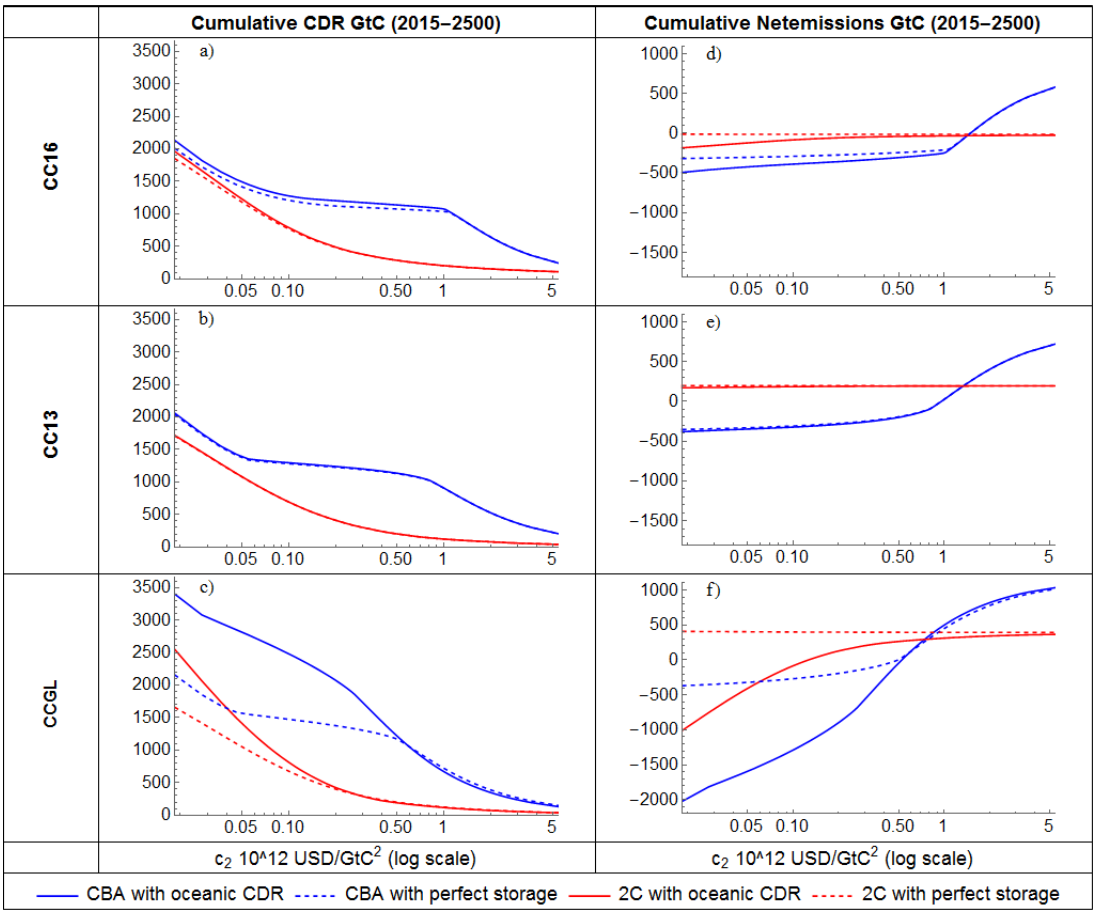

Figure 4.1: Cumulative CDR and Net Emissions as Function of Convexity of CDR cost for the period 2015 until 2500.

The figure shows the cumulative optimal amount of CDR (left panel) and cumulative optimal amounts of net emissions (right panel) as function of c_2, the slope of the marginal CDR cost curve. The upper panel corresponds to *CC16* (the carbon cycle model from DICE2016R), the middle panel corresponds to *CC13* (the carbon cycle model from DICE2013R), and the lower panel corresponds to *CCGL* (the carbon cycle model from Gerlagh and Liski (2017)). Each box displays the optimal amounts for *CBA* (blue lines) and *2C* (red lines) for two CDR options, oceanic CDR (solid lines) and perfect storage (dashed lines).

Due to increasing exogenous forcing (up to 1 W/m^2 until the year 2100 and constant at this value thereafter) there is some non-CO_2 induced warming, causing damages. Accordingly, it would be optimal for a flat marginal CDR cost curve to decrease atmospheric carbon concentration below its preindustrial level to achieve negative CO_2 forcing (compared to the preindustrial level) to compensate for the non-CO_2 forcing. Accordingly, without that constraint we would observe more cumulative CDR to the left of this kink. The second kink which is only present for *CC13* and *CCGL* (in *CC16* the transition is smooth) coincides with a substitution effect

becoming present: here the amount of emissions actually increases in response to the availability of CDR. We discuss this issue in more detail below.

Looking at the optimal amounts of net emissions for the *2C* framework indicates that *CC16* is most restrictive in terms of the (remaining) emission budget. While both, *CC13* and *CCGL*, still allow for positive cumulative net emissions for compliance with the 2°C degree goal, *CC16* requires already negative cumulative net emissions for this goal. Note that *CCGL* shows significant negative cumulative net negative emissions for a flatter marginal CDR cost curve in case of oceanic CDR but not in case of perfect storage due to the compensation for carbon leakage and carbon cycle feedbacks. However, for all three carbon cycle models, the optimal amounts of CDR and net emission are higher in the *CBA* frameworks than in the *2C* framework. This can be explained by the different time profile of CDR utilization and in turn different substitution effect to which we turn next.

Figure 4.2 shows in the left panel a similar information as Figure 4.1, but including the time profile of cumulative oceanic CDR (until 2500). The right panel shows the distribution of carbon emissions in the different carbon boxes in the year 4000 as function of the cumulative amount of CDR. Furthermore, the right panel contains information about peak and average temperature for the period 2015 until 2500 and for the period 2500 until 4000. Both panels provide the information for the three climate policy scenarios, *CBA*, *2C*, and *2C2100* from the top to the bottom, respectively. The figure provides the information for *CC16* (the corresponding figures for *CC13* and *CCGL* are provided in Supplement C, respectively).

The time profile reveals the different utilization of CDR in DICE in the different mitigation frameworks. In the *CBA* framework the bulk of CDR is carried out beyond 2100 and CDR is used as long-term strategy to reduce the atmospheric carbon concentration (a). This becomes evident by looking at the corresponding distribution of emissions in the carbon cycle (e) as function of cumulative CDR. First, there is almost no substitution effect with respect to emissions present until cumulative CDR reach 1200 Gt C. Second, there is only a modest decline in peak

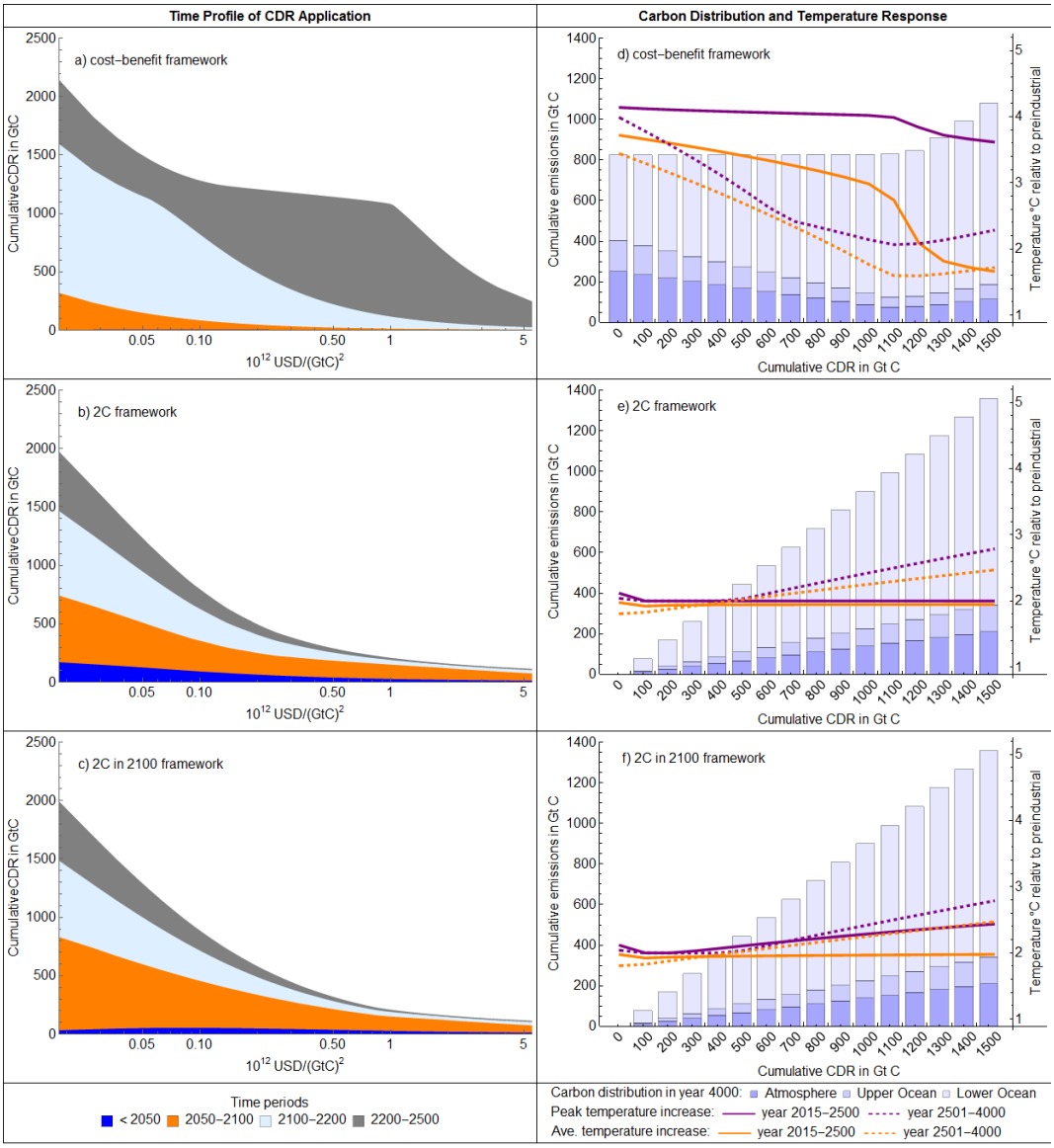

Figure 4.2: Time Profile of CDR Application (until year 2500), Carbon Distribution in year 4000, and Temperature Response until year 2500 and 4000 in CC16.

The left panel shows similar information as Figure 4.1, but including the time profile of CDR utilization for the different mitigation frameworks (*CBA*, *2C*, and *2C2100* in a), b) and c), respectively). The right panel shows the distribution of the carbon emissions (from 2015 until 2500) in the year 4000 across the different carbon reservoirs in dependence of the cumulative amount of CDR for the different mitigation frameworks (*CBA*, *2C*, and *2C2100* in d), e) and f), respectively). The right panel also includes information about peak and average temperature for the period 2015-2500 and 2501 until 4000.

temperature (red line) compared to the situation without CDR. The reason is that the DICE model (also in the 2016R specification) has a rather modest estimate for climate impacts, suggesting that in a framework where the cost of abatement are weighted

against the avoided damages of climate change a peak temperature increase of about 4°C is optimal. Consequently, the optimal amount of emissions is strongly influenced by the evolution of carbon intensity and the backstop price for emission-free energy (which are both given exogenously). CDR is postponed into the future when the economy is very rich (due to continuous growth in the DICE economic model), making CDR cheaply affordable. This is indicated by the stronger decline in average temperature. While without CDR the decline in temperature is limited by the rather slow natural carbon uptake, with CDR this option is used to speed up this process. Only for a rather flat marginal CDR cost function we observe some substitution effect and some effect on atmospheric peak temperature. Turning to the long term effects, we see that for CDR up to a cumulative amount of 1100 Gt C, also peak and average temperature beyond 2500 are declining because of speeding up the natural carbon uptake. However, for larger CDR amounts, resulting in increasing cumulative emissions, we observe that peak and average temperature are increasing in the cumulative amount of CDR, indicating that carbon previously removed returns to the atmosphere (as indicated by the increasing grey atmospheric bar), causing peak and average temperature to rise again.

In the *2C* framework, CDR has a very different role compared to the *CBA* framework. A significant amount of CDR is deployed already before 2100 with an increasing share relative to the total amount of CDR with steeper marginal CDR cost curve. Furthermore, CDR is already deployed before 2050 and we observe a significant emission substitution effect. As discussed above, *CC16* is most restrictive in terms of the (remaining) emission budget. Without CDR the 2°C target cannot be achieved, however, already a cumulative amount of 100 Gt C CDR is sufficient (here the solid red line indicating peak temperature drops to 2°C) for compliance with 2°C. Increasing amounts of CDR result in increasing amounts of cumulative emissions, in turn with consequences for the temperature response beyond 2500. Without sustained CDR, the carbon added to the oceanic reservoir equilibrates with the upper ocean and atmosphere and we observe both, a peak and average warming beyond 2500.

The utilization of CDR in the *2C2100* framework is only slightly different compared to the *2C* framework. The time profile in the lower left panel (c) shows that

less carbon is removed from the atmosphere before 2050, instead the majority of CDR is utilized in the period 2050 until 2100 because the 2°C goal has to be achieved by 2100. Accordingly, the lower right panel (f) shows that peak temperature and therefore temperature overshooting increases in the cumulative amount of CDR with the same consequences for long-term warming (after switching CDR off) as in the *2C* framework.

The time profiles and distribution plots for *CC13* and *CCGL* look similar (Figure C2 and Figure C3 in the Supplementary Information, respectively), however there are two noticeable differences. First, due to the very slow exchange between carbon reservoirs in *CC13* all emissions end up in the deep ocean in the year 4000 for CDR application which cumulatively exceeds 1,000 Gt C in the *CBA* framework. Furthermore, we even observe that extra carbon, in excess of the cumulative emissions is removed from the atmosphere to the deep ocean, implying that atmospheric carbon content is lower than in the reference scenario without any emissions from the year 2015 to the year 4000. However, for *2C* and *2C2100* we do not observe this effect for *CC13* because here the substitution effect with respect to abatement results in a too strong emission increase. Still, the atmospheric carbon content in the year 4000 is significantly lower with *CC13* than with *CC16* or even *CCGL*. Accordingly, peak and average temperature are not increasing beyond 2500 in *CC13*. Second, due to the fast exchange between carbon reservoirs in *CCGL* the substitution effect with respect to abatement is very low in the *CBA* framework, at least within the displayed scale of CDR (up 1500 Gt C). Here, a significant increase in emissions can only be observed for cumulative CDR larger than 2,500 Gt C. In the *2C* and *2C2100* frameworks the substitution effect is present, however, resulting in a less step increase in cumulative emissions for increasing cumulative CDR compared to *CC13* and in particular *CC16*.

The faster exchange between reservoirs in *CCGL* also results in a stronger difference between oceanic CDR and oceanic CDR under the (false) conjecture of perfect storage. Figure 4.3 shows the time profile of the difference between these two CDR options for all three carbon cycles in the *2C* framework. We have chosen CDR cost scenarios which correspond to a cumulative amount of 1500 Gt C CDR until

2500. For a smaller cumulative amount of CDR (i.e. steeper marginal CDR cost) the difference shrinks. As shown already in Figure 4.1, there is a significant difference between perfect storage and oceanic storage for *CCGL*. Because of the rather fast exchange, the substitution effect is smaller with oceanic CDR (and only present for very flat CDR cost which allow carry out the extra CDR to compensate for the carbon cycle feedbacks) than with perfect storage. Accordingly, a planner who falsely assumes perfect storage would set emission reductions too low (and in turn emissions are too high) such that more CDR is needed to compensate for carbon returning to atmosphere. In sum, the false assumption with respect to CDR results in an extra cumulative amount of CDR of about 180 Gt C in comparison to the optimal amount of 1500 Gt C under the correct assumption. With *CC13* there is almost no difference due to the effect that there is almost no difference between perfect and oceanic CDR in that model (cf. Figure 4.1). With *CC16* we observe a small difference, resulting from the same mechanism as for *CCGL* but the cumulative extra amount of CDR is below 10 Gt C (in comparison to the optimal amount of 1500 Gt C).

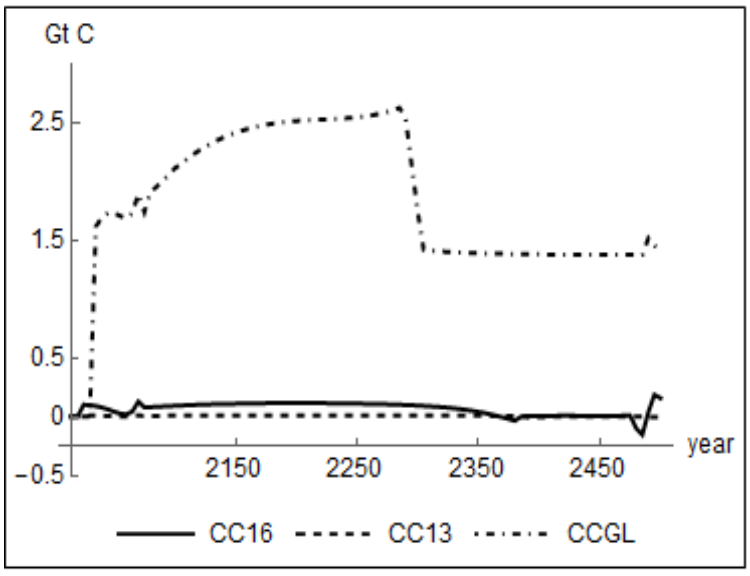

Figure 4.3: Implications of oceanic CDR under the (false) assumption of perfect storage.

The figure shows the annual difference between oceanic CDR andoceanic CDR under the (false) assumption of perfect storagein the *2C* framework for all three carbon cycles for the case of 1500 Gt C cumulative CDR under oceanic CDR.

We turn now to the question how well the atmospheric carbon and global mean temperatures trajectories obtained from optimal mitigation policies are reflected by corresponding simulations obtained in more sophisticated carbon cycle and Earth system models. We focus here on the optimal mitigation policies derived with *CC16*, and implement those also in *CC13*, *CCGL*, BEAM ,and UVic ESCM. Until the year 2500 the optimal polices were implemented, followed by zero emissions and zero CDR until the end of the simulation horizon in the year 4000. We look first at mitigation policies without CDR before we turn to selected CDR policies. Figure 4.4 shows the development of atmospheric carbon content and the increase in global mean temperature for business-as-usual emissions, for the *CBA* framework, and for the *2C* framework where in the CBA framework the optimal amount of emissions was obtained from *CC16*. Note that with *CC16* the 2C goal cannot be achieved (without changing the assumptions underlying exogenous forcing) and we implemented zero emissions throughout the entire period.

The results indicate that *CC16* has significantly improved with respect to the long-term dynamics, in particular for high emission scenarios, as becomes evident by the much smaller gap to the simulated atmospheric carbon content and global mean temperature increase obtained with BEAM and UVic for business-as-usual emissions compared to the gap with *CC13* and *CCGL*. For the cumulative business usual emissions of 5630 Gt C (until the year 2500), peak atmospheric concentration (global mean temperature increase relative to preindustrial) increases to about 2330 and 2594 ppm (4.57°C and 4.97°C) in UVic ESCM and BEAM, respectively. In *CC16* the corresponding figures are 1884 ppm and 4.3°C, whereas in *CC13* only 1232 ppm and 3.42°C and in *CCGL* even lower with 953 ppm and 2.8862°C. However, the improved long-term dynamics in *CC16* comes apparently at the cost of being too restrictive with respect to the short term dynamics for mitigation scenarios (i.e. with less emission). In the *CBA* framework, global mean temperature increase obtained with UVic ESCM is rather matched by *CC13* than by *CC16* (atmospheric carbon content obtained with UVic is between atmospheric carbon content of *CC13* and *CC16*) (see middle panel in Figure 4.4). Similarly, the decrease in atmospheric carbon content and global mean temperature is much slower in *CC16* for zero emissions than in the other carbon

cycles (see lower panel in Figure 4.4). Consequently, using *CC13* instead of *CC16* for the derivation of optimal abatement in the *2C* framework, the implementation in UVic ECSM shows that compliance with the 2°C goal is achieved up until the year 2500 (beyond that long-term warming increases up to 2.65°C). However, using instead *CCGL*, the 2°C goal is already violated in UVic ECSM by the year 2165 (yet, the long-term peak increase is with 2.92°C degrees not that much higher as with the CC13 abatement path).

Noteworthy is the high concordance between BEAM and UVic for business-as-usual emissions and also in parts for zero emissions, but BEAM overestimates the short-term atmospheric carbon concentration increase and accordingly temperature increase in the *CBA* framework. For the *2C* framework (lower panel in Figure 4.4) we observe that with zero emissions compliance can be achieved in *CC13*, *CCGL* and almost in BEAM (peak temperature increase is 2.02605°C). Still, it needs to be kept in mind that we have left the DICE2016R assumptions with respect to exogenous land-use emissions and exogenous forcing unchanged. Still, even with zero land-use emissions and linearly decreasing exogenous forcing from 0.5 W/m^2 in the year 2015 to 0 W/m^2 in the year 2100, application of *CC16* result for zero emissions from 2015 onwards in a committed warming of 1.43°C temperature increase relative to preindustrial (starting in 2015 with a temperature increase of 0.85°C). Noteworthy is that UVic ECSM allows for compliance up until the year 3500 (with the DICE2016R assumptions of exogenous forcing and land-use emissions), confirming that *CC16* can be considered too pessimistic with respect to its remaining emission budget. However, we observe for the UVic ECSM trajectory an irregularity in the temperature increase (which is also present as small increase in the atmospheric carbon content via the temperature feedback) due to an ocean deep convection event. We discuss this issue in more detail below.

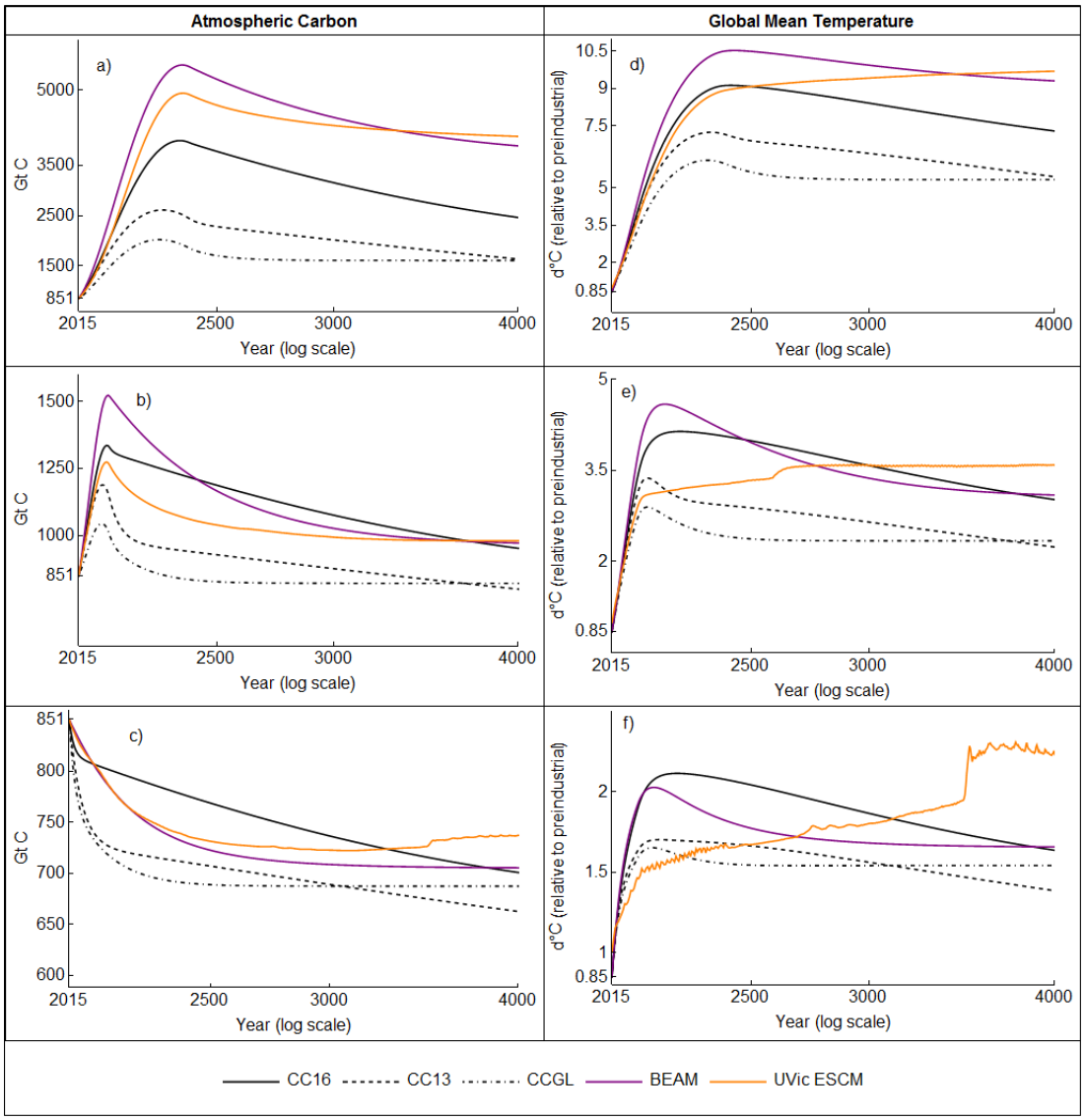

Figure 4.4: Comparison of carbon cycle models without CDR until the year 4000.

The figure shows atmospheric carbon content (left panel) and global mean temperature increase (right panel) for business-as-usual emissions (a) and d), respectively), for the *CBA* framework (b) and e), respectively), and for zero emissions (c) and f) respectively) for *CC16*, *CC13*, *CCGL*, BEAM, and UVic ESCM. The optimal emissions in *CBA* until the year 2500 were derived with *CC16*.

Noteworthy is the high concordance between BEAM and UVic for business-as-usual emissions and also in parts for zero emissions, but BEAM overestimates the short-term atmospheric carbon concentration increase and accordingly temperature increase in the *CBA* framework. For the *2C* framework (lower panel in Figure 4.4) we observe that with zero emissions compliance can be achieved in *CC13*, *CCGL* and almost in BEAM (peak temperature increase is 2.02605°C). Still, it needs to be kept

in mind that we have left the DICE2016R assumptions with respect to exogenous land-use emissions and exogenous forcing unchanged. Still, even with zero land-use emissions and linearly decreasing exogenous forcing from 0.5 W/m^2 in the year 2015 to 0 W/m^2 in the year 2100, application of *CC16* result for zero emissions from 2015 onwards in a committed warming of 1.43°C temperature increase relative to preindustrial (starting in 2015 with a temperature increase of 0.85°C). Noteworthy is that UVic ECSM allows for compliance up until the year 3500 (with the DICE2016R assumptions of exogenous forcing and land-use emissions), confirming that *CC16* can be considered too pessimistic with respect to its remaining emission budget. However, we observe for the UVic ECSM trajectory an irregularity in the temperature increase (which is also present as small increase in the atmospheric carbon content via the temperature feedback) due to an ocean deep convection event. We discuss this issue in more detail below.

Figure 4.5 shows the development of atmospheric carbon content and the increase in global mean temperature for the *CBA*, *2C*, and *2C2100* framework until the year 4000 (in the upper, middle, and lower panel, respectively.) The optimal emission and CDR paths in the three frameworks until the year 2500 where derived with *CC16.* We selected a cost scenario corresponding to cumulative CDR of 1200 Gt C as the amount is large enough to result in sufficient carbon cycle feedbacks and also goes in line with a substitution effect, resulting in more emissions.

In general, the paths obtained with *CC16* appear reasonably close to the paths obtained with UVic ECSM, suggesting that integrated assessment of CDR in DICE2016R is sensible. In particular simulated atmospheric carbon content is rather similar in *CC16* and UVIC, at least until the year 2500, concurring therefore also for the short-term increase and decrease in the *2C2100* framework (see c) in the lower panel). Beyond 2500 there is an increasing gap between UVic and *CC16* because not all long-term saturation and carbon cycle feedbacks can be accounted for in *CC16*. However, as mentioned above, this gap is considerably smaller for *CC16* than for *CC13.* Given the close match of atmospheric carbon content it appears somewhat surprising that *CC16* overestimates the short-term increase in global mean temperature, suggesting that i) rather the climate module of *CC16* requires further

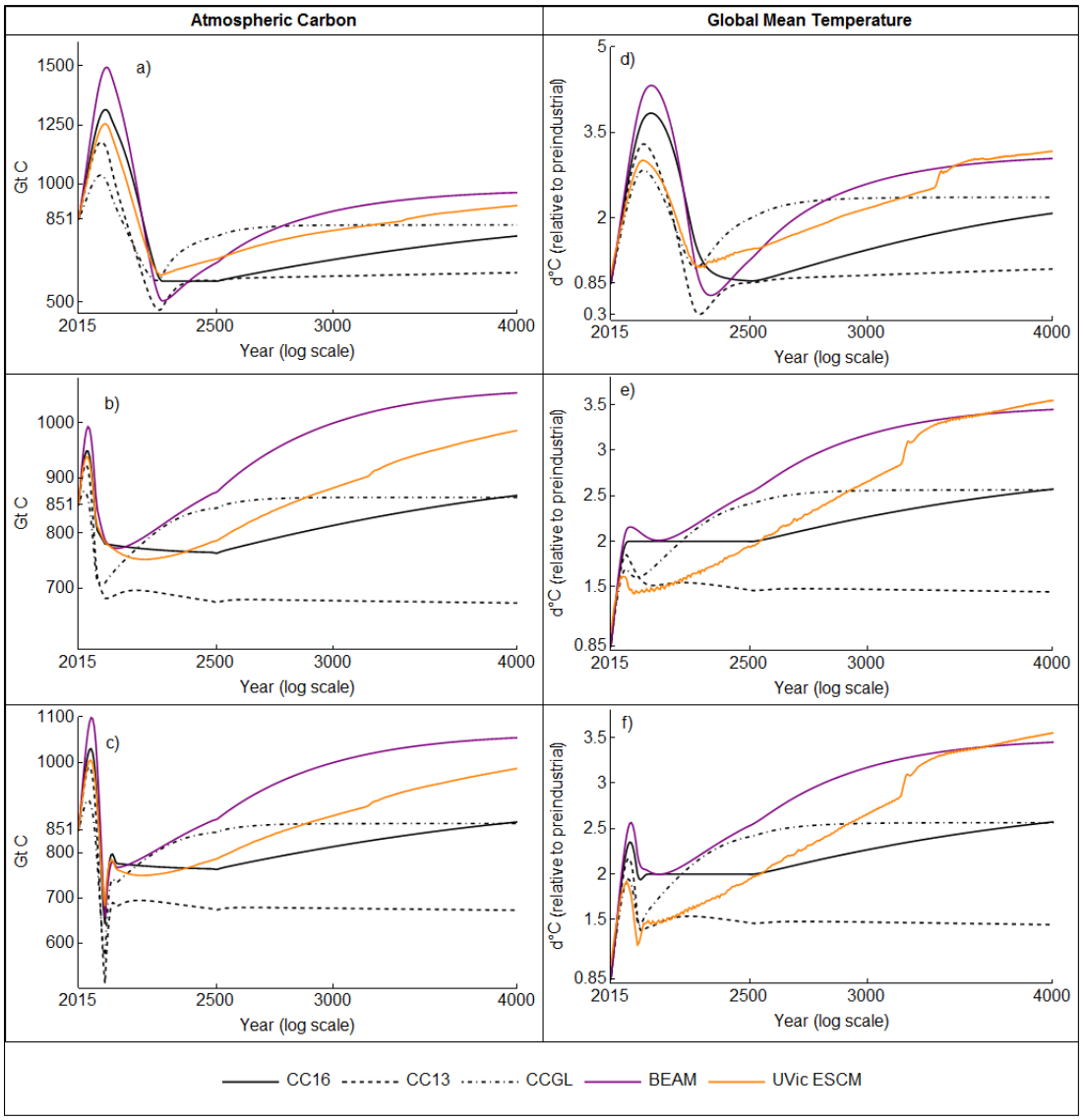

Figure 4.5: Comparison of carbon cycle models with CDR until the year 4000.

The figure shows atmospheric carbon content (left panel) and global mean temperature increase (right panel) for the *CBA* framework, (a) and d), respectively), for the *2C* framework (b) and e), respectively), and for the *2C2100* framework (c) and f) respectively) for *CC16*, *CC13*, *CCGL*, BEAM, and UVic ESCM. The optimal emission and CDR paths in the three frameworks where derived with *CC16* for a CDR cost scenario which corresponds to cumulative 1200 Gt C.

adjustments than the carbon cycle model and ii) the derived mitigation policies are probably too conservative, at least with respect to the short run. For all three mitigation framework, *CCGL* shows stronger (short-term) increase in atmospheric carbon content and consequently global mean temperature than *CC16* or UVic ECSM, while for scenarios without CDR is close or even below the trajectories obtained with

CC13. Again, the reason is the rather fast exchange between carbon reservoirs in *CCGL*, implying that the amount of CDR obtained with *CC16* is simply too small to compensate for the extra emissions resulting from the substitution effect. The increase in atmospheric carbon content and global mean temperature in only exceeded by BEAM which shows again a good match of the long-term dynamics but appears to be too restrictive for the short-term dynamics, compared UVic ESCM. Again, we observe for UVic ESCM towards the end of the simulation horizon irregularities in the temperature response to which we turn next.

Global mean temperature shows a significant increase in the UVic ESCM simulations around the year 3300 which means at a point in time when emissions (and CDR) have been zero already for almost 1000 years. The increase is explained by an ocean deep convection event, resulting in a temporary carbon flux from the ocean to the atmosphere with a total of about 8 Gt C outgassing in a region of the Southern Ocean and in substantial amount of heat loss of the ocean adding to the warming triggered by the ongoing leakage of formerly injected carbon into the deep ocean. This becomes also evident in the sensitivity experiments where we considered different parameterization of vertical mixing (Figure 4.6). A slower vertical ocean mixing (kv low) results in a slower air-sea gas exchange, postponing therefore the ocean deep convection event whereas faster vertical ocean mixing brings the event forward.

Such open ocean deep convection in the Southern Ocean have been identified in many CMIP5 models (Lavergne et al., 2014), the UVic model (Meissner et al., 2008; Reith et al., 2016) and also in the Kiel Climate Model, for which the cause could be linked to internal climate variability (Martin et al., 2013). An important model limitation in this respect is a coarse grid resolution, which for example prevents the correct representation of bottom water formation processes on the continental shelf and thus might favor such events (Bernardello et al., 2014). Clearly, capturing such effects is beyond the capability of simple carbon-cycle and climate models used for integrated assessment.

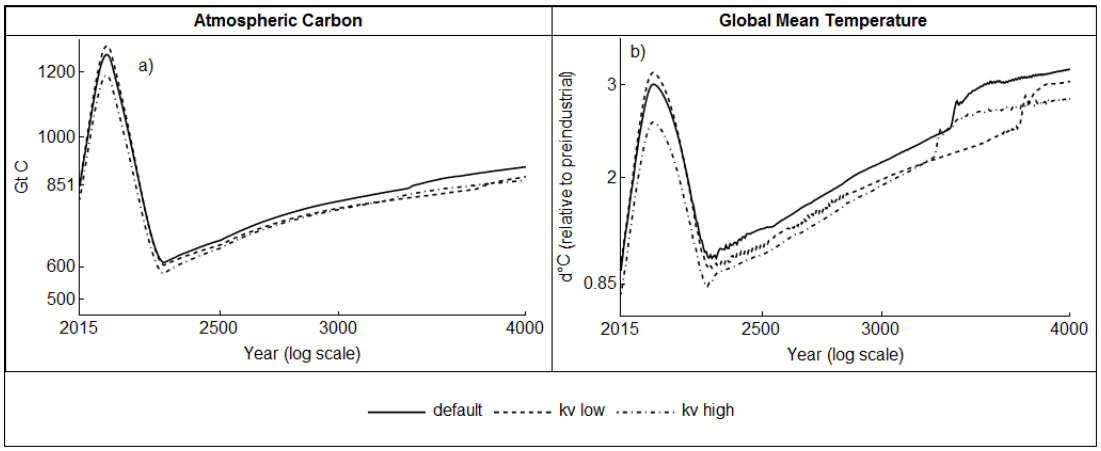

Figure 4.6: Sensitivity with respect to vertical ocean mixing.

The figure shows atmospheric carbon content (left panel) and global mean temperature increase (right panel) for the *CBA* framework with CDR, (a) and d), respectively). The optimal emission and CDR paths until the year 2500 were derived with *CC16*. The solid line shows the default parametrization, the dashed and dot-dashed line shows the results for 50 percent lower and higher parametrization for vertical ocean mixing, respectively.

4.4 Discussion

Obviously, our results are strongly affected by the general specifications of the DICE2016R model, which we maintained in our analysis. Introducing abatement options for land-use emissions and in particular allowing to alter the exogenous forcing (assumed in DICE2016R to be linearly increasing from 0.5 W/m^2 in the year 2015 to 1W/m^2 in the year 2100 and constant thereafter) might allow compliance with the 2°C or even 1.5°C goal without CDR (Su et al., 2017). Furthermore, the substitution effect is strongly dependent on the assumptions in DICE2016R with respect to the exogenous development of the carbon intensity and the backstop price. With less optimistic assumptions in this regard, we would observe a much stronger substitution effect also in the cost-benefit framework. While the magnitude of the substitution effect influences the magnitude of the outgassing and temperature increase beyond the year 2500, both are not inevitable outcomes of CDR policies obtained from the DICE2016R model. We have derived the optimal polices only until the year 2500 (the DICE2016R specification) and simulated the response of the carbon cycle model for the remaining 1500 years under the assumption of zero

emissions and zero CDR. The purpose was to investigate to which extent the carbon cycle models used in integrated assessment capture stylized facts of the carbon cycle. Extending the optimization period would result in continuous CDR to remove carbon from the atmosphere and pump it into the deep ocean at the rate at which it leaks back to the atmosphere. Due to discounting, such continuous long-term CDR application would however have negligible effects on near term policies.

The carbon cycle models applied in the integrated assessment would require endless CDR application to prevent outgassing as aspects of the carbon cycle like for example sedimentary processes are not included. Furthermore, many processes relevant for different CDR methods are not included, implying that our generic treatment of CDR may be too coarse to study details of specific CDR methods. For example, termination of alkalinity management is expect to result in smaller outgassing of removed carbon than termination of macro- or micronutrient fertilization and would rather correspond to the perfect storage scenario in our investigation than oceanic CDR (Paquay and Zeebe, 2013; Keller et al., 2014). However, if alkalinity increase would be achieved by spreading olivine (e.g. in the catchment area of large rivers) also nutrient cycles would be affected, resulting in additional fertilization effects, making the estimation of the actual net removal (after termination) more complex than suggested by the basic ocean chemistry (Köhler et al., 2013). Still, even under the assumption of perfect storage for alkalinity management, opposing carbon cycle feedbacks would be at play, resulting from the response of the terrestrial carbon reservoir (which is captured in our investigation by reduced ambient carbon uptake of the upper box for *CC13* and *CC16* and reduced uptake of the terrestrial biosphere in CCGL).

Finally, by choosing the deterministic DICE2016R model as point of reference we have neglected uncertainty in our analysis. Introducing uncertainty in the climate system would have allowed investigating to which extend CDR is used to increase the likelihood of compliance with the 2°C goal by for example a less pronounced substitution effect. Introducing uncertainty with respect to the carbon intensity and the development of the backstop price would also have implications for the application of CDR and the corresponding substitution effect. However, also the CDR methods

themselves are uncertain with respect to their costs, their side-effects, and their carbon cycle implications (Fuss et al., 2014; Field and Mach, 2017). In particular CDR specific (uncertain) side-effects could limit their applications. The magnitude of the side effects depends on the material cycles affected and the scale of application (Klepper and Rickels, 2014). Furthermore, the formation of CO_2 plumes or lakes and the potential risk of fast rising CO_2 bubbles (both potentially resulting from deep sea carbon injection) was neglected (IPCC, 2005; Bigalke et al., 2008). Despite no explicit treatment of uncertainty, our analysis of oceanic storage under the false assumption of perfect storage provides some insights. At least for *CC16* and *CC13* we can conclude that appropriate updating of the information on carbon stock levels reduces the misguidance from neglecting potential uncertainties about carbon cycle feedbacks.

4.5 Conclusion

Given the worlds shrinking carbon budget for ambitious climate change mitigation, achieving (net) negative carbon emissions appears to be inevitable. However, they would not linearly extend the carbon budget because in an interacting carbon cycle their net contribution is strongly influenced by feedbacks and saturation effects. So far, the investigation of these interactions and the net contribution of CDR has been restricted to scenario analysis in earth system models, which cannot answer how the presence of these feedbacks affects endogenously derived optimal or cost-effective mitigation policies. Consequently, the aim of our study was to investigate how well these feedbacks and effects are captured in integrated assessment models, which are suitable to analyze a broad set of possible CDR scenarios. We have investigated (oceanic) CDR in the integrated assessment model DICE, in its most recent version (DICE2016R) and considered in addition two further carbon cycle models (DICE2013R) and (Gerlagh and Liski, 2017). We have considered three different mitigation frameworks, cost-benefit-analysis, compliance with the 2°C goal, and cost-effective compliance with the 2°C by the year 2100. In contrast to the literature we did not imposed annual limits on the amount of CDR but considered a convex CDR

cost function, as we believe that the operational cost are characterized by increasing marginal costs, both within any specific CDR method and across CDR methods.

We found that the role of CDR depends on the mitigation framework in our integrated assessment analysis. While cost-effective compliance with the 2°C target requires significant CDR application already before the year 2050, application of CDR in a cost-benefit framework (with endogenous amount of climate change) is a long-term strategy to speed up the otherwise rather slow natural reduction of atmospheric carbon concentration after peak atmospheric temperature. In turn, near-term application of CDR goes in line with a strong substitution effect, resulting in less emission reductions. For this mode of application, the main effect of CDR is to extend the near-term emission budget, as only a very small or even zero emission can still be emitted to the atmosphere without CDR. Using CDR to bring down the atmospheric carbon content in the long-term shows only a moderate substitution effect, provided CDR is sufficiently cheap. The magnitude of these effects is dependent on the carbon cycle feedbacks in the applied carbon cycle model. For a model that assumes a rather slow exchange between the carbon reservoirs, oceanic CDR is close to 'perfect' storage. This makes CDR very effective and results in turn in a strong substitution effect. For a model that assumes a fast exchange between the carbon reservoirs, oceanic CDR becomes less effective, resulting in a weaker substitution effect. However, decreased effectiveness of CDR results in extra CDR efforts to compensate for the carbon leaking back to the atmosphere if the CDR cost function is sufficiently flat. Consequently, modelling the effectiveness of CDR in dependence of the carbon cycle explicitly results in different results than obtained by adjusting simply the effectiveness of CDR as in (Chen and Tavoni, 2013).

The strongest carbon cycle feedbacks are observed in the carbon cycle model introduced by Gerlagh and Liski (2017), while with the DICE2013R carbon cycle model oceanic CDR is almost equivalent to perfect storage. Overall, the carbon cycle model in DICE2016R has significantly improved compared to DICE2013R, capturing very well long-term outgassing of carbon injected into the deep ocean and corresponding increases in the temperature beyond 2500 for large CDR scenarios. Comparing DICE2016R to UVIC ESCM simulations indicates that the improved

long-term dynamics come at the cost of a (too) tight short-term remaining emission budget. Ignoring other abatement options with respect to land-use emissions and non-CO_2 greenhouse gases, compliance with the 2°C goal cannot be achieved in DICE2016R without CDR. Consequently, one could argue that short-term mitigation policies derived with DICE2016R are too restrictive, however, in a cost-benefit framework the rather restrictive carbon cycle model is overcompensated by the modest estimates for climate change impacts in DICE2016R. Furthermore, the match between DICE2016R and UVic ESCM is closer for atmospheric carbon content than for global mean temperature increase, suggesting that adjustments of the climate module could be a strategy for achieving better estimates for mitigation policies.

In conclusion, investigating CDR in DICE2016R appears to be sensible and the derivation of endogenous mitigation policies provides relevant insights because the optimal amount of CDR is derived under i) accounting for the emission substitution effect and ii) compensation for carbon cycle feedbacks. Clearly, simple carbon cycle box models cannot capture all relevant processes and feedbacks. However, for the DICE2016R carbon cycle model we find that appropriate updating of carbon stocks (based either on observations or more complex models) can provide a good workaround to correct for misspecifications of the carbon cycle model or unforeseen leakage events.

Acknowledgments, Samples, and Data

The authors declare that there are no conflicts of interest. All model files and corresponding data data used in this analysis are available in the Supporting Information. Any real or perceived financial conflicts of interests for any author.

5 Conclusions and Outlook

Chapters 2-4 of this dissertation have revisited the idea of ocean carbon sequestration by direct CO_2 injection and advance its current scientific understanding with respect to the addressed research questions (see section 1.3). The following conclusions can be drawn.

Achieving a specific atmospheric carbon reduction via ocean carbon sequestration requires accounting for carbon-cycle feedbacks and backfluxes. The investigated targeted atmospheric carbon reduction of 70 Gt C via direct CO_2 injection into the deep ocean is missed by 16 to 30 % under the RCP/ECP 8.5 (Chapter 2). Hence, the respective response of the global carbon cycle implies that direct CO_2 injection cannot be 100 % efficient and provide 100 % of the targeted atmospheric carbon reduction on decadal to centennial timescales (see Fig. 2.3 in Chapter 2).

The influence of the carbon-cycle feedbacks on the targeted atmospheric carbon reduction is mainly caused by the partial outgassing of injected CO_2 and a reduced rate of air-sea gas exchange when compared to the control run without injection.

The model's terrestrial ecosystems respond to the CO_2 injections and reduced atmospheric CO_2 concentrations through a reduced CO_2 fertilization effect and a temperature-induced decrease in soil respiration, relative to the control simulation. However, a high level of uncertainty is associated with the larger signal of the terrestrial response to the scaling of the default CO_2 fertilization parameterizations when compared to the targeted atmospheric carbon reduction in the injection experiments with the default setting of the terrestrial photosynthesis model (see Fig. 2.6 in Chapter 2).

Overall, the influence of the highly uncertain carbon-cycle feedbacks highlight the challenge of quantitatively detecting, attributing, and eventually accounting for carbon storage and carbon fluxes generated by direct CO_2 injection into the deep

ocean even in a relatively coarse-resolution model with little internal climate variability. The observational monitoring of the evolution of injected CO_2 plumes and hence an accurate verification of its effectiveness in the real ocean has been shown to be extremely difficult, even if a dye such as sulfur hexafluoride (SF_6) would be devised to track the injected CO_2 (Matsumoto and Mignone, 2005). This is reasoned by the fact that the injected CO_2 would spread too quickly and widely from the injection site(s) in order to be fully recorded by even the most ambitious ocean survey. However, their ocean-only model study neglects the influence of carbon-cycle feedbacks upon direct CO_2 injections. The results presented in Chapter 2 hence add another level of complexity on observational monitoring and verification of CO_2-injection, especially in the real Earth system with its much larger internal variability. Consequently, these aspects indicate the limited viability of direct CO_2 injection, because these would challenge any potential future transnational authority to accurately assign carbon credits under a respective global climate accord unless model derived estimates could be accepted at face value.

Under the assumption of a world with CO_2 emissions of the RCP/ECP 4.5 and its corresponding climate impacts, it is found that a total mass of 1562 Gt C would have to be injected at 3000m water depth in order to reach and maintain the 1.5°C climate target on a millennium timescale. The inclusion of $CaCO_3$ sediment and terrestrial weathering feedbacks in the UVic-model reduce this amount by about 11 %, providing a more realistic estimate because those feedbacks are always present in the Earth System.

The suitability of direct CO_2 injection to reach a specific climate target gets most obvious by comparing the injected CO_2 amount of 1562 Gt C noted above with the amount of CO_2 emission reduction necessary to comply with 1.5°C on a 1000 year timescale. This required emission reduction amounts to about 955 Gt C (39 % less) and is defined by the difference of the cumulative CO_2 injections and the diagnosed leakage of injected CO_2. It represents the emission reductions required for a perfect carbon storage technology. The amount of required emission reduction required to cool the model predicted global mean temperature by 1°C is quantified to be 446 Gt C / 1°C in the near-term (year 2100) and about 595 Gt C / 1°C in the long-term (year

3020). The near-term estimate is approximately the same for direct CO_2 injection, because only a tiny fraction has outgassed until that point in time. However, in the long-term the amount is about 951 Gt C / 1°C (37 % more) for oceanic CCS when compared to the required emission reduction.

This comparison highlights that the suitability of direct CO_2 injection to reach a specific climate target is in the long-term limited by its leaked amount of CO_2. Accordingly, the near-term benefits of direct CO_2 injection come at the price of a burden for future generations, because the outgassed fraction would need to be re-captured by some additional CDR methods such as direct air capture facilities and re-injected into the deep ocean long time (generations) after humans took benefit from energy production associated to the CO_2 emissions in the first place. Hence, direct CO_2 injection of the size needed to reach the 1.5°C would likely lead to a lock-in effect for many centuries after its deployment.

An important constraint of these model-derived estimates is the neglect of non-CO_2 greenhouse gases in the applied forcing, which very likely results in an underestimation of the required cumulative CO_2 injections and in consequence of the required emission reduction. In general, it is estimated that non-CO_2 greenhouse gases contribute between 10-30 % of the total forcing (Friedlingstein et al., 2014) until the year 2100 and for a business-as-usual CO_2 emission scenario. Extrapolating the present contribution of non-CO_2 greenhouse gases qualitatively into the future, the cumulative CO_2 injections that are compatible with the 1.5°C climate target are expected to be on the order of about 2200 Gt C. That is of similar magnitude as represented by the oceanic CCS modeling experiment in which an amount of CO_2 that allows to closely follow the atmospheric CO_2 concentration of the RCP/ECP 2.6 is injected (see Chapter 3).

Furthermore, direct CO_2 injection result in a trade-off between injection-related reductions in atmospheric CO_2 accompanied by decreased upper ocean acidification and strongly acidified water masses in the intermediate and deep ocean, with maximum pH reductions in the vicinity of the injection sites. Accordingly, the global community would have to decide if severe stress, potential loss of deep ocean

ecosystems is bearable when paid-off by the conservation or restoration of marine ecosystems in the upper ocean to a large extent. This trade-off stresses the necessity of a careful evaluation of local harm against global benefit, which holds very likely true for the potential deployment of direct CO_2 injections into the deep ocean as well as for any other deliberate CO_2 removal method.

The findings of the integrated assessment of direct CO_2 injection into the deep ocean as proxy for ocean-based CDR methods (Chapter 4) shows that the box-type carbon cycle model used in the most recent version of the Dynamic Integrated Climate-Economy Model (DICE2016R) have significantly improved when compared to its predecessor DICE2013R. This is due to the fact that it captures the long-term outgassing of injected CO_2 into the deep ocean as well as the related increase in global mean temperatures. However, this improvement comes with the expense of a small near-term remaining emission budget, when compared to the UVic model, which limits the accurate assessment of low emission scenarios. As a consequence, DICE2016R suggests that the 2°C climate target cannot be achieved without negative emissions through CDR. In model runs with DICE2013R, we find that the efficiency of direct CO_2 injection is close to that of geological storage, because the model assumes a rather slow exchange between the different carbon reservoirs. Furthermore, the strongest carbon cycle feedbacks are observed in the carbon cycle model by Gerlagh and Liski (2017).

Overall, these findings show that assessment of direct CO_2 injections and more generally CDR seems to be sensible in such an integrated assessment framework, where the amount of CDR is determined, taking into account less ambitious emission reductions as consequence of direct CO_2 injections and the extra amount of carbon required to compensate for carbon cycle feedbacks. Simulating the effectiveness of CDR in dependence of the carbon cycle explicitly results in different results than obtained by adjusting simply the effectiveness of CDR as for instance done in the study of Chen and Tavoni (2013). This demonstrates the necessity of the accounting for carbon cycle feedbacks in an integrated assessment of any CDR method(s).

Furthermore, Earth system models should be used for validation in order to enable a more robust derivation of policy recommendations. As the computational power increases, some type of Earth system models of intermediate complexity may replace the climate model component of IAMs (Hajima et al., 2014) and thus allow for a more comprehensive coupling of relevant economic and carbon cycle feedbacks.

The findings of this dissertation have been derived by or validated against a single Earth system climate model of intermediate complexity, i.e., the UVic-model. Several model intercomparison studies (Friedlingstein et al., 2006; Plattner et al., 2008; Eby et al., 2013; Zickfeld et al., 2013) have shown that the UVic model predictions of the land and ocean carbon uptake and temperature change under different CO_2 emissions and concentration scenarios are comparable to a number of atmosphere and ocean general circulation models, as well as Earth system models of intermediate complexity. Nevertheless, it is difficult to derive uncertainty ranges of, e.g., the effectiveness of direct CO_2-injections from the process-oriented work presented here. A more complete uncertainty estimate could be either derived from a multi-model study or from systematic model-parameter perturbation studies with a single model. Future work with the UVic model could for instance include a suite of parameter perturbation simulations focusing on specific processes both in the ocean and on land, which have been identified in this study to impact the net carbon storage of the Earth system in relation to direct CO_2 injection into the deep ocean.

As the leakage of injected CO_2 from the ocean determines the effectiveness of direct CO_2 injection, varying physical parameters of the ocean model (e.g. of vertical diffusivity or of advection) that dictate the transport of injected CO_2, would help to constrain associated uncertainties. Furthermore, the occurrence of ocean deep convection events observed in some of the conducted injection experiments raises the question if these could happen in reality (Bernadello et al., 2014) or if those events are rather a model artefact, e.g. caused by the coarse grid resolution, which hinders, for instance, the correct representation of bottom water formation processes on the continental shelf. However, even if unrealistic, such events could be viewed as an analogue of future climate surprises, meaning that unexpected events could occur in

reality due to the non-linearity of the climate system that might offset or favor any targeted atmospheric carbon reduction. In a future study, the relative frequency of outgassing events and hence their quantitative feedback in relation to direct CO_2 injections could be better quantified by a larger ensemble of model runs with slightly perturbed greenhouse gas forcing.

The CO_2 fertilization effect and the temperature sensitivity of soil respiration have been identified to drive the model's terrestrial carbon cycle response to reduced atmospheric carbon through direct CO_2 injection into the deep ocean. In addition to the sensitivity experiments carried out with respect to CO_2-fertilization, future work should address also the uncertainty related to the default parameterization of the influence of temperature on the soil respiration rate, e.g. by sensitivity runs in which the Q10 value is varied, e.g., by ±50 %. Further, a better disentangling of terrestrial feedback processes involved in the terrestrial response to the targeted atmospheric carbon reduction via direct CO_2 injection is required, for example by separately performing additional radiatively and biogeochemically un-coupled simulations. Models that feature a nitrogen-cycle control of terrestrial productivity and resolve regional changes in temperature and precipitation predict a smaller terrestrial feedback and hence a larger increase in projected future atmospheric CO_2 concentrations for given CO_2 emission scenarios (e.g., IPCC, 2013; Hajima et al., 2014) compared to less complex models of the biosphere. Hence, the introduction of nutrient control in the land component of the UVic-model would likely result in a different terrestrial response to the direct CO_2 injections.

Overall, further trans- and interdisciplinary research on the response of the global carbon cycle to any anthropogenic perturbation is needed in order to reduce or overcome associated uncertainties, which would in turn improve the decision-making process on the most viable option(s) to address dangerous consequences of anthropogenic climate change.

Finally, the author would like to clarify that the results of this dissertation should neither be viewed for nor against the potential deployment of direct CO_2 injection into

the deep ocean. If seriously considered, a transparent and iterative evaluation of the potential benefits and adverse side effects as well as ethical, legal, and governance issues must be included in a comprehensive assessment of direct CO_2 injection as well as any deliberate intervention into the climate system.

Supporting Information

Supplement A

Revisiting ocean carbon sequestration by direct injection: a global carbon budget perspective

Supplement A provides two tables showing the absolute DIC and PH values of the *RCP 8.5 Control* run at the injection sites and the respective changes in the WE simulations (section 2.3.2). Figure A1 illustrates the cumulative CO_2 emissions in the *RCP 8.5 control* run. Plus, the Figures A2 to A5 for section 2.3.4.2 that illustrate the explanation of the high correlation and apparent synchronicity in land carbon uptake between the WE simulations (Fig. 2.4 e) as well as Figure A6 that shows the deep convection related carbon uptake in the Southern Ocean in *I-1500* (section 2.3.4.2).

Table A1: Absolute values of the DIC concentration near the injection sites at the end of the injection period (year 2119) of the RCP 8.5 Control run and comparison of absolute changes in the DIC concentration near the injection sites at the end of the injection period (year 2119) between Orr [2004] (Full range) and our WE simulations (WE simulations minus RCP 8.5 Control run).

DIC [µmol/kg^{-1}]	**Biscay**	**New York**	**Rio**	**Frisco**	**Tokyo**	**Jakarta**	**Mumbai**
I-800 (RCP 8.5)	2246	2217	2249	2340	2301	2262	2307
I-1500 (RCP 8.5)	2207	2195	2187	2361	2341	2272	2307
I-3000 (RCP 8.5)	2184	2171	2186	2354	2338	2254	2287
Δ DIC [µmol/kg^{-1}]	**Biscay**	**New York**	**Rio**	**Frisco**	**Tokyo**	**Jakarta**	**Mumbai**
Full range at 800m (Orr, 2004)	261–1821	52 - 406	95 - 360	123 - 3178	58 - 271	79 -1095	159 - 1542
I-800	357	307	187	356	111	211	232
Full range at 1500m (Orr, 2004)	143 - 4165	79 - 904	52 - 495	112 -1565	158 - 514	97 - 811	136 -1209
I-1500	257	281	155	263	260	209	190
Full range at 3000m (Orr, 2004)	210 - 976	162 - 1222	109 - 1211	88 - 780	125 - 393	70 - 517	198 - 1966
I-3000	299	463	245	215	265	175	199

Table A2: Absolute PH values near the injection sites at the end of the injection period (year 2119) of the RCP 8.5 Control run and comparison of absolute changes in PH near the injection sites at the end of the injection period (year 2119) between Orr [2004] (Full range) and our WE simulations (WE simulations minus RCP 8.5 Control run).

PH	**Biscay**	**New York**	**Rio**	**Frisco**	**Tokyo**	**Jakarta**	**Mumbai**
I-800(RCP 8.5)	7.78	7.84	7.74	7.55	7.72	7.80	7.68
I-1500 (RCP 8.5)	7.84	7.87	7.93	7.56	7.78	7.90	7.88
I-3000 (RCP 8.5)	7.97	7.98	7.97	7.86	7.88	7.93	7.95
Δ PH	**Biscay**	**New York**	**Rio**	**Frisco**	**Tokyo**	**Jakarta**	**Mumbai**
Full range at 800m (Orr, 2004)	(-1.98) - (-.74)	(-1.08) – (-.12)	(-1.03) - (-.24)	(-2.43) - (-.29)	(-0.8) - (-.13)	(-1.8) - (-.17)	(-2.08) - (-.36)
I-800	-.91	-.85	-.57	-.74	-.36	-.64	-.65
Full range at 1500m (Orr, 2004)	(-2.34) – (-.39)	(-1.69) - (-.19)	(-1.29) - (-.12)	(-2.05) - (-.27)	(-1.3) - (-.036)	(-1.67) - (-.22)	(-1.78) - (-.3)
I-1500	-.77	-.83	-.49	-.72	-.73	-.68	-.59
Full range at 3000m (Orr, 2004)	(-1.7) - (-.65)	(-1.63) - (-.42)	(-1.77) - (-.25)	(-1.59) - (-.21)	(-1.09) - (-.33)	(-1.29) - (-.16)	(-2.02) - (-.54)
I-3000	-.90	-1.2	-.77	-.67	-.78	-.57	-.53

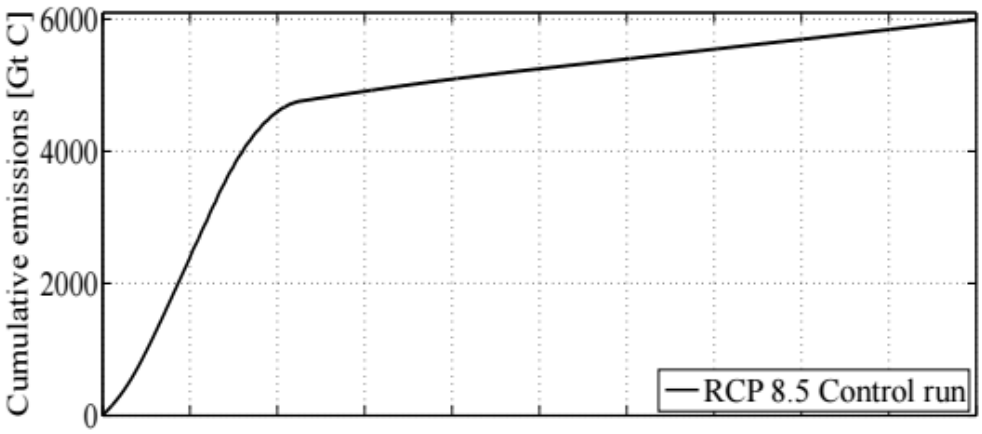

Figure A1: (a) Cumulative CO_2 emissions in the RCP 8.5 control run.

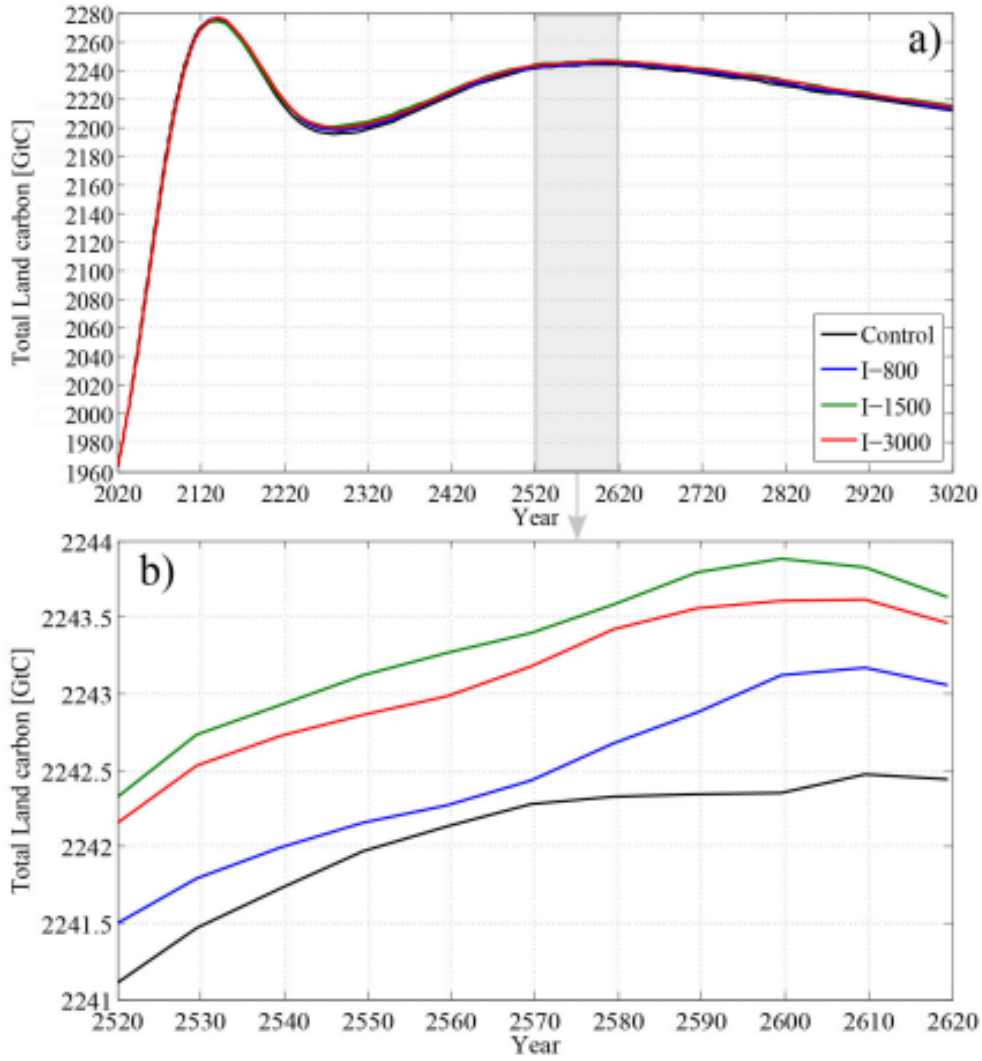

Figure A2: Total land carbon of the RCP 8.5 control run and the WE simulations for (a) the whole simulation period and (b) the simulation period between the years 2520 and 2620.

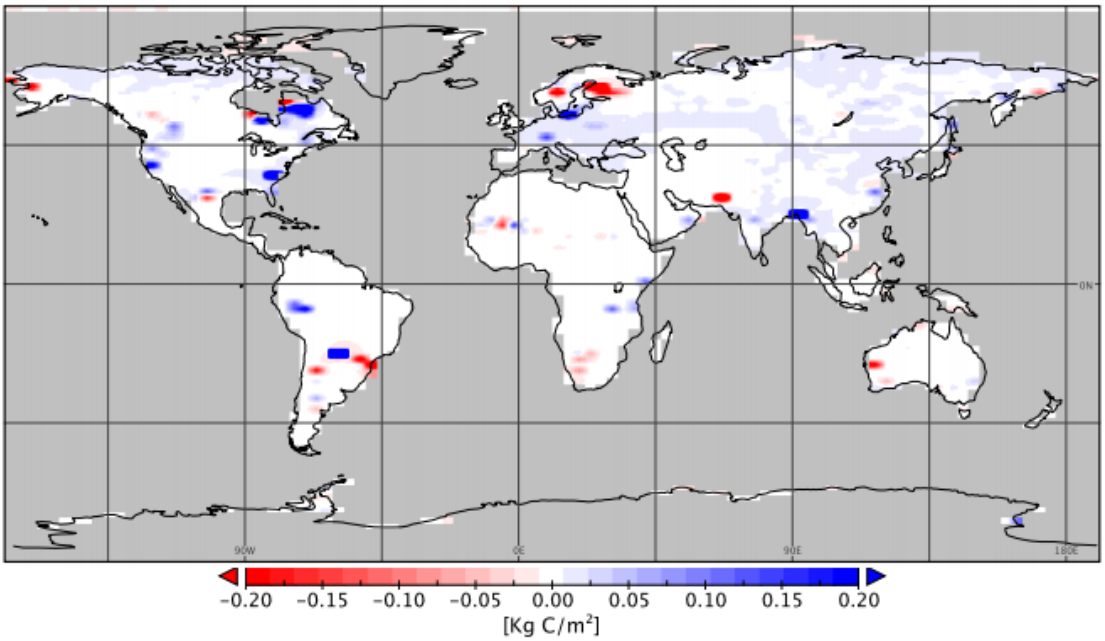

Figure A3: Absolute changes in land carbon between I-800 and the RCP 8.5 control run for the synchronic increase illustrated in Figure 2.2 g, i.e., year 2600 minus 2570.

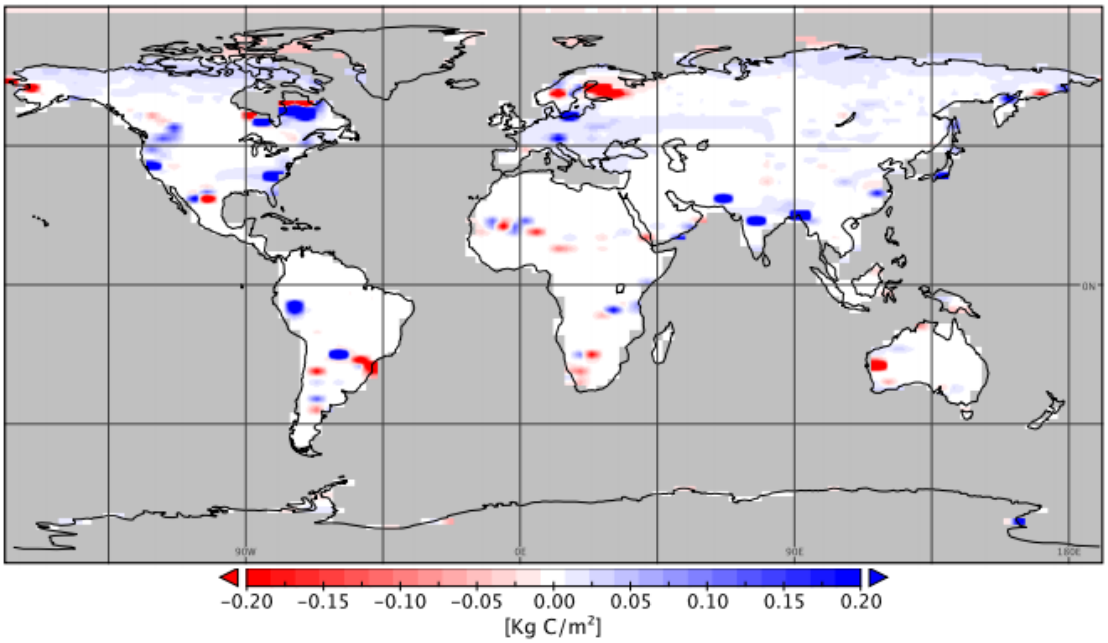

Figure A4: Absolute changes in land carbon between I-1500 and the RCP 8.5 Control run for the synchronic increase illustrated in Figure 2.2 g, i.e., year 2600 minus 2570.

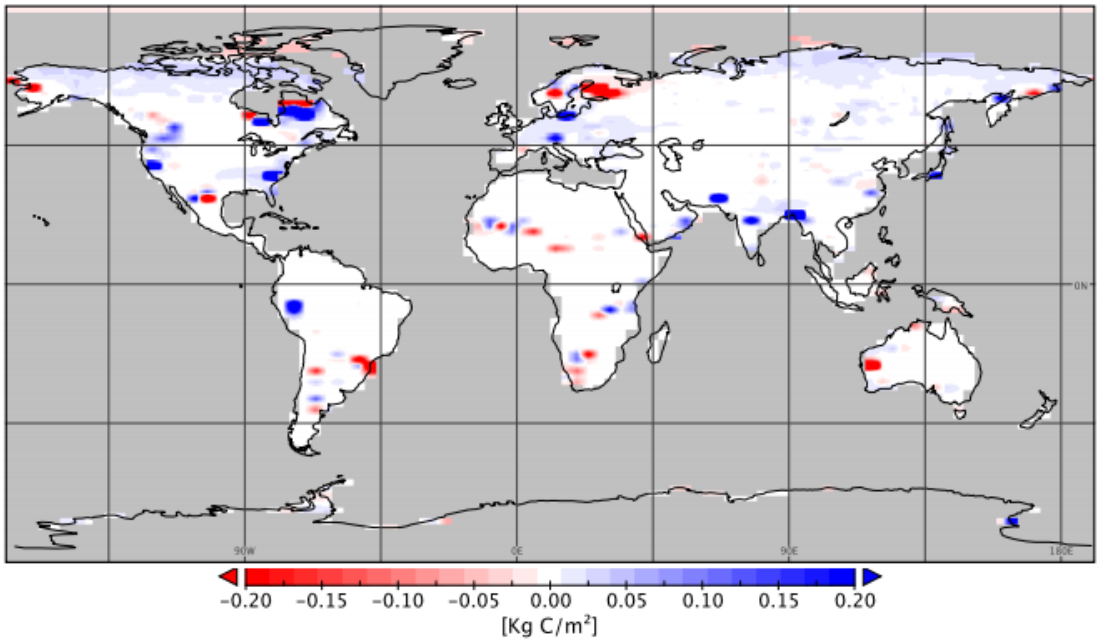

Figure A5: Absolute changes in land carbon between I-3000 and the RCP 8.5 Control run for the synchronic increase illustrated in Figure 2.2 g, i.e., year 2600 minus 2570.

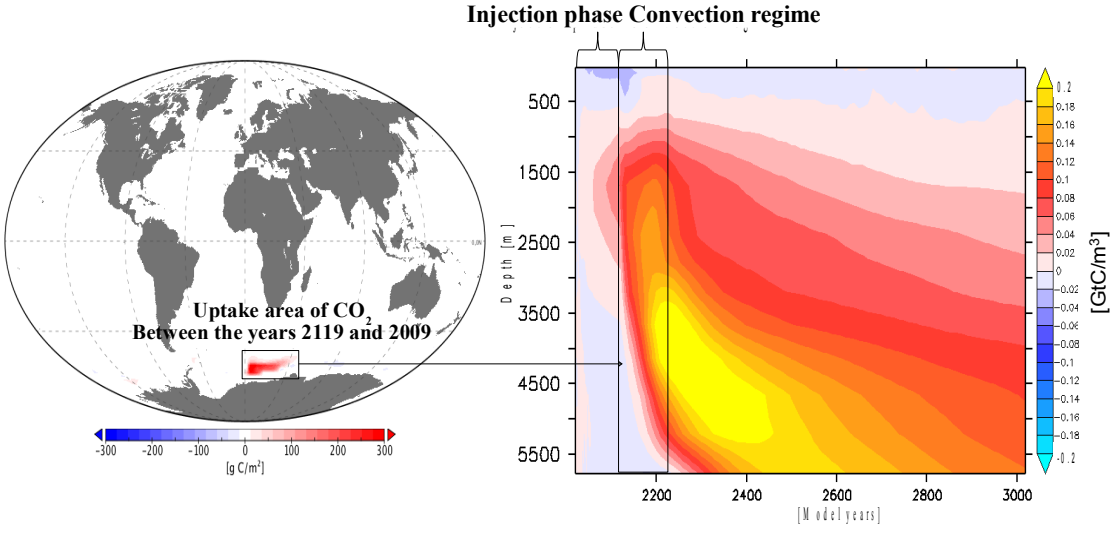

Figure A6: Downward carbon flux between the years 2119 and 2209 (I-1500 minus RCP 8.5 Control run) (left panel) Absolute change in total oceanic carbon (I-1500 minus RCP 8.5 Control run) (left panel)

Supplement B

Direct CO_2 injections to meet the 1.5°C climate target: What price would the ocean have to pay?

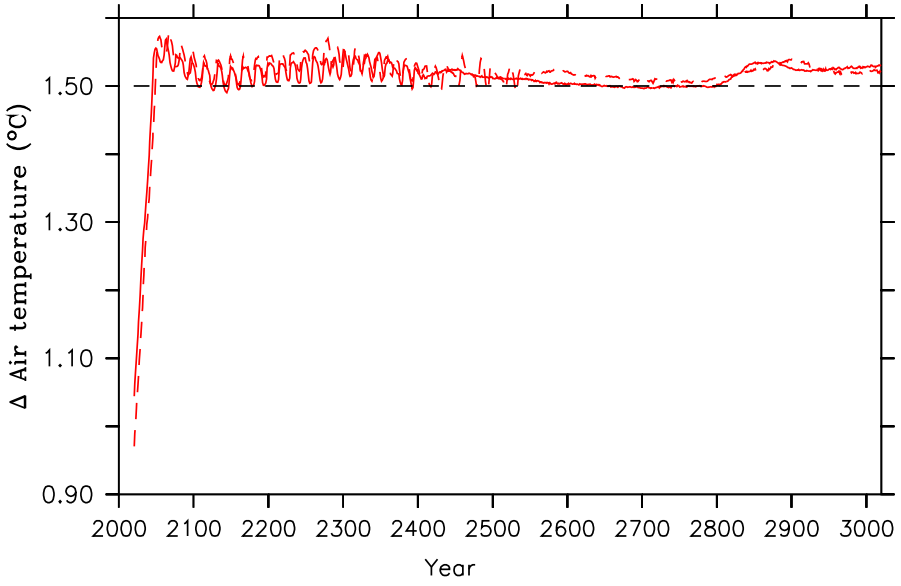

Figure B1: Global mean surface air temperature, relative to preindustrial, of the 1.5°C_target_Comitw simulation (solid) and the 1.5°C_target_Comitw_sed run (dashed). The horizontal dashed black line denotes the 1.5°C climate target.

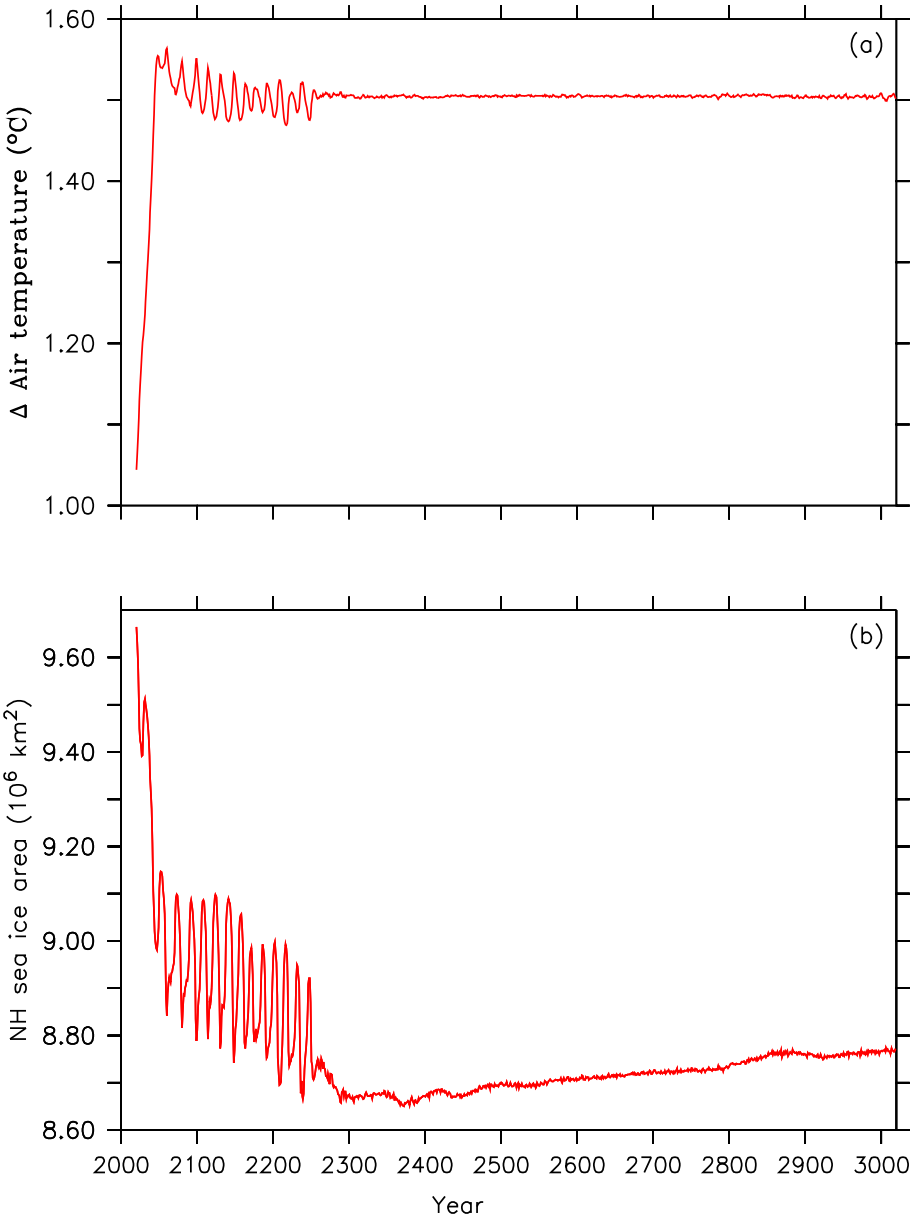

Figure B2: Time-series of the default 1.5°C_target simulation for (a) global mean surface air temperature, relative to preindustrial, and (b) northern hemisphere (NH) sea ice area.

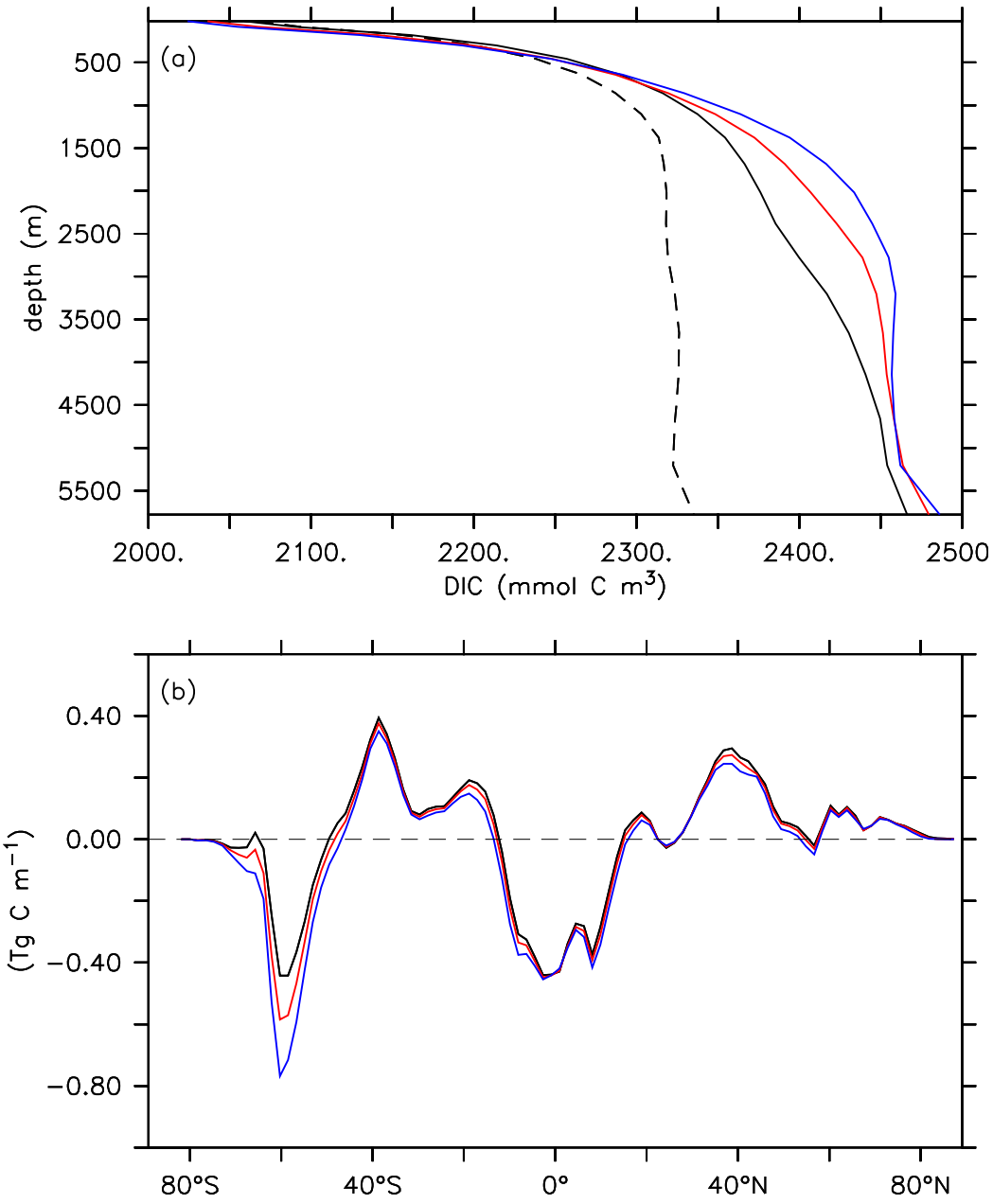

Figure B3: Comparison between the different default injection experiments, i.e., 1.5°C_target_Cemit simulation (black lines), 1.5°C_target simulation (red lines) and CO_2target_RCP2.6 simulation (blue lines) for (a) global mean profile of DIC in year 2020 (dashed black line) and global mean profiles in year 3020 (solid lines), and (b) cumulative atmosphere-to-ocean carbon flux in year 3020.

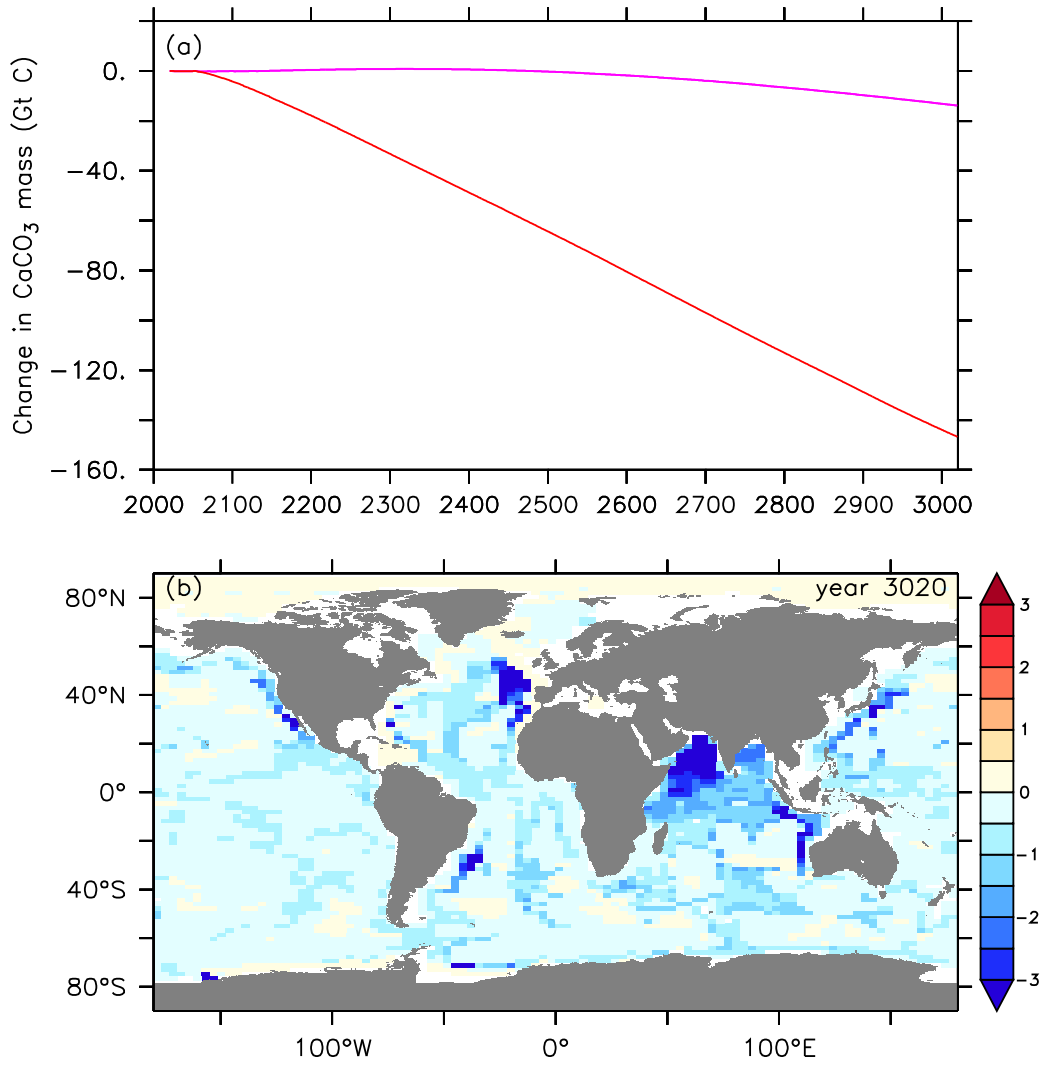

Figure B4: (a) Time-series of change in $CaCO_3$ mass for the RCP 4.5 control_sed simulation (purple line) and the 1.5°C_target_sed run, relative to the year 2020, and (b) global distribution of change in $CaCO_3$ mass (Kg C/m^2) in the 1.5°C_target_sed run (year 3020 minus year 2020).

Supplement C

Integrated Assessment of Carbon Dioxide Removal

Introduction

Additional information with respect to the linear carbon cycle box models and the validation with BEAM and UVic ESCM are provided in Text C1 and Text C2. Figure C3 corresponds to Figure 4.1 in the main text. While Figure 4.1 in the main text displays cumulative CDR and cumulative net emissions as function of the convexity of the CDR cost function for the two mitigation frameworks, CBA and 2C, Figure 4.2 provides the same information but for the two mitigation frameworks, CBA and 2C2100. The comparison between Figure 4.1 and Figure C3 indicates that there is only a very small difference between the mitigation frameworks 2C and 2C2100 when it comes to cumulative CDR and cumulative net emissions as function of the cost. Figure C4 and Figure C5 correspond to Figure 4.2 in the main text. Figure 4.2 shows the time profile for cumulative CDR as function of the convexity of the CDR cost for all three mitigation frameworks and the long-term carbon cycle and climate response for the CC16. Figure C4 and Figure C5 provide this information for CC13 and CCGL, respectively. The additional compressed file DICE_AMPL_IAM_CDR.rar includes all model files, the required run files to execute the different model files in AMPL, the required data to run the models (either included for single parameters in the model files or for time series of parameters as txt files which are automatically imported into the model upon execution), and a readme.txt file with additional information on the content.

C.1 Linear Carbon Cycle Models and Implementation of CDR in DICE

The carbon cycle model in DICE2016R (Nordhaus, 2017), DICE2013R (Nordhaus and Sztorc, 2013), and (Gerlagh and Liski, 2017) are three-box models:

$$\begin{pmatrix} S_1(t) \\ S_2(t) \\ S_2(t) \end{pmatrix} = \begin{pmatrix} \sigma_{11} & \sigma_{12} & \sigma_{13} \\ \sigma_{21} & \sigma_{22} & \sigma_{23} \\ \sigma_{31} & \sigma_{32} & \sigma_{33} \end{pmatrix} \begin{pmatrix} S_1(t) \\ S_2(t) \\ S_2(t) \end{pmatrix} + \begin{pmatrix} q_1 \\ q_2 \\ q_3 \end{pmatrix} E(t-1) + \begin{pmatrix} w_1 \\ w_2 \\ w_3 \end{pmatrix} CDR(t-1).$$

In DICE2016R and DICE2013R, S_1, S_2, and S_3, correspond to the atmosphere (MAT), upper ocean (MUP), and lower ocean (MLO), respectively. In Gerlagh and Liski (2017), they correspond to upper box containing atmosphere and upper ocean at constant fractions , terrestrial biosphere, and lower ocean, respectively. Consequently, in two DICE models the parameters σ_{13} and σ_{31} are zero because there is no direct exchange between atmosphere and deep ocean, while this parameters are non-negative in Gerlagh and Liski (2017). Table C1 below displays the parameter values of the transition matrix for the three models (for 5 year time steps).

Table C1: Parameter values of the transition matrix for the three carbon cycle models for 5 year time steps (displayed here rounded to 4 decimal places).

	σ_{11}	σ_{12}	σ_{13}	σ_{21}	σ_{22}	σ_{23}	σ_{31}	σ_{32}	σ_{33}
CC16	0.8800	0.1200	0	0.1960	0.7970	0.0070	0	0.0015	0.9985
CC13	0.9120	0.0880	0	0.0383	0.9592	0.0025	0	0.0003	0.9997
CCGL	0.8351	0.1199	0.0151	0.1104	0.8771	0.0008	0.0545	0.0030	0.9841

In DICE2016R and DICE2013R, emissions enter only the atmosphere, implying that q_2 and q_3 are zero, in Gerlagh and Liski (2017) it is assumed for time steps larger than one year, part of the ambient carbon exchange between reservoirs is captured by non-negative values for q_2 and q_3, implying that a certain fraction directly enters other reservoirs. Accordingly, we have followed their approach for the calibration of w_1, w_2, and w_3 by using these parameters to obtain a closer fit of the 5 year time step

calibration with the given 1 year time step calibration (where the three parameter values are zero). Consequently, the parameter w_1 displays the fraction of carbon removed which has returned to the atmosphere within a five year time period. Table C2 below displays the parameter values for the distribution of emissions and CDR.

Table C2: Parameter values of the distribution of emissions and CDR for the three carbon cycle models for 5 year time steps (displayed here rounded to 4 decimal places).

	q_1	q_2	q_3	w_1	w_2	w_3
CC16	1	0	0	0	0	1
CC13	1	0	0	0	0	1
CCGL	0.9318	0.0460	0.0221	0.0062	0.0002	0.9936

Both, DICE2013 and CCGL have been simulated with "historical emissions" such that they have the same initial conditions for atmospheric carbon stock as DICE2016R (i.e., 851 Gt C) in the year 2015. Table C3 below displays the initial values for the three carbon cycles.

Table C3: Initial values for the three carbon cycle models in 2015 in Gt C.

	$S_1(0)$	$S_2(0)$	$S_3(0)$
CC16	851.000	460.0	1,740.00
CC13	851.000	1,541.0	10,010.50
CCGL	290.836	159.4	158.34

For CCGL, the constant fraction 0.904409 of S_1 corresponds to the atmospheric carbon stock. Furthermore, in CCGL the carbon stocks are measured in deviation to the preindustrial values, implying that in order to obtain the initial value for atmospheric carbon stock of 851 Gt C one needs to add the preindustrial value of 588 Gt C.

All other equations with respect to the climate module (i.e., forcing equation and temperature equation) and assumptions with respect to exogenous land-use emissions and exogenous forcing are specified like in DICE2016R.

C.2 Validation with BEAM and UVic ESCM

The parameter values for the non-linear three-box Bolin and Eriksson Adjusted Model (BEAM) are obtained from Glotter et al. (2014) and validated with the documentation of webDICE (http://webdice.rdcep.org/). Like with the linear carbon cycles models, we derived "historical emission" up until the year 2015 such that the atmospheric carbon stock is as DICE2016R (i.e., 851 Gt C).

To insure that the carbon cycle models in the IAMs and UVic ESCM are initialized with nearly the same mean annual atmospheric CO_2 and temperature conditions, we first prescribe all forcing, following historical observations, to reach the same year 2015 conditions as in the IAMs. Then, we diagnose compatible CO_2 emissions and use these to force the model until the year 2015. The model has been spun-up for 10,000 years and then run from 850 to 2005, where historical atmospheric CO_2 forcing is prescribed along with known natural (orbital, volcanic, and solar) and other anthropogenic forcing (greenhouse gases, sulfate aerosols, and land cover change), following the Paleoclimate Modelling Intercomparison Project Phase 3 (PMIP3) and the Coupled Model Intercomparison Project Phase 5 (CMIP5)-recommended datasets (Taylor et al., 2011).

From the year 2006 until the year 2015 simulations continue with prescribed historical CO_2 forcing, which is then held constant from 2014 to 2015 at 2014 levels. From 2006 onwards, natural forcings as well as land cover change are held constant at 2005-levels. Non-CO_2 greenhouse gases and aerosols follow the RCP 8.5 specifications from 2006 to 2015 (Meinshausen et al., 2011). Further, prescribed, monthly varying, National Center for Environmental Prediction (NCEP) reanalysis winds are used together with a dynamical feedback from a first-order approximation of geostrophic wind anomalies associated with changing winds in a changing climate (Weaver et al., 2001).

Compatible CO_2 emissions from 850 to 2015 are diagnosed in the prescribed CO_2 run presented above and then used to conduct an emission driven simulation until

the year 2015. All other forcing remains the same. From the year 2016 onwards, the UVic simulations follow the same forcing as used in the respective IAM simulations. Table C4 below displays the initial values for BEAM and UVic ECSM in 2015, showing for the latter the initial values for atmosphere, land, and total ocean.

Table C4: Initial values for BEAM and UVic ECSM in 2015 in Gt C.

	$S_1(0)$/Atmosphere	$S_2(0)$/Land	$S_3(0)$ / Total Ocean
BEAM	851	727	35,646.00
UVic ECSM	850.89	1789.02	37391.18

Like in the carbon cycle models in the IAMs, CDR/deep ocean CO_2 injections are simulated by adding carbon to the lower box, $S_3(t)$. In UVic ESCM, deep ocean CO_2 injections in the respective CDR scenarios is simulated, in terms of the locations of the injections sites and the general deployment methodology, based on the OCMIP carbon sequestration protocols (Orr et al., 2001) and carried out in an idealized manner by adding CO_2 directly to the dissolved inorganic carbon (DIC) pool (Orr et al., 2001). Thus, we neglect any gravitational effects and assume that the injected CO_2 instantaneously dissolves into seawater and is transported quickly away from the injection point and distributed homogenously over the entire model grid box with lateral dimensions of a few hundred kilometers and many tens of meters in the vertical direction (Reith et al., 2016). Consequently, the formation of CO_2 plumes or lakes as well as the potential risk of fast rising CO_2 bubbles are neglected (IPCC, 2005; Bigalke et al., 2008).

Following Orr et al. (2001) and Reith et al. (2016) CO_2 is injected at seven separate injections sites, which are located in individual grid boxes near the Bay of Biscay (42.3° N, 16.2° W), New York (36.9° N, 66.6° W), Rio de Janeiro (27.9° S, 37.8° W), San Francisco (31.5° N, 131.4° W), Tokyo (33.3° N, 142.2° E), Jakarta (11.7° S, 102.6° E) and Mumbai (13.5° N, 63° E) (Reith et al., 2016; their Figure 1). Direct CO_2 injections are carried out at 2900 m depth to minimize leakage and maximize retention time. At this depth, liquid CO_2 is denser than seawater, which has

the additional advantage that any undissolved droplets would sink rather than rise to the surface (e.g., IPCC, 2005).

Additional Figures

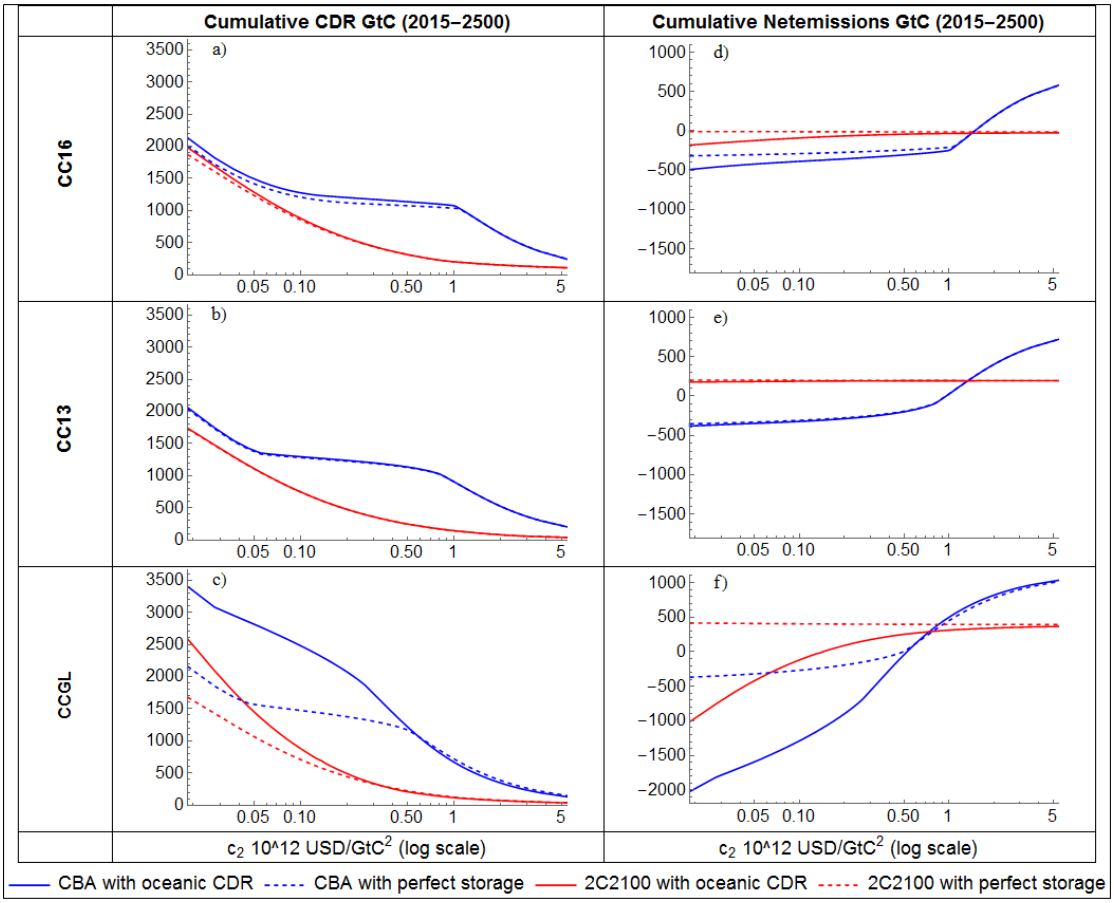

Figure C1: Cumulative CDR and Net Emissions as Function of Convexity of CDR cost for the period 2015 until 2500 for the CBA and 2C2100 Framework.

The figure shows the cumulative optimal amount of CDR (left panel) and cumulative optimal amounts of net emissions (right panel) as function of c2, the slope of the marginal CDR cost curve. The upper panel corresponds to CC16 (the carbon cycle model from DICE2016R), the middle panel corresponds to CC13 (the carbon cycle model from DICE2013R), and the lower panel corresponds to CCGL (the carbon cycle model from Gerlagh and Liski (2017)). Each box displays the optimal amounts for CBA (blue lines) and 2C2100 (red lines) for two CDR options, oceanic CDR (solid lines) and perfect storage (dashed lines).

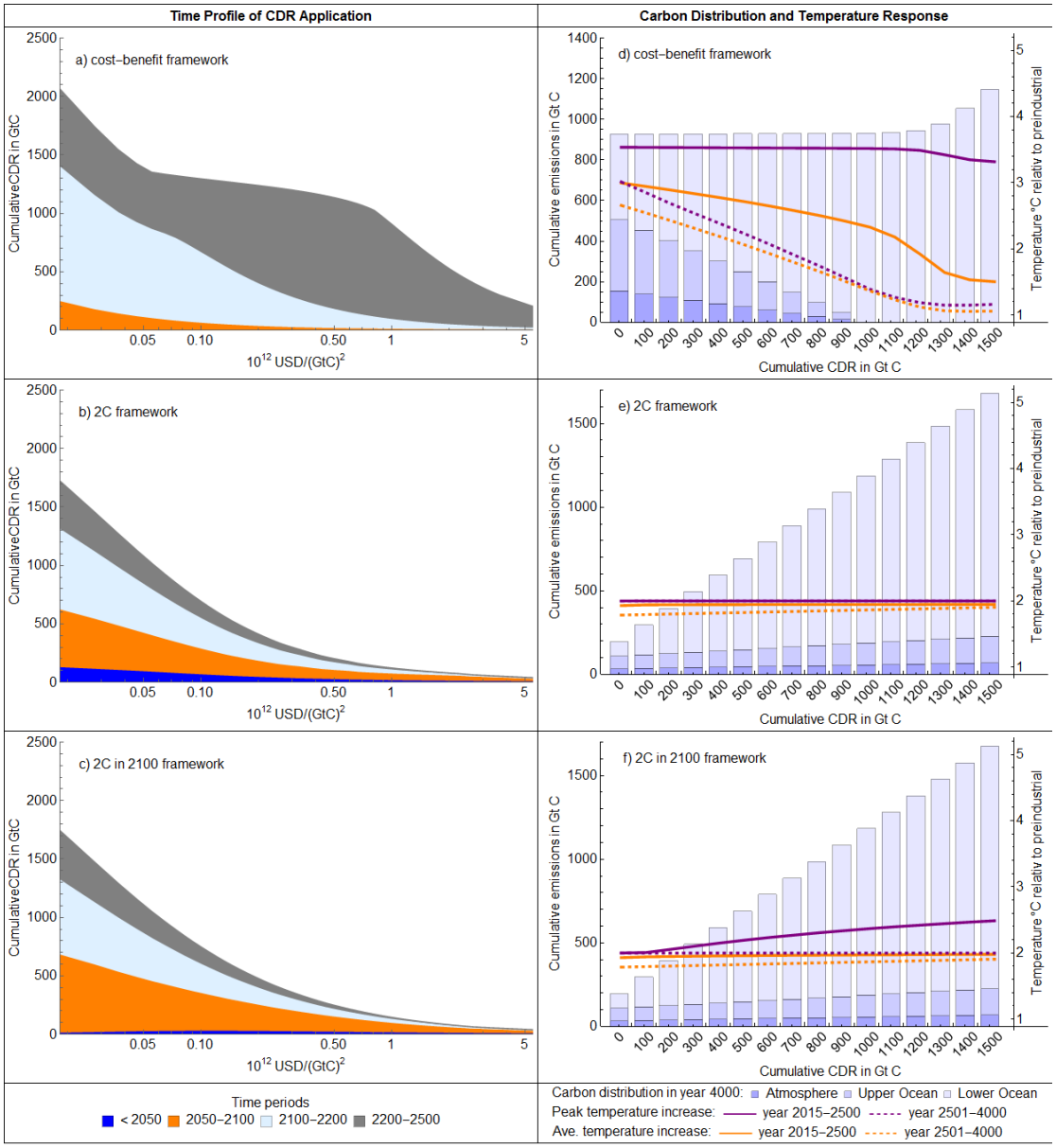

Figure C2: Time Profile of CDR Application (until year 2500), Carbon Distribution in year 4000, and Temperature Response until year 2500 and 4000 in CC13.

The left panel shows the cumulative optimal amount of CDR as function of c2, the slope of the marginal CDR cost curve, including the time profile of CDR utilization for the different mitigation frameworks (CBA, 2C, and 2C2100 in a), b) and c), respectively). The right panel shows the distribution of the carbon emissions (from 2015 until 2500) in the year 4000 across the different carbon reservoirs in dependence of the cumulative amount of CDR for the different mitigation frameworks (CBA, 2C, and 2C2100 in d), e) and f), respectively). The right panel also includes information about peak and average temperature for the period 2015-2500 and 2501 until 4000.

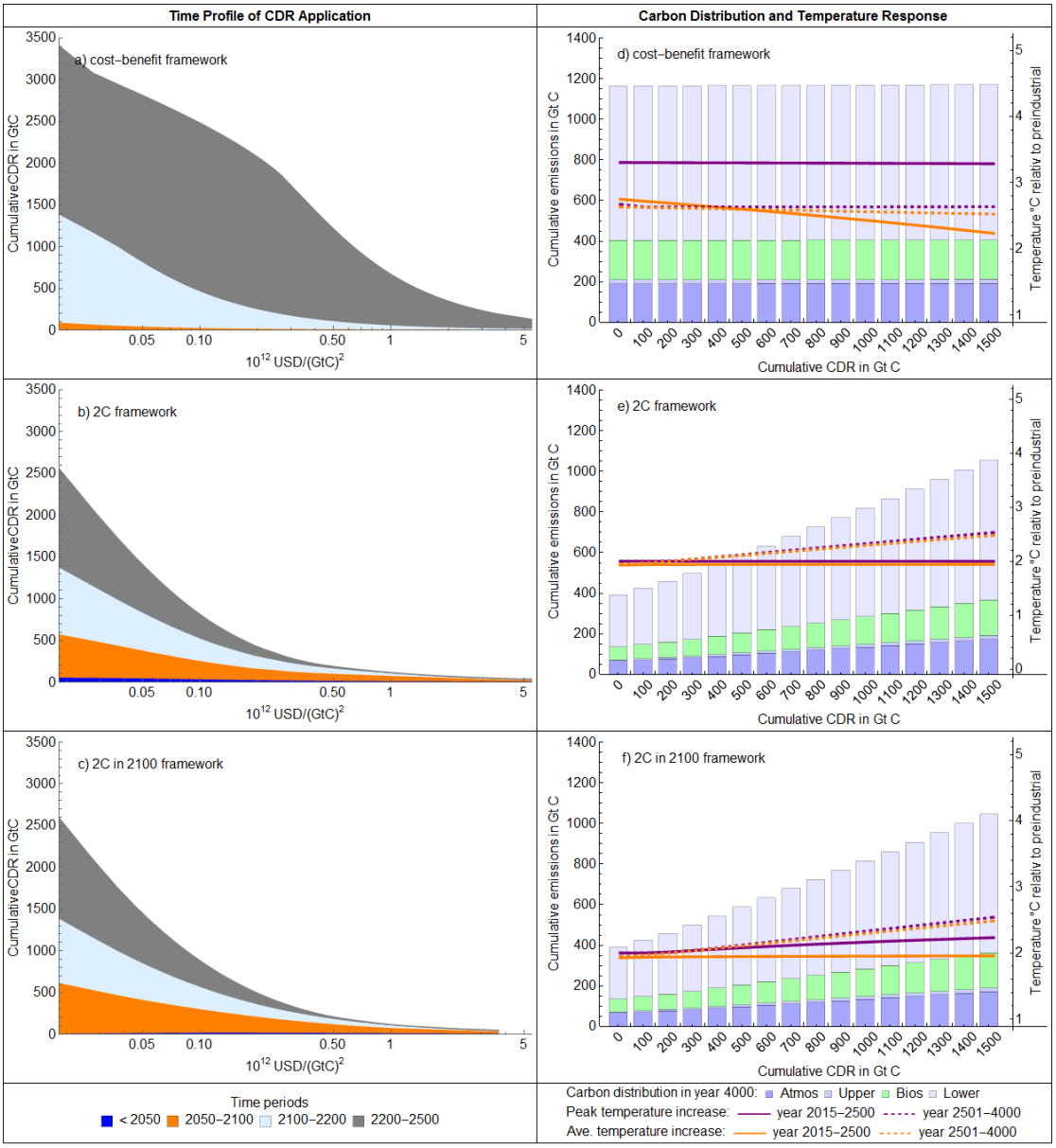

Figure C3: Time Profile of CDR Application (until year 2500), Carbon Distribution in year 4000, and Temperature Response until year 2500 and 4000 in CCGL.

The left panel shows the cumulative optimal amount of CDR as function of c_2, the slope of the marginal CDR cost curve, including the time profile of CDR utilization for the different mitigation frameworks (CBA, 2C, and 2C2100 in a), b) and c), respectively). The right panel shows the distribution of the carbon emissions (from 2015 until 2500) in the year 4000 across the different carbon reservoirs in dependence of the cumulative amount of CDR for the different mitigation frameworks (CBA, 2C, and 2C2100 in d), e) and f), respectively). The right panel also includes information about peak and average temperature for the period 2015-2500 and 2501 until 4000.

BIBLIOGRAPHY

Ahlström, A., Schurgers, G., Arneth, A., and Smith, B.: Robustness and uncertainty in terrestrial ecosystem carbon response to CMIP5 climate change projections, Environ. Res. Lett., 7, 044008, doi:10.1088/1748-9326/7/4/044008, 2012.

Allen, M. R., Frame, D. J., Huntingford, C., Jones, C. D., Lowe, J. A., Meinshausen, M. and Meinshausen, N.: Warming caused by cumulative carbon emissions towards the trillionth tonne, Nature, 458(7242), 1163–1166, doi:10.1038/nature08019, 2009.

Anderson, K. and Peters, G.: The trouble with negative emissions, Science, 354, 182–183, doi:10.1126/science.aah4567, 2016.

Archer, D., Eby, M., Brovkin, V., Ridgwell, A., Cao, L., Mikolajewicz, U., Caldeira, K., Matsumoto, K., Munhoven, G., Montenegro, A. and Tokos, K.: Atmospheric Lifetime of Fossil Fuel Carbon Dioxide, Annu. Rev. Earth Pl. Sc., 37, 117–134, doi:10.1146/annurev.earth.031208.100206, 2009.

Archer, D., Kheshgi, H., and Maier-Reimer, E.: Dynamics of fossil fuel CO_2 neutralization by marine $CaCO_3$, Global Biogeochem. Cy., 12, 259–276, doi:10.1029/98GB00744, 1998.

Archer, D.: A data-driven model of the global calcite lysocline, Global Biogeochem. Cycles, 10(3), 511–526, doi:10.1029/96GB01521, 1996.

Archer, D.: Fate of fossil fuel CO_2 in geologic time, J. Geophys. Res. C Ocean., 110(9), 1–6, doi:10.1029/2004JC002625, 2005.

Arora, V. K., Boer, G. J., Friedlingstein, P., Eby, M., Jones, C. D., Christian, J. R., Bonan, G., Bopp, L., Brovkin, V., Cadule, P., Hajima, T., Ilyina, T., Lindsay, K., Tjiputra, J. F., and Wu, T.: Carbon–Concentration and Carbon–Climate Feedbacks in CMIP5 Earth System Models, J. Climate, 26, 5289–5314, doi:10.1175/JCLI-D-12-00494.1, 2013.

Azar, C., Lindgren, K., Obersteiner, M., Riahi, K., van Vuuren, D. P., den Elzen, K. M. G. J., Möllersten, K., and Larson, E. D.: The feasibility of low CO_2 concentration targets and the role of bio-energy with carbon capture and storage (BECCS), Climatic Change, 100, 195–202, doi:10.1007/s10584-010-9832-7, 2010.

Bernardello, R., Marinov, I., Palter, J. B., Galbraith, E. D., and Sarmiento, J. L.: Impact of Weddell Sea deep convection on natural and anthropogenic carbon in a climate model, Geophys. Res. Lett., 41, 7262–7269, doi:10.1002/2014GL061313, 2014.

Bigalke, N. K., Rehder, G., and Gust, G.: Experimental investigation of the rising behavior of CO_2 droplets in seawater under hydrate-forming conditions, Environ. Sci. Technol., 42, 5241–5246, doi:10.1021/es800228j, 2008.

Bitz, C. M. and Lipscomb, W. H.: An energy-conserving thermodynamic model of sea ice, J. Geophys. Res., 104, 15669, doi:10.1029/1999JC900100, 1999.

Bopp, L., Resplandy, L., Orr, J. C., Doney, S. C., Dunne, J. P., Gehlen, M., Halloran, P., Heinze, C., Ilyina, T., Séférian, R., Tjiputra, J., and Vichi, M.: Multiple stressors of ocean ecosystems in the 21st century: projections with CMIP5 models, Biogeosciences, 10, 6225–6245, doi:10.5194/bg-10-6225-2013, 2013.

Boucher, O., Halloran, P. R., Burke, E. J., Doutriaux-Boucher, M., Jones, C. D., Lowe, J., Ringer, M. A., Robertson, E., and Wu, P.: Reversibility in an Earth System model in response to CO_2 concentration changes, Environ. Res. Lett., 7, 24013, doi:10.1088/1748-9326/7/2/024013, 2012.

Boysen, L. R., Lucht, W., and Gerten, D.: Trade-offs for food production, nature conservation and climate limit the terrestrial carbon dioxide removal potential, Global change biology, doi:10.1111/gcb.13745, 2017b.

Boysen, L. R., Lucht, W., Gerten, D., Heck, V., Lenton, T. M., and Schellnhuber, H. J.: The limits to global-warming mitigation by terrestrial carbon removal, Earth's Future, 5, 463–474, doi:10.1002/2016EF000469, 2017a.

Burke, M., Hsiang, S. M., and Miguel, E.: Global non-linear effect of temperature on economic production, Nature, 527, 235–239, doi:10.1038/nature15725, 2015.

Caldeira, K. and Wickett, M. E.: Anthropogenic carbon and ocean pH, Nature, 425(6956), 365, doi:10.1038/425365a, 2003.

Cao, L. and Caldeira, K.: Atmospheric carbon dioxide removal: Long-term consequences and commitment, Environ. Res. Lett., 5, 24011, doi:10.1088/1748-9326/5/2/024011, 2010.

Cao, L., Eby, M., Ridgwell, A., Caldeira, K., Archer, D., Ishida, A., Joos, F., Matsumoto, K., Mikolajewicz, U., Mouchet, A., Orr, J. C., Plattner, G.-K., Schlitzer, R., Tokos, K., Totterdell, I., Tschumi, T., Yamanaka, Y. and Yool, A.: The role of ocean transport in the uptake of anthropogenic CO_2, Biogeosciences, 6(3), 375–390, doi:10.5194/bg-6-375-2009, 2009.

Carvalhais, N., Forkel, M., Khomik, M., Bellarby, J., Jung, M., Migliavacca, M., Mingquan, M., Saatchi, S., Santoro, M., Thurner, M., Weber, U., Ahrens, B., Beer, C., Cescatti, A., Randerson, J. T., and Reichstein, M.: Climate in Terrestrial Ecosystems, Nature, 514, 213–217, doi:10.1038/nature13731, 2014.

Chen, C. and Tavoni, M.: Direct air capture of CO_2 and climate stabilization: A model based assessment, Climatic Change, 118, 59–72, doi:10.1007/s10584-013-0714-7, 2013.

Ciais, P., Sabine, C., Bala, G., Bopp, L., Brovkin, V., Canadell, J., Chhabra, a, DeFries, R., Galloway, J., Heimann, M., Jones, C., Quéré, C. Le, Myneni, R. B., Piao, S. and Thornton, P.: Carbon and Other Biogeochemical Cycles, Clim. Chang., 2013 - Phys. Sci. Basis, doi:10.1017/CBO9781107415324.015, 2013.

Clarke, L. E., Jiang, K., Akimoto, K., Babiker, M., Blanford, G., Fisher-Vanden, K., Hourcade, J.-C., Krey, V., Kriegler, E., Löschel, A., McCollum, D., Paltsev, S., Rose, S., Shukla, P. R., Tavoni, M., van der Zwaan, B. C. C. and van Vuuren, D. P.: Assessing transformation pathways, Clim. Chang. 2014 Mitig. Clim. Chang. Contrib. Work. Gr. III to Fifth Assess. Rep. Intergov. Panel Clim. Chang., 413–510, 2014.

Claussen, M., Mysak, L., Weaver, A., Crucifix, M., Fichefet, T., Loutre, M. F., Weber, S., Alcamo, J., Alexeev, V., Berger, A., Calov, R., Ganopolski, A., Goosse, H., Lohmann, G., Lunkeit, F., Mokhov, I., Petoukhov, V., Stone, P. and Wang, Z.: Earth system models of intermediate complexity: Closing the gap in the spectrum of climate system models, Clim. Dyn., 18(7), 579–586, doi:10.1007/s00382-001-0200-1, 2002.

Clémençon, R.: The Two Sides of the Paris Climate Agreement, J. Environ. Dev., 25(1), 3–24, doi:10.1177/1070496516631362, 2016.

Collins, M., Knutti, R., Arblaster, J., Dufresne, J. L., Fichefet, T., Friedlingstein, P., Gao, X., Gutowski, W. J., Johns, T., Krinner, G., Shongwe, M., Tebaldi, C., Weaver, A. J., and Wehner, M.: Chapter 12 - Long-term climate change: Projections, commitments and irreversibility, in: Climate Change 2013: The Physical Science Basis. IPCC Working Group I Contribution to AR5, IPCC (Ed.), Cambridge University Press, Cambridge, 2013.

De Lavergne, C., Palter, J. B., Galbraith, E. D., Bernardello, R., and Marinov, I.: Cessation of deep convection in the open South-ern Ocean under anthropogenic climate change, Nature Climate Change, 4, 278–282, doi:10.1038/nclimate2132, 2014.

DeVries, T. and Primeau, F.: Dynamically and Observationally Constrained Estimates of Water-Mass Distributions and Ages in the Global Ocean, J. Phys. Oceanogr., 41, 2381–2401, doi:10.1175/JPO-D-10-05011.1, 2011.

Dickson, A. G. and Millero, F. J.: A comparison of the equilibrium constants for the dissociation of carbonic acid in seawater media, Deep Sea Res. Part A, Oceanogr. Res. Pap., 34(10), 1733–1743, doi:10.1016/0198-0149(87)90021-5, 1987.

Doney, S. C., Fabry, V. J., Feely, R. a and Kleypas, J. a: Ocean acidification: the other CO_2 problem., Ann. Rev. Mar. Sci., 1, 169–92, doi:10.1146/annurev.marine.010908.163834, 2009.

Doney, S. C.: The growing human footprint on coastal and open-ocean biogeochemistry, Science, 328, 1512–1516, doi:10.1126/science.1185198, 2010.

Duteil, O. and Oschlies, A.: Sensitivity of simulated extent and future evolution of marine suboxia to mixing intensity, Geophys. Res. Lett., 38, n/a-n/a, doi:10.1029/2011GL046877, 2011.

Eby, M., Weaver, A. J., Alexander, K., Zickfeld, K., Abe-Ouchi, A., Cimatoribus, A. A., Crespin, E., Drijfhout, S. S., Edwards, N. R., Eliseev, A. V., Feulner, G., Fichefet, T., Forest, C. E., Goosse, H., Holden, P. B., Joos, F., Kawamiya, M., Kicklighter, D., Kienert, H., Matsumoto, K., Mokhov, I. I., Monier, E., Olsen, S., M., Pedersen, J. O. P., Perrette, M., Philippon-Berthier, G., Ridgwell, A., Schlosser, A., Schneider von Deimling, T., Shaffer, G., Smith, R. S., Spahni, R., Sokolov, A. P., Steinacher, M., Tachiiri, K., Tokos, K., Yoshimori, M., Zeng, N., and Zhao, F.: Historical and idealized climate model experiments: an intercomparison of Earth system models of intermediate complexity, Clim. Past, 9, 1111–1140, doi:, 2013.

Fabricius, K. E., Kluibenschedl, A., Harrington, L., Noonan, S. and De'ath, G.: In situ changes of tropical crustose coralline algae along carbon dioxide gradients, Sci. Rep., 5, 9537, doi:10.1038/srep09537, 2015.

Fanning, A. F. and Weaver, A. J.: An atmospheric energy-moisture balance model: Climatology, interpentadal climate change, and coupling to an ocean general circulation model, J. Geophys. Res., 101, 15111–15128, doi:10.1029/96JD01017, 1996.

Feng, E. Y., Keller, D. P., Koeve, W. and Oschlies, A.: Could artificial ocean alkalinization protect tropical coral ecosystems from ocean acidification?, Environ. Res. Lett., 11(7), 74008, doi:10.1088/1748-9326/11/7/074008, 2016.

Field, C. B. and Mach, K. J.: Rightsizing carbon dioxide removal, Science (New York, N.Y.), 356, 706–707, doi:10.1126/science.aam9726, 2017.

Field, C., Barros, V., Stocker, T. and Dahe, Q.: IPCC workshop on impacts of ocean acidification on marine biology and ecosystems. Workshop report. [online] Available from: https://www.etde.org/etdeweb/details_open.jsp?osti_id=1032894, 2011.

Flögel, S., Dullo, W. C., Pfannkuche, O., Kiriakoulakis, K. and Rüggeberg, A.: Geochemical and physical constraints for the occurrence of living cold-water corals, Deep. Res. Part II Top. Stud. Oceanogr., 99, 19–26, doi:10.1016/j.dsr2.2013.06.006, 2014.

Friedlingstein, P., Andrew, R. M., Rogelj, J., Peters, G. P., Canadell, J. G., Knutti, R., Luderer, G., Raupach, M. R., Schaeffer, M., Van Vuuren, D. P., and Le Quéré, C.: Persistent growth of CO_2 emissions and implications for reaching climate targets, Nat. Geosci., 7, 709–715, doi:10.1038/ngeo2248, 2014.

Friedlingstein, P., Cox, P., Betts, R., Bopp, L., von Bloh, W., Brovkin, V., Cadule, P., Doney, S., Eby, M., Fung, I., Bala, G., John, J., Jones, C., Joos, F., Kato, T., Kawamiya, M., Knorr, W., Lindsay, K., Matthews, H. D., Raddatz, T., Rayner, P., Reick, C., Roeckner, E., Schnitzler, K.-G., Schnur, R., Strassmann, K., Weaver, A. J., Yoshikawa, C., and Zeng, N.: Climate–Carbon Cycle Feedback Analysis: Results from the C4 MIP Model Intercomparison, J. Climate, 19, 3337–3353, doi:10.1175/JCLI3800.1, 2006.

Frölicher, T. L., Winton, M., and Sarmiento, J. L.: Continued global warming after CO_2 emissions stoppage, Nature Climate change, 4, 40–44, doi:10.1038/nclimate2060, 2013.

Fuss, S., Canadell, J. G., Peters, G. P., Tavoni, M., Andrew, R. M., Ciais, P., Jackson, R. B., Jones, C. D., Kraxner, F., Nakicenovic, N., Le Quéré, C., Raupach, M. R., Sharifi, A., Smith, P., and Yamagata, Y.: Betting on negative emissions, Nature Climate change, 4, 850–853, doi:10.1038/nclimate2392, 2014.

Gasser, T., Guivarch, C., Tachiiri, K., Jones, C. D., and Ciais, P.: Negative emissions physically needed to keep global warming below 2 °C, Nature communications, 6, 7958, doi:10.1038/ncomms8958, 2015.

Gehlen, M., Séférian, R., Jones, D. O. B., Roy, T., Roth, R., Barry, J., Bopp, L., Doney, S. C., Dunne, J. P., Heinze, C., Joos, F., Orr, J. C., Resplandy, L.,

Segschneider, J., and Tjiputra, J.: Projected pH reductions by 2100 might put deep North Atlantic biodiversity at risk, Biogeosciences, 11, 6955–6967, doi:10.5194/bg-11-6955-2014, 2014.

Gerlagh, R. and Liski, M.: Consistent climate policies, Journal of the European Economic Association, doi:10.1093/jeea/jvx010, 2017.

Gillett, N. P., Arora, V. K., Zickfeld, K., Marshall, S. J., and Merryfield, W. J.: Ongoing climate change following a complete cessation of carbon dioxide emissions, Nature Geosci, 4, 83–87, doi:10.1038/ngeo1047, 2011.

Glotter, M. J., Pierrehumbert, R. T., Elliott, J. W., Matteson, N. J., and Moyer, E. J.: A simple carbon cycle representation for economic and policy analyses, Climatic Change, 126, 319–335, doi:10.1007/s10584-014-1224-y, 2014.

Guinotte, J. M. and Fabry, V. J.: Ocean acidification and its potential effects on marine ecosystems, Ann. N. Y. Acad. Sci., 1134, 320–342, doi:10.1196/annals.1439.013, 2008.

Guinotte, J. M., Orr, J., Cairns, S., Freiwald, A., Morgan, L. and George, R.: Will human-induced changes in seawater chemistry alter the distribution of deep-sea scleractinian corals?, Front. Ecol. Environ., 4(3), 141–146, doi:10.1890/1540-9295(2006)004[0141:WHCISC]2.0.CO;2, 2006.

Hagerty, S. B., van Groenigen, K. J., Allison, S. D., Hungate, B. A., Schwartz, E., Koch, G. W., Kolka, R. K., and Dijkstra, P.: Accelerated microbial turnover but constant growth efficiency with warming in soil, Nature Climate Change, 4, 903–906, doi:10.1038/nclimate2361, 2014.

Hajima, T., Tachiiri, K., Ito, A., and Kawamiya, M.: Uncertainty of concentration-terrestrial carbon feedback in earth system models, J. Climate, 27, 3425–3445, doi:10.1175/JCLI-D-13-00177.1, 2014.

Hansen, J., Sato, M., Kharecha, P., Schuckmann, K. Von and Beerling, D. J.: Young people ' s burden : requirement of negative CO_2 emissions, , 577–616, 2017.

Hansen, J., Sato, M., Ruedy, R., Nazarenko, L., Lacis, A., Schmidt, G. A., Russell, G., Aleinov, I., Bauer, M., Bauer, S., Bell, N., Cairns, B., Canuto, V., Chandler, M., Cheng, Y., Del Genio, A., Faluvegi, G., Fleming, E., Friend, A., Hall, T., Jackman, C., Kelley, M., Kiang, N., Koch, D., Lean, J., Lerner, J., Lo, K., Menon, S., Miller, R., Minnis, P., Novakov, T., Oinas, V., Perlwitz, J., Perlwitz, J., Rind, D., Romanou, A., Shindell, D., Stone, P., Sun, S., Tausnev, N., Thresher, D., Wielicki, B., Wong, T., Yao, M. and Zhang, S.: Efficacy of climate forcings, J. Geophys. Res. D Atmos., 110(18), 1–45, doi:10.1029/2005JD005776, 2005.

Harvey, L. D. D.: Mitigating the atmospheric CO_2 increase and ocean acidification by adding limestone powder to upwelling regions, J. Geophys. Res., 113, 1669, doi:10.1029/2007JC004373, 2008.

Heinze, C., Meyer, S., Goris, N., Anderson, L., Steinfeldt, R., Chang, N., Le Quéré, C. and Bakker, D. C. E.: The ocean carbon sink - Impacts, vulnerabilities and challenges, Earth Syst. Dyn., 6(1), 327–358, doi:10.5194/esd-6-327-2015, 2015.

Herrington, T. and Zickfeld, K.: Path independence of climate and carbon cycle response over a broad range of cumulative carbon emissions, Earth Syst. Dynam., 5, 409–422, doi:10.5194/esd-5-409-2014, 2014.

Hof, A. F., Hope, C. W., Lowe, J., Mastrandrea, M. D., Meinshausen, M., and van Vuuren, D. P.: The benefits of climate change mitigation in integrated assessment models: The role of the carbon cycle and climate component, Climatic Change, 113, 897–917, doi:10.1007/s10584-011-0363-7, 2012.

Hoffert, M. I., Wey, Y. C., Callegari, A. J., and Broecker, W. S.: Atmospheric response to deep-sea injections of fossil-fuel carbon dioxide, Climatic Change, 2, 53–68, doi:10.1007/BF00138226, 1979.

Hofmann, M. and Schellnhuber, H. J.: Ocean acidification: a millennial challenge, Energy Environ. Sci., 3(12), 1883, doi:10.1039/c000820f, 2010.

Horton, J. B., Keith, D. W. and Honegger, M.: Implications of the Paris Agreement for Carbon Dioxide Removal and Solar Geoengineering, , 1–10, 2016.

Houghton, R. A.: Balancing the Global Carbon Budget, Annu. Rev. Earth Planet. Sci., 35(1), 313–347, doi:10.1146/annurev.earth.35.031306.140057, 2007.

Intergovernmental Panel on Climate Change (IPCC): Workshop Report of the IPCC Workshop on Impacts of Ocean Acidification on Marine Biology and Ecosystems [Field, C.B., Barros, V., Stocker, T.F., Qin, D. , Mach, K.J., Plattner, G.-K., Mastrandrea, M.D., Tignor, M., and Ebi, K.L. (eds.)]. IPCC Working Group II Technical Support Unit, Carnegie Institution, Stanford, California, United States of America, pp. 164, 2011.

IPCC: Climate Change 2013: The Physical Science Basis, Contribution of Working Group I to the Fifth Assessment Report of the Intergovernmental Panel on Climate Change, edited by: Stocker, T. F., Qin, D., Plattner, G.-K., Tignor, M., Allen, S. K., Boschung, J., Nauels, A., Xia, Y., Bex, V., and Midgley, P. M., Cambridge University Press, Cambridge, United Kingdom and New York, NY, USA, 1535 pp., 2013.

IPCC: Climate Change 2014: Impacts, Adaptation, and Vulnerability. Part A: Global and Sectoral Aspects. Contribution of Working Group II to the Fifth Assessment Report of the Intergovernmental Panel on Climate Change [Field, C.B., V.R. Barros, D.J. Dokken, K.J., Cambridge University Press, Cambridge, United 1599 Kingdom and New York, NY, USA, 2014.

IPCC: IPCC Special Report on Carbon Dioxide Capture and Storage, Prepared by Working Group III of the Intergovernmental Panel on Climate Change, edited by: Metz, B., Davidson, O., de Coninck, H. C., Loos, M., and Meyer, L. A., Cambridge University Press, Cambridge, United Kingdom and New York, NY, USA, 442 pp., 2005.

Israelsson, P. H., Chow, A. C. and Eric Adams, E.: An updated assessment of the acute impacts of ocean carbon sequestration by direct injection, Energy Procedia, 1(1), 4929–4936, doi:10.1016/j.egypro.2009.02.324, 2009.

Jain, A. K. and Cao, L.: Assessing the effectiveness of direct injection for ocean carbon sequestration under the influence of climate change, Geophys. Res. Lett., 32, L09609, doi:10.1029/2005GL022818, 2005.

Jenkinson, D., Adams, D., Wild, A.: Model estimates of CO_2 emissions from soil in response to global warming, Nature, 351(6324), 304-306, 1991.

Jones, C. D., Ciais, P., Davis, S. J., Friedlingstein, P., Gasser, T., Peters, G. P., Rogelj, J., van Vuuren, D. P., Canadell, J. G., Cowie, A., Jackson, R. B., Jonas, M., Kriegler, E., Littleton, E., Lowe, J. A., Milne, J., Shrestha, G., Smith, P., Torvanger, A., and Wiltshire, A.: Simulating the Earth system response to negative emissions, Environmental Research Letters, 11, 95012, doi:10.1088/1748-9326/11/9/095012, 2016.

Jones, C., Robertson, E., Arora, V., Friedlingstein, P., Shevliakova, E., Bopp, L., Brovkin, V., Hajima, T., Kato, E., Kawamiya, M., Liddicoat, S., Lindsay, K., Reick, C. H., Roelandt, C., Segschneider, J., and Tjiputra, J.: Twenty-first-century compatible CO_2 emissions and airborne fraction simulated by cmip5 earth sys- tem models under four representative concentration pathways, J. Climate, 26, 4398–4413, doi:10.1175/JCLI-D-12-00554.1, 2013.

Keeling, R. F.: Triage in the greenhouse, Nat. Geosci., 2(12), 820–822, doi:10.1038/ngeo701, 2009.

Keller, D. P., Feng, E. Y., and Oschlies, A.: Potential climate engineering effectiveness and side effects during a high carbon dioxide-emission scenario, Nature Communications 5, 3304, doi:10.1038/ncomms4304, 2014.

Keller, D. P., Lenton, A., Scott, V., Vaughan, N. E., Bauer, N., Ji, D., Jones, C. D., Kravitz, B., Muri, H., and Zickfeld, K.: The Carbon Dioxide Removal Model Intercomparison Project (CDR-MIP): Rationale and experimental design, Geosci. Model Dev. Discuss., https://doi.org/10.5194/gmd-2017-168, in review, 2017.

Keller, D. P., Oschlies, A., and Eby, M.: A new marine ecosystem model for the University of Victoria Earth System Climate Model, Geosci. Model Dev., 5, 1195–1220, doi:10.5194/gmd-5-1195-2012, 2012.

Klein R.J.T., Midgley, G. F., Preston, B. L., Alam, M., Berkhout, F. G. H., Dow, K. and Shaw, M. R.: 16. Adaptation Opportunities, Constraints, and Limits, Assess. Rep. 5- Clim. Chang. 2014 Impacts, Adapt. Vulnerability. Part A Glob. Sect. Asp., 899–943, doi:10.1017/CBO9780511807756.003, 2014.

Klepper, G. and Rickels, W.: Climate Engineering: Economic Considerations and Research Challenges, Rev Environ Econ Policy, 8, 270–289, doi:10.1093/reep/reu010, 2014.

Klepper, G. and Rickels, W.: The Real Economics of Climate Engineering, Economics Research International, 2012, 1–20, doi:10.1155/2012/316564, 2012.

Kleypas, J. A., et al.: Environmental limits to coral reef development: Where do we draw the line?, Am. Zool., 39(1), 146–159, 1999.

Knopf, B., Fuss, S., Hansen, G., Creutzig, F., Minx, J. and Edenhofer, O.: From Targets to Action: Rolling up our Sleeves after Paris, Glob. Challenges, 1(2), 1600007, doi:10.1002/gch2.201600007, 2017.

Knutti, R., Rogelj, J., Sedláček, J. and Fischer, E. M.: A scientific critique of the two-degree climate change target, Nat. Geosci., 9(1), doi:10.1038/ngeo2595, 2015.

Koeve, W. and Oschlies, A.: Potential impact of DOM accumulation on fCO_2 and carbonate ion computations in ocean acidification experiments, Biogeosciences, 9(10), 3787–3798, doi:10.5194/bg-9-3787-2012, 2012.

Köhler, P., Abrams, J. F., Völker, C., Hauck, J., and Wolf-Gladrow, D. A.: Geoengineering impact of open ocean dissolution of olivine on atmospheric CO_2 surface ocean pH and marine biology, Environ. Res. Lett., 8, 14009, doi:10.1088/1748-9326/8/1/014009, 2013.

Körtzinger, A.: Betrachtung aus meereschemischer perspektive: Der globale kohlenstoffkreislauf im Anthropozän, Chemie Unserer Zeit, 44(2), 118–129, doi:10.1002/ciuz.201000507, 2010.

Kriegler, E., Edenhofer, O., Reuster, L., Luderer, G., and Klein, D.: Is atmospheric carbon dioxide removal a game changer for climate change mitigation?, Climatic Change, 118, 45–57, doi:10.1007/s10584-012-0681-4, 2013.

Lavergne, C. de, Palter, J. B., Galbraith, E. D., Bernardello, R., and Marinov, I.: Cessation of deep convection in the open Southern Ocean under anthropogenic climate change, Nature Climate change, 4, 278–282, doi:10.1038/nclimate2132, 2014.

Le Quéré, C., Andrew, R. M., Friedlingstein, P., Sitch, S., Pongratz, J., Manning, A. C., Korsbakken, J. I., Peters, G. P., Canadell, J. G., Jackson, R. B., Boden, T. A., Tans, P. P., Andrews, O. D., Arora, V. K., Bakker, D. C. E., Barbero, L., Becker, M., Betts, R. A., Bopp, L., Chevallier, F., Chini, L. P., Ciais, P., Cosca, C. E., Cross, J., Currie, K., Gasser, T., Harris, I., Hauck, J., Haverd, V., Houghton, R. A., Hunt, C. W., Hurtt, G., Ilyina, T., Jain, A. K., Kato, E., Kautz, M., Keeling, R. F., Klein Goldewijk, K., Körtzinger, A., Landschützer, P., Lefèvre, N., Lenton, A., Lienert, S., Lima, I., Lombardozzi, D., Metzl, N., Millero, F., Monteiro, P. M. S., Munro, D. R., Nabel, J. E. M. S., Nakaoka, S.-I., Nojiri, Y., Padín, X. A., Peregon, A., Pfeil, B., Pierrot, D., Poulter, B., Rehder, G., Reimer, J., Rödenbeck, C., Schwinger, J., Séférian, R., Skjelvan, I., Stocker, B. D., Tian, H., Tilbrook, B., van der Laan-Luijkx, I. T., van der Werf, G. R., van Heuven, S., Viovy, N., Vuichard, N., Walker, A. P., Watson, A. J., Wiltshire, A. J., Zaehle, S., and Zhu, D.: Global Carbon Budget 2017, Earth Syst. Sci. Data Discuss., https://doi.org/10.5194/essd-2017-123, in review, 2017.

"Le Quéré, C., Peters, G. P., Andres, R. J., Andrew, R. M., Boden, T. A., Ciais, P., Friedlingstein, P., Houghton, R. A., Marland, G., Moriarty, R., Sitch, S., Tans, P., Arneth, A., Arvanitis, A., Bakker, D. C. E., Bopp, L., Canadell, J. G., Chini, L. P., Doney, S. C., Harper, A., Harris, I., House, J. I., Jain, A. K., Jones, S. D., Kato, E., Keeling, R. F., Klein Goldewijk, K., Körtzinger, A., Koven, C., Lefèvre, N., Maignan, F., Omar, A., Ono, T., Park, G.-H., Pfeil, B., Poulter, B., Raupach, M. R.,

Regnier, P., Rödenbeck, C., Saito, S., Schwinger, J., Segschneider, J., Stocker, B. D., Takahashi, T., Tilbrook, B., van Heuven, S., Viovy, N., Wanninkhof,

R., Wiltshire, A., and Zaehle, S.: Global carbon budget 2013, Earth Syst. Sci. Data, 6, 235–263, doi:10.5194/essd-6-235-2014, 2014."

Le Quéré, C., Peters, G. P., Andres, R. J., Andrew, R. M., Boden, T. a., Ciais, P., Friedlingstein, P., Houghton, R. a., Marland, G., Moriarty, R., Sitch, S., Tans, P., Arneth, a., Arvanitis, a., Bakker, D. C. E., Bopp, L., Canadell, J. G., Chini, L. P., Doney, S. C., Harper, a., Harris, I., House, J. I., Jain, a. K., Jones, S. D., Kato, E., Keeling, R. F., Klein Goldewijk, K., Körtzinger, a., Koven, C., Lefèvre, N., Maignan, F., Omar, a., Ono, T., Park, G. H., Pfeil, B., Poulter, B., Raupach, M. R., Regnier, P., Rödenbeck, C., Saito, S., Schwinger, J., Segschneider, J., Stocker, B. D., Takahashi, T., Tilbrook, B., Van Heuven, S., Viovy, N., Wanninkhof, R., Wiltshire, a. and Zaehle, S.: Global carbon budget 2013, Earth Syst. Sci. Data, 6, 235–263, doi:10.5194/essd-6-235-2014, 2014.

Leung, D. Y. C., Caramanna, G., and Maroto-Valer, M. M.: An overview of current status of carbon dioxide capture and storage technologies, Renewable and Sustainable Energy Reviews, 39, 426–443, doi:10.1016/j.rser.2014.07.093, 2014.

Lewis, E. and Wallace, D.: Program developed for CO_2 system calculations, Ornl/Cdiac-105, 1–21, doi:4735, 1998.

Lischka, S., Büdenbender, J., Boxhammer, T. and Riebesell, U.: Impact of ocean acidification and elevated temperatures on early juveniles of the polar shelled pteropod Limacina helicina: Mortality, shell degradation, and shell growth, Biogeosciences, 8(4), 919–932, doi:10.5194/bg-8-919-2011, 2011.

MacDougall, A. H.: Reversing climate warming by artificial atmospheric carbon-dioxide removal: Can a Holocene-like climate be restored?, Geophys. Res. Lett., 40, 5480–5485, doi:10.1002/2013GL057467, 2013.

MacDougall, A. H.: The Transient Response to Cumulative CO_2 Emissions: a Review, Curr. Clim. Chang. Reports, 2(1), 39–47, doi:10.1007/s40641-015-0030-6, 2016.

Marchetti, C.: On geoengineering and the CO_2 problem, Climatic Change, 1, 59–68, doi:10.1007/BF00162777, 1977.

Martin, T., Park, W., and Latif, M.: Multi-centennial variability controlled by Southern Ocean convection in the Kiel Climate Model, Clim. Dynam., 40, 2005–2022, doi:10.1007/s00382-012-1586-7, 2013.

Matsumoto, K. and Mignone, B. K.: Model simulations of carbon sequestration in the Northwest Pacific by direct injection, J. Oceanogr., 61(4), 747–760, doi:10.1007/s10872-005-0081-8, 2005.

Matthews, H. D. and Caldeira, K.: Stabilizing climate requires near-zero emissions, Geophys. Res. Lett., 35(4), 1–5, doi:10.1029/2007GL032388, 2008.

Matthews, H. D., Gillett, N. P., Stott, P. a and Zickfeld, K.: The proportionality of global warming to cumulative carbon emissions., Nature, 459(7248), 829–32, doi:10.1038/nature08047, 2009.

Matthews, H. D.: Implications of CO_2 fertilization for future climate change in a coupled climate-carbon model, Glob. Change Biol., 13, 1068–1078, doi:10.1111/j.1365-2486.2007.01343.x, 2007.

Mauritsen, T. and Pincus, R.: Committed warming inferred from observations, Nature Climate change, 215, 56, doi:10.1038/nclimate3357, 2017.

McKinsey&Company: Impact of the financial crisis on carbon emissions: Version 2.1 of the Global Greenhouse Gas Abatement Cost Curve, McKinsey&Company, 2010.

Mehrbach, C., Culberson, C. H., Hawley, J. E. and Pytkowicx, R. M.: Measurement of the Apparent Dissociation Constants of Carbonic Acid in Seawater At Atmospheric Pressure1, Limnol. Oceanogr., 18(6), 897–907, doi:10.4319/lo.1973.18.6.0897, 1973.

Meinshausen, M., Smith, S. J., Calvin, K., Daniel, J. S., Kainuma, M. L. T., Lamarque, J., Matsumoto, K., Montzka, S. A., Raper, S. C. B., Riahi, K., Thomson, A., Velders, G. J. M., and van Vuuren, D. P. P.: The RCP greenhouse gas concentrations and their extensions from 1765 to 2300, Climatic Change, 109, 213–241, doi:10.1007/s10584-011-0156-z, 2011.

Meissner, K. J., Eby, M., Weaver, A. J., and Saenko, O. A.: CO_2 threshold for millennial-scale oscillations in the climate system: implications for global warming scenarios, Clim. Dynam., 30, 161–174, doi:10.1007/s00382-007-0279-0, 2007.

Meissner, K. J., Weaver, A. J., Matthews, H. D., and Cox, P. M.: The role of land surface dynamics in glacial inception: A study with the UVic Earth System Model, Clim. Dynam., 21, 515–537, doi:10.1007/s00382-003-0352-2, 2003.

Moss, R. H., Edmonds, J. a, Hibbard, K. a, Manning, M. R., Rose, S. K., van Vuuren, D. P., Carter, T. R., Emori, S., Kainuma, M., Kram, T., Meehl, G. a, Mitchell, J. F. B., Nakicenovic, N., Riahi, K., Smith, S. J., Stouffer, R. J., Thomson, A. M., Weyant, J. P. and Wilbanks, T. J.: The next generation of scenarios for climate change research and assessment., Nature, 463(7282), 747–56, doi:10.1038/nature08823, 2010.

Mucci A.: The solubility of calcite and aragonite in seawater at various salinities, temperatures and one atmosphere total pressure. Amer. Jour. Sci. 283: 780-799, 1983.

Mueller, K., Cao, L., Caldeira, K., and Jain, A.: Differing methods of accounting ocean carbon sequestration efficiency, J. Geophys. Res., 109, C12018, doi:10.1029/2003JC002252, 2004.

Myhre, G., Samset, B. H., Schulz, M., Balkanski, Y., Bauer, S., Berntsen, T. K., Bian, H., Bellouin, N., Chin, M., Diehl, T., Easter, R. C., Feichter, J., Ghan, S. J., Hauglustaine, D., Iversen, T., Kinne, S., Kirkeväg, A., Lamarque, J. F., Lin, G., Liu, X., Lund, M. T., Luo, G., Ma, X., Van Noije, T., Penner, J. E., Rasch, P. J., Ruiz, A., Seland, Skeie, R. B., Stier, P., Takemura, T., Tsigaridis, K., Wang, P., Wang, Z., Xu, L., Yu, H., Yu, F., Yoon, J. H., Zhang, K., Zhang, H. and Zhou, C.: Radiative forcing of the direct aerosol effect from AeroCom Phase II simulations, Atmos. Chem. Phys., 13(4), 1853–1877, doi:10.5194/acp-13-1853-2013, 2013.

National Research Council: Climate Intervention: Carbon Dioxide Removal and Reliable Sequestration, National Academies Press, 2015b.

National Research Council: Climate Intervention: Reflecting Sunlight to Cool Earth, National Academies Press, 2015a.

Nordhaus, W. and Sztorc, P.: DICE 2013R: Introduction and User's Manual, Cowles Found, New Haven, CT, 2013.

Nordhaus, W. D.: Revisiting the social cost of carbon, Proceedings of the National Academy of Sciences of the United States of America, 114, 1518–1523, doi:10.1073/pnas.1609244114, 2017.

Nordhaus, W.: Estimates of the Social Cost of Carbon: Concepts and Results from the DICE-2013R Model and Alternative Approaches, Journal of the Association of Environmental and Resource Economists, 1, 273–312, doi:10.1086/676035, 2014.

Ogden, L. E.: Marine Life on Acid, Bioscience, 63(5), 322–328, doi:10.1525/bio.2013.63.5.3, 2013.

Orr, J. C., Aumont, O., Yool, A., Plattner, K., Joos, F., Maier-Reimer, E., Weirig, M.-F., Schlitzer, R., Caldeira, K., Wicket, M., and Matear, R.: Ocean CO_2 Sequestration Efficiency from 3-D Ocean Model Comparison, in: Greenhouse Gas Control Technologies, edited by: Williams, D., Durie, B., McMullan, P., Paulson, C., and Smith, A., CSIRO, Colligwood, Australia, 469–474, 2001.

Orr, J. C., Najjar, C. R., Sabine, C. L., and Joos, F.: Abiotic- Howto, Internal OCMIP Report, LCSE/CEA Saclay, Gif-sur- Yvette, France, 25 pp., 1999.

Orr, J. C.: Modelling of ocean storage of CO_2 – The GOSAC study, Report PH4/37, IEA Greenhouse gas R&D Programme, 96 pp., 2004.

Oschlies, A., Pahlow, M., Yool, A., and Matear, R. J.: Climate engineering by artificial ocean upwelling: Channelling the sorcerer's apprentice, Geophys. Res. Lett., 37, L04701, doi:10.1029/2009GL041961, 2010.

Pacanowski, R. C.: MOM2: Documentation, User's Guide and Reference Manual, GFDL Ocean Tech. Rep. 3.2, 329 pp., 1996.

Pandolfi, J. M., Connolly, S. R., Marshall, D. J. and Cohen, A. L.: Projecting Coral Reef Futures Under Global Warming and Ocean Acidification, Science (80-.)., 333(6041), 418–422, doi:10.1126/science.1204794, 2011.

Paquay, F. S. and Zeebe, R. E.: Assessing possible consequences of ocean liming on ocean pH, atmospheric CO_2 concentration and associated costs, International Journal of Greenhouse Gas Control, 17, 183–188, doi:10.1016/j.ijggc.2013.05.005, 2013.

Peters, G. P., Andrew, R. M., Boden, T., Canadell, J. G., Ciais, P., Le Quéré, C., Marland, G., Raupach, M. R., and Wilson, C.: The challenge to keep global warming below 2°C, Nature Climate Change, 3, 4–6, doi:10.1038/nclimate1783, 2013.

Plattner, G. K., Knutti, R., Joos, F., Stocker, T. F., von Bloh, W., Brovkin, V., Cameron, D., Driesschaert, E., Dutkiewicz, S., Eby, M., Edwards, N. R., Fichefet, T., Hargreaves, J. C., Jones, C. D., Loutre, M. F., Matthews, H. D., Mouchet, A.,

Müller, S. A., Nawrath, S., Price, A., Sokolov, A., Strassmann, K. M. and Weaver, A. J.: Long-term climate commitments projected with climate-carbon cycle models, J. Clim., 21(12), 2721–2751, doi:10.1175/2007JCLI1905.1, 2008.

Prentice, I. C, Farquhar, G. D., Fasham, M. J. R., Goulden, M. L., Heimann, M., Jaramillo, V. J., Kheshgi, H. S., Le Quéré, C., Scholes, R. J., and Wallace, D. W. R.: The Carbon Cycle and Atmospheric Carbon Dioxide, in: Climate Change 2001: The Scientific Basis: Contribution of Working Group I to the Third Assessment Report of the Intergovernmental Panel on Climate Change, edited by: Houghton, J. T., Ding, Y., Griggs, D. J., Noguer, M., van der Linden, P. J., Dai, X., Maskell, K., and Johnson, C. A., Cambridge Univ. Press, New York, 881 pp., 2001.

Raftery, A. E., Zimmer, A., Frierson, D. M. W., Startz, R., and Liu, P.: Less than 2 °C warming by 2100 unlikely, Nature Climate change, 109, 13915, doi:10.1038/nclimate3352, 2017.

Randall, D. A., Wood, R. A., Bony, S., Colman, R., Fichefet, T., Fyve, J., Kattsov, V., Pitman, A., Shukla, J., Srinivasan, J., Stouffer, R. J., Sumi, A. and Taylor, K. E.: Climate Models and Their Evaluation, Clim. Chang. 2007 Phys. Sci. Basis. Contrib. Work. Gr. I to Fourth Assess. Rep. Intergov. Panel Clim. Chang., 591–662, doi:10.1016/j.cub.2007.06.045, 2007.

Rao, S., Klimont, Z., Smith, S. J., Van Dingenen, R., Dentener, F.,Bouwman, L., Riahi, K., Amann, M., Bodirsky, B. L., van Vuuren, D. P., Reis, L. A., Calvin, K., Drouet, L., Fricko, O., Fujimori, S., Gernaat, D., Havlik, P., Harmsen, M., Hasegawa, T., Heyes, C., Hilaire, J., Luderer, G., Masui, T., Stehfest, E., Strefler, J., van der Sluis, S., and Tavoni, M.: Future air pollution in the Shared Socio-economic Pathways, Global Environ. Change, 42, 346–358, 2017.

Reith, F., Keller, D. P., and Oschlies, A.: Revisiting ocean carbon sequestration by direct injection: A global carbon budget perspective, Earth Syst. Dyn., 7(4), 797–812, doi:10.5194/esd-7-797-2016, 2016.

Renforth, P., Jenkins, B. G. and Kruger, T.: Engineering challenges of ocean liming, Energy, 60, 442–452, doi:10.1016/j.energy.2013.08.006, 2013.

Resplandy, L., Bopp, L., Orr, J. C. and Dunne, J. P.: Role of mode and intermediate waters in future ocean acidification: Analysis of CMIP5 models, Geophys. Res. Lett., 40(January), 3091–3095, doi:10.1002/grl.50414, 2013.

Riahi, K., van Vuuren, D. P., Kriegler, E., Edmonds, J., O'Neill, B. C., Fujimori, S., Bauer, N., Calvin, K., Dellink, R., Fricko, O., Lutz, W., Popp, A., Cuaresma, J. C., KC, S., Leimbach, M., Jiang, L., Kram, T., Rao, S., Emmerling, J., Ebi, K., Hasegawa, T., Havlik, P., Humpenöder, F., Da Silva, L. A., Smith, S., Stehfest, E., Bosetti, V., Eom, J., Gernaat, D., Masui, T., Rogelj, J., Strefler, J., Drouet, L., Krey, V., Luderer, G., Harmsen, M., Takahashi, K., Baumstark, L., Doelman, J. C., Kainuma, M., Klimont, Z., Marangoni, G., Lotze-Campen, H., Obersteiner, M., Tabeau, A. and Tavoni, M.: The Shared Socioeconomic Pathways and their energy, land use, and greenhouse gas emissions implications: An overview, Glob. Environ. Chang., 42, 153–168, doi:10.1016/j.gloenvcha.2016.05.009, 2017.

Ricke, K. L., Orr, J. C., Schneider, K. and Caldeira, K.: Risks to coral reefs from ocean carbonate chemistry changes in recent earth system model projections, Environ. Res. Lett., 8(3), 34003, doi:10.1088/1748-9326/8/3/034003, 2013.

Rickels, W. and Lontzek, T. S.: Optimal global carbon management with ocean sequestration, Oxford Economic Papers, 64, 323–349, doi:10.1093/oep/gpr027, 2012.

Rickels, W., Klepper, G., Dovern, J.; Betz, G., Brachatzek, N.; Cacean, S.; Güssow, K., Heintzenberg, J., Hiller, S.; Hoose, C., Leisner, T., Oschlies, A., Platt, U., Proelß, A., Renn, O., Schäfer, S., Zürn M.: Large-Scale Intentional Interventions into the Climate System? Assessing the Climate Engineering Debate. Scoping report conducted on behalf of the German Federal Ministry of Education and Research (BMBF), Kiel Earth Institute, Kiel, 2011.

Ridgwell, A., Rodengen, T. J., and Kohfeld, K. E.: Geographical variations in the effectiveness and side effects of deep ocean carbon sequestration, Geophys. Res. Lett., 38, 1–6, doi:10.1029/2011GL048423, 2011.

Roberts, J. M. and Cairns, S. D.: Cold-water corals in a changing ocean, Curr. Opin. Environ. Sustain., 7, 118–126, doi:10.1016/j.cosust.2014.01.004, 2014.

Rockström, J., Steffen, W., Noone, K., Persson, Å., Chapin III, F. S., Lambin, E. F., Lenton, T. M., Scheffer, M., Folke, C., Schellnhuber, H., Nykvist, B., de Wit, C. A., Hughes, T., van der Leeuw, S., Rodhe, H., Sörlin, S., Snyder, P. K., Costanza, R. and Al., E.: Planetary Boundaries: Exploring the Safe Operating Space for Humanity, Ecol. Soc., 14(2), 32, doi:10.1038/461472a, 2009.

Rogelj, J., and Lucht, W.: The world's biggest gamble, Earth's Future, 4, 465–470, doi:10.1002/2016EF000392, 2016.

Rogelj, J., Chen, C., Nabel, J., Macey, K., Hare, W., Schaeffer, M., Markmann, K., Höhne, N., Krogh Andersen, K., and Meinshausen, M.: Analysis of the Copenhagen Accord pledges and its global climatic impacts – a snapshot of dissonant ambitions, Environ. Res. Lett., 5, 034013, doi:10.1088/1748-9326/5/3/034013, 2010.

Rogelj, J., den Elzen, M., Höhne, N., Fransen, T., Fekete, H., Winkler, H., Schaeffer, R., Sha, F., Riahi, K., and Meinshausen, M.: Paris Agreement climate proposals need a boost to keep warming well below 2 °C, Nature, 534, 631–639, doi:10.1038/nature18307, 2016.

Rogelj, J., Luderer, G., Pietzcker, R. C., Kriegler, E., Schaeffer, M., Krey, V., and Riahi, K.: Energy system transformations for limiting end-of-century warming to below 1.5 °C, Nature Climate change, 5, 519–527, doi:10.1038/nclimate2572, 2015.

Rogelj, J., Schaeffer, M., Friedlingstein, P., Gillett, N. P., van Vuuren, D. P., Riahi, K., Allen, M., and Knutti, R.: Differences between carbon budget estimates unravelled, Nature Climate change, 6, 245–252, doi:10.1038/nclimate2868, 2016.

Rogelj, J., Schaeffer, M., Meinshausen, M., Knutti, R., Alcamo, J., Riahi, K., and Hare, W.: Zero emission targets as long-term global goals for climate protection, Environ. Res. Lett., 10, 105007, doi:10.1088/1748-9326/10/10/105007, 2015.

Rose, S. K., Kriegler, E., Bibas, R., Calvin, K., Popp, A., van Vuuren, D. P., and Weyant, J.: Bioenergy in energy transformation and climate management, Climatic Change, 123, 477–493, doi:10.1007/s10584-013-0965-3, 2014.

Sabine, C. L., Feely, R. A., Gruber, N., Key, R. M., Lee, K., Bullister, J. L., Wanninkhof, R., Wong, C. S., Wallace, D. W. R., Tilbrook, B., Millero, F. J., Peng, T.-H., Kozyr, A., Ono, T. and Rios, A. F.: The oceanic sink for anthropogenic CO_2., Science, 305(5682), 367–71, doi:10.1126/science.1097403, 2004.

Sanderson, B. M., O'Neill, B. C. and Tebaldi, C.: What would it take to achieve the Paris temperature targets?, Geophys. Res. Lett., 43(13), 7133–7142, doi:10.1002/2016GL069563, 2016.

Sarmiento, J. L. and Gruber, N.: Sinks for Anthropogenic Carbon, Phys. Today, 55(8), 30–36, doi:10.1063/1.1510279, 2002.

Sarmiento, J. L. and Toggweiler, J. R.: A new model for the role of the oceans in determining atmospheric pCO_2, Nature, 308(5960), 621–624 [online] Available from: http://dx.doi.org/10.1038/308621a0, 1984.

Schimel, D., Stephens, B. B., and Fisher, J. B.: Effect of increasing CO_2 on the terrestrial carbon cycle, P. Natl. Acad. Sci. USA, 112, 436–441, doi:10.1073/pnas.1407302112, 2015.

Schubert, R., Schellnhuber, H. J., Buchmann, N., Epiney, A., Griesshammer, R., Kulessa, M., Messner, D., Rahmstorf, S. and Schmid, J.: The Future Oceans – Warming Up, Rising High, Turning Sour., 2006.

Scott, V., Haszeldine, R. S., Tett, S. F. B. and Oschlies, A.: Fossil fuels in a trillion tonne world, Nat. Clim. Chang., 5(5), 419–423 [online] Available from: http://dx.doi.org/10.1038/nclimate2578, 2015.

Shepherd, J. G.: Geoengineering the climate: science, governance and uncertainty, Philos. T. Roy. Soc. A, 370, 4166–4175, doi:10.1098/rsta.2012.0186, 2009.

Siegenthaler, U.: Stable Carbon Cycle – Climate Relationship During the Late Pleistocene Stable Carbon Cycle – Climate Relationship During the Late Pleistocene, , 1313(25), 1313–1317, doi:10.1126/science.1120130, 2005.

Smith, P., Davis, S. J., Creutzig, F., Fuss, S., Minx, J., Gabrielle, B., Kato, E., Jackson, R. B., Cowie, A., Kriegler, E., van Vuuren, D. P., Rogelj, J., Ciais, P., Milne, J., Canadell, J. G., McCollum, D., Peters, G., Andrew, R., Krey, V., Shrestha, G., Friedlingstein, P., Gasser, T., Grübler, A., Heidug, W. K., Jonas, M., Jones, C. D., Kraxner, F., Littleton, E., Lowe, J., Moreira, J. R., Nakicenovic, N., Obersteiner, M., Patwardhan, A., Rogner, M., Rubin, E., Sharifi, A., Torvanger, A., Yamagata, Y., Edmonds, J., and Yongsung, C.: Biophysical and economic limits to negative CO_2 emissions, Nature Climate change, 6, 42–50, doi:10.1038/nclimate2870, 2015.

Su, X., Takahashi, K., Fujimori, S., Hasegawa, T., Tanaka, K., Kato, E., Shiogama, H., Masui, T., and Emori, S.: Emission pathways to achieve 2.0°C and 1.5°C climate targets, Earth's Future, 5, 592–604, doi:10.1002/2016EF000492, 2017.

Sun, Y., Gu, L., Dickinson, R. E., Norby, R. J., Pallardy, S. G., and Hoffman, F. M.: Impact of mesophyll diffusion on estimated global land CO_2 fertilization, P. Natl. Acad. Sci. USA, 11, 15774–15779, doi:10.1073/pnas.1418075111, 2014.

Taylor, K. E., Stouffer, R. J., and Meehl, G. A.: An Overview of CMIP5 and the Experiment Design, Bulletin of the American Meteorological Society, 93, 485–498, doi:10.1175/BAMS-D-11-00094.1, 2011.

Tokarska, K. B. and Zickfeld, K.: The effectiveness of net negative carbon dioxide emissions in reversing anthropogenic climate change, Environmental Research Letters, 10, 94013, doi:10.1088/1748-9326/10/9/094013, 2015.

UNFCCC: Conference of the Parties: Adoption of the Paris Agreement, Proposal by the President, Paris Clim. Chang. Conf. November 2015, COP 21, available at: http://unfccc.int/resource/docs/2015/cop21/eng/l09.pdf, last access: 2 January 2016, 2015.

van der Ploeg, F. and Rezai, A.: Cumulative emissions, unburnable fossil fuel, and the optimal carbon tax, Technological Forecasting and Social Change, 116, 216–222, doi:10.1016/j.techfore.2016.10.016, 2017.

van der Sleen, P., Groenendijk, P., Vlam, M., Anten, N. P. R., Boom, A., Bongers, F., Pons, T. L., Terburg, G., and Zuidema, P. A.: No growth stimulation of tropical trees by 150 years of CO_2 fertilization but water-use efficiency increased, Nat. Geosci., 8, 24–28, doi:10.1038/ngeo2313, 2014.

van Heuven, S., Pierrot, D., Lewis, E., and Wallace, D. W.R.: MATLAB Program Developed for CO_2 System Calculations, ORNL/CDIAC-105b, Carbon Dioxide Information Analysis Center, Oak Ridge National Laboratory, US Department of Energy, Oak Ridge, Tennessee, ftp://cdiac.ornl.gov/pub/co2sys/CO2SYScalcMATLAB, 2009.

van Vuuren, D. P., Deetman, S., van Vliet, J., van den Berg, M., van Ruijven, B. J., and Koelbl, B.: The role of negative CO_2 emissions for reaching 2 °C—insights from integrated assessment modelling, Climatic Change, 118, 15–27, doi:10.1007/s10584-012-0680-5, 2013.

van Vuuren, D. P., Lowe, J., Stehfest, E., Gohar, L., Hof, A. F., Hope, C., Warren, R., Meinshausen, M., and Plattner, G.-K.: How well do integrated assessment models simulate climate change?, Climatic Change, 104, 255–285, doi:10.1007/s10584-009-9764-2, 2011.

Vichi, M., Navarra, A., and Fogli, P. G.: Adjustment of the natural ocean carbon cycle to negative emission rates, Climatic Change, 118, 105–118, doi:10.1007/s10584-012-0677-0, 2013.

Volk, T. and Hoffert, M. I.: Ocean carbon pumps: Analysis of relative strengths and efficiencies in ocean driven atmospheric CO_2 changes, in The Carbon Cycle and Atmospheric CO_2: Natural variations Archaean to present, ed. by Sundquist, E.T. and Broecker, W.S., Geophys. Monogr. Ser., 32, 99-110, AGU, Washington, D.C., 1985.

Warren, R., Mastrandrea, M. D., Hope, C., and Hof, A. F.: Variation in the climatic response to SRES emissions scenarios in integrated assessment models, Climatic Change, 102, 671–685, doi:10.1007/s10584-009-9769-x, 2010.

Weaver, A. J., Eby, M., Wiebe, E. C., Bitz, C. M., Duffy, P. B., Ewen, T. L., Fanning, A. F., Holland, M. M., MacFadyen, A., Matthews, H. D., Meissner, K. J., Saenko, O., Schmittner, A., Wang, H., and Yoshimori, M.: The UVic earth system climate model: Model description, climatology, and applications to past, present and future climates, Atmos. Ocean, 39, 361–428, doi:10.1080/07055900.2001.9649686, 2001.

Williamson, P.: Emissions reduction: Scrutinize CO_2 removal methods, Nature, 530(153), 5–7, doi:10.1038/530153a, 2016.

Wise, M., Calvin, K., Thomson, A., Clarke, L., Bond-Lamberty, B., Sands, R., Smith, S. J., Janetos, A., and Edmonds, J.: Implications of limiting CO_2 concentrations for land use and energy, Science (New York, N.Y.), 324, 1183–1186, doi:10.1126/science.1168475, 2009.

Zeebe, R. E.: History of Seawater Carbonate Chemistry, Atmospheric CO_2, and Ocean Acidification, Annu. Rev. Earth Pl. Sc., 40, 141–165, doi:10.1146/annurev-earth-042711-105521, 2012.

Zickfeld, K. and Herrington, T.: The time lag between a carbon dioxide emission and maximum warming increases with the size of the emission, Environ. Res. Lett., 10, 31001, doi:10.1088/1748-9326/10/3/031001, 2015.

Zickfeld, K., Eby, M., Weaver, A. J., Alexander, K., Crespin, E., Edwards, N. R., Eliseev, A. V., Feulner, G., Fichefet, T., Forest, C. E., Friedlingstein, P., Goosse, H., Holden, P. B., Joos, F., Kawamiya, M., Kicklighter, D., Kienert, H., Matsumoto, K., Mokhov, I. I., Monier, E., Olsen, S. M., Pedersen, J. O. P., Perrette, M., Philippon-Berthier, G., Ridgwell, A., Schlosser, A., Schneider Von Deimling, T., Shaffer, G., Sokolov, A., Spahni, R., Steinacher, M., Tachiiri, K., Tokos, K. S., Yoshimori, M., Zeng, N., and Zhao, F.: Long-Term Climate Change Commitment and Reversibility: An EMIC Intercomparison, J. Climate, 26, 5782– 5809, doi:10.1175/JCLI-D-12-00584.1, 2013.

Acknowledgements

First of all, I would like to thank Andreas Oschlies very much for giving me the opportunity to join his group as a PhD candidate, for the support and supervision, the discussions, for giving me the opportunities to visit summer schools, workshops, and conferences and for always being supportive and constructive in a very friendly manner.

A very special thanks goes to David Keller, Wolfgang Koeve and Wilfried Rickels! During my time as a PhD candidate, I could always rely on their help. Without your guidance this thesis would have never been possible - Thank you very much!

Further, I would like to thank Julia Getzlaff, Rita Erven, Ulrike Löptien and Iris Kriest for their great help! Also, a big thank you to Ulrike Bernitt and Monika Peschke, who have always helped with administrational stuff!

Further, I would like to thank my fellow PhD candidates, especially Nadine Mengis, Levin Nickelsen, Lionel Arteaga, Tronje Kemena, Wanxuan Wao, Shubham Krishna, and Daniela Niemeyer for making the work much more pleasant!

And finally, I want to deeply thank my girlfriend Inga, my father and the rest of my family and friends for their great support and endless patience!

Eidesstattliche Erklärung

Hiermit erkläre ich an Eides statt, dass die vorliegende Arbeit mit dem Titel: 'Ocean carbon sequestration by direct CO_2 injection' von mir selbstständig angefertigt wurde. Bis auf zitierte Referenzen und Beratung meiner Betreuer wurden keine weiteren Quellen verwendet. Diese Arbeit ist unter Einhaltung der Regeln guter wissenschaftlicher Praxis der Deutschen Forschungsgemeinschaft entstanden. Sie wurde weder im Rahmen eines Prüfungsverfahrens an anderer Stelle vorgelegt noch veröffentlicht. Ich erkläre mich einverstanden, dass diese Arbeit an die Bibliothek des GEOMAR und die Universitätsbibliothek der Christian-Albrechts-Universität zu Kiel weitergeleitet wird.

Kiel, Dezember 2017

_____

(Fabian Reith)